



Universitetet
i Stavanger

Faculty of Science and Technology

MASTER'S THESIS

Study program / Specialization Constructions and Materials Offshore Constructions	Spring semester, 2016 Open / Restricted Access
Writer: Torstein Kristensen
Faculty supervisor: Sudath Siriwardane External supervisor: Oddrun A. Kristensen (Marine Aluminium)	
Thesis title: Study of production tolerances' impact on capacities with regards to EN-1999	
Credits (ECTS): 30	
Key words: Imperfections Flexural buckling Eurocode 9 NS-EN 1090-3 Perry-Robertson equation Buckling curves	Pages: 85 + enclosure: 40 Stavanger, June 13 th 2016

Summary

The goal of this thesis was to investigate the effect that production tolerances has on the strength capacities of a beam or column. The out-of-straightness imperfection on a pinned column, and its effect on the flexural buckling resistance, was chosen as the main consideration. The production standard NS-EN 1090-3 has different production tolerances that must be followed if a beam or column is going to be approved according to Eurocode 9. This includes a tolerance limit for the out-of-straightness imperfection. This tolerance limit was investigated in order to determine if it was safe to follow. Imperfections in the cross-section geometry, and its respective tolerance limits, was also considered in this thesis.

The effect of the out-of-straightness imperfection was investigated using the Perry-Robertson formula. This Perry-Robertson method is in part used to develop the buckling curves that are presented in both Eurocode 3 and Eurocode 9 today. However, these buckling curves have been strengthened by tests results and experiments. As a simplified method, the Perry-Robertson formula can therefore not offer a perfect representation of the actual buckling behavior of an imperfect column, but it can be used to illustrate the effect of an out-of-straightness imperfection rather well. Several Perry-Robertson calculations were performed for different cross-section types and for different imperfection values. The results from these calculations showed a large drop in flexural buckling resistance for an imperfect column compared with a perfectly straight column. The loss in load carrying capacity also grew with larger imperfections. It was shown that cross-sections, which has a low resistance to buckling, was effected more severely by the imperfection. The production tolerance for an out-of-straightness imperfection, as given in NS-EN 1090-3, was compared with these calculations. With this comparison, it was found that trusting the tolerance limit might prove dangerous in some situations. An ANSYS finite element analysis was carried at Marine Aluminium for multiple columns with an imperfection of 10 mm, in order to verify the Perry-Robertson calculations. The results from this analysis indicated that the Perry-Robertson method was conservative, but that it simulated the effect of the imperfection well.

The same column-models was then used in Eurocode 9 capacity calculations. The Eurocode 9 guidelines for flexural buckling resistance has an imperfection safety factor that is used in all buckling calculations. The results from these calculations yielded a lower flexural buckling resistance than the Perry-Robertson method for all the columns that were tested. The Eurocode 9 calculations proved to be conservative enough that no dangerous situation was found while staying true to the tolerance limits given in NS-EN 1090-3. An argument that the imperfection safety factor is too conservative in some situations is made and the optimization of Eurocode 9 buckling calculations is discussed.

Preface

This paper is written as a master's thesis at the University of Stavanger, in the spring of 2016. It shall account for 30 credits and mark the end of my studies at the University. In the thesis, the effect that initial imperfections have on Eurocode 9 capacities is investigated. Since this is a rather large subject the main focus became the out-of-straightness imperfection. While my previous experience with aluminium as a structural material is limited to two summer internships and a bachelor thesis, imperfections were a whole new subject for me. I feel that I have learned a lot from my work with this thesis.

When the time came for me to choose a subject for my master's thesis, I did not have a clue what I wanted to write about. I would therefore like to thank Steinar Lundberg and Oddrun A. Kristensen at Marine Aluminium, for producing several different alternatives for me to choose from. I would also like to thank them both for helping me through my thesis. A huge thank you must also go out to their coworker Fabio Garcia. With his help, my calculations were validated through an ANSYS analysis. It is hard to come by nicer people than the people working at Marine Aluminium!

I would also like to thank my supervisor from the University of Stavanger, Sudath Siriwardane. Although most of my work on this thesis was done away from Stavanger, I hugely appreciated our meetings and discussions.

Lastly I would like to thank my family and especially my parents. Their continuous support throughout my education has been priceless. I am truly lucky to have such a kind and loving family.

Stavanger, spring 2016

Torstein Kristensen

Contents

Summary	1
Preface.....	3
Figures	7
Tables	9
1. Introduction.....	11
1.1. Background for thesis.....	12
1.2. Aluminium as a structural material	13
1.3. Imperfections	14
1.4. Overview of NS-EN 1090-3:2008	15
2. Theoretical background.....	17
2.1. Buckling	17
2.2. Euler's critical load.....	19
2.3. Deriving Euler's critical load equation.....	21
2.4. Buckling of imperfect columns:.....	25
2.5. Slenderness ratio	28
2.6. Different methods of buckling.....	29
2.7. The Perry-Robertson equation.....	31
2.8. Deriving the Perry Robertson equation.....	32
2.9. Eurocode 9 calculation method	35
3. Previous works	39
3.1. A new design method for stainless steel columns subjected to flexural buckling.....	39
3.2. Stability of 6082-T6 aluminium alloy column with H-section and rectangular hollow sections.....	40
4. Calculations of imperfect columns	41
4.1. Buckling curve of an imperfect quadratic hollow section column	41
4.2. NS-EN 1090-3: Permitted deviation	45
4.3. Assumptions in the Perry-Robertson equation.....	49
4.4. ANSYS analysis	51
4.5. Eurocode 9 column calculations.....	56
4.6. Eurocode 9, imperfect column design.....	61
4.7. H-400 calculations	66
4.8. Result discussion	71
5. Cross-section imperfection and local buckling.....	75

5.1. Imperfect cross-section	75
6. Conclusion	81
7. Future work	83
References.....	85
Appendix A: Cross-section properties and classification	87
A.1. The 200x10 mm quadratic hollow section	87
A.2. The H-400 cross-section	89
Appendix B: Eurocode 9 design calculations.....	91
B.1. 200x10 mm quadratic hollow section	91
B.2. H-400 cross-section	94
Appendix C: Eurocode 9 imperfect column design	99
C.1. Equivalent horizontal forces method.....	99
C.2: Imperfection effect	102
Appendix D: Perry-Robertson calculations.....	105
D.1. 10 mm imperfection, 200x10 mm quadratic hollow section	105
D.2. 15 mm imperfection, 200x10 mm quadratic hollow section	108
D.3. 5 mm imperfection, 200x10 mm quadratic hollow section	110
D.4. No imperfection, 200x10 mm quadratic hollow section.....	112
D.5. 10 mm imperfection, H-400 cross-section - Minor axis	114
D.6. No imperfection, H-400 cross-section - Minor axis.....	117
D.7. 10 mm imperfection, H-400 cross-section - Major axis	119
D.8. No imperfection, H-400 cross-section - Major axis.....	121
Appendix E: Imperfect cross-section calculations.....	123
E.1. H-400 Cross-section with varying geometry	123
E.2. H-200 Cross-section with varying geometry	125

Figures

Figure 1: Imperfect loading + deformed shape	14
Figure 2: Bending deformation	18
Figure 3: Buckling deformation	18
Figure 4: Crushing deformation and buckling deformation	18
Figure 5: Fixed column	20
Figure 6: Free end column.....	20
Figure 7: Forces on crooked column	21
Figure 8: Column with a half sine-wave deflection	23
Figure 9: Buckling of imperfect column	25
Figure 10: Buckling of imperfect beam	32
Figure 11: Eurocode 9, equivalent horizontal forces [1]	37
Figure 12: 200x10 mm quadratic hollow section	42
Figure 13: Buckling curve, 10 mm imperfection	42
Figure 14: Buckling curve, no imperfection.....	43
Figure 15: Buckling curve comparison, 10 mm imperfection and no imperfection.....	44
Figure 16: Buckling curve comparison with tolerance line, 10 mm imperfection	45
Figure 17: Buckling curve comparison with tolerance line, 15 mm imperfection	46
Figure 18: Buckling curve comparison with tolerance line, 5 mm imperfection	47
Figure 19: Buckling curve comparison, varying imperfections.....	48
Figure 20: Imperfect column model.....	51
Figure 21: Top end support	52
Figure 22: Bottom end support	52
Figure 23: Buckling deformation, L = 2000 mm	53
Figure 24: Buckling deformation, L = 5000 mm	53
Figure 25: Buckling curve comparison, ANSYS and Perry-Robertson.....	55
Figure 26: Buckling curve comparison, Perry-Robertson (no imperfection) and Eurocode 9	58
Figure 27: Buckling curve comparison, Perry-Robertson with varying imperfection and Eurocode 9 .	59
Figure 28: Buckling curve comparison, various imperfections.....	59
Figure 29: Buckling curve comparison with tolerance line, Perry-Robertson with 5 mm imperfection and Eurocode 9.....	60
Figure 30: Eurocode 9, imperfection effect	64
Figure 31: H-400 cross-section	66
Figure 32: Rotated H-400 cross-section	66
Figure 33: H-400 cross-section dimensions.....	67
Figure 34: Buckling curve comparison, H-400 minor axis	68
Figure 35: Buckling curve comparison, H-400 major axis	69
Figure 36: Buckling curve comparison, varying imperfection, H-400 minor axis and Eurocode 9.....	70
Figure 37: Buckling curve comparison, varying imperfection, H-400 major axis and Eurocode 9.....	70
Figure 38: Eurocode 3, buckling curves [2]	72
Figure 39: Eurocode 9, buckling curves [1]	72
Figure 40: Capacities with variable cross-section, H-400.....	78
Figure 41: Capacities with variable cross-section, H-200.....	78
Figure 42: 200x10 mm quadratic hollow section	87
Figure 43: H-400 cross-section	89

Figure 44: Imperfect column model, 10 mm imperfection	105
Figure 45: 200x10 mm quadratic hollow section	105
Figure 46: Imperfect column model, 15 mm imperfection	108
Figure 47: Imperfect column model, 5 mm imperfection	110
Figure 48: H-400 cross-section	114
Figure 49: H-400 cross-section	123
Figure 50: H-200 cross-section	125

Tables

Table 1: Effective length factor [14]	19
Table 2: ANSYS analysis results	54
Table 3: ANSYS and Perry-Robertson stress ratio comparison	54
Table 4: Eurocode 9, compression resistance and flexural buckling resistance	56
Table 5: Eurocode 9, critical resistance and stress ratio	57
Table 6: Eurocode 9, design resistances and maximum allowable axial force	62
Table 7: Eurocode 9, Bending moment + axial force criteria check	63
Table 8: Eurocode 9, imperfection effect on design resistances	65
Table 9: Stress comparison: Eurocode 9, Perry-Robertson and ANSYS	65
Table 10: Table 6.2 from Eurocode 9 [1]	88
Table 11: Eurocode 9 resistances, 200x10 mm quadratic hollow section	93
Table 12: Eurocode 9 resistances, H-400	97
Table 13: Eurocode 9, imperfection effect	103
Table 14: Perry-Robertson results, 10 mm imperfection, 200x10 mm quadratic hollow section	107
Table 15: Perry-Robertson results, 15 mm imperfection, 200x10 mm quadratic hollow section	109
Table 16: Perry-Robertson results, 5 mm imperfection, 200x10 mm quadratic hollow section	111
Table 17: Perry-Robertson results, no imperfection, 200x10 mm quadratic hollow section	113
Table 18: Perry-Robertson results, 10 mm imperfection, H-400 minor axis	116
Table 19: Perry-Robertson results, no imperfection, H-400 minor axis	118
Table 20: Perry-Robertson results, 10 mm imperfection, H-400 major axis	120
Table 21: Perry-Robertson results, no imperfection, H-400 major axis	122
Table 22: Classification and thickness reduction, H-400	124
Table 23: Moment of inertia, H-400	124
Table 24: Compression and flexural buckling resistance, H-400	124
Table 25: Classification and thickness reduction, H-200	125
Table 26: Moment of inertia, H-200	126
Table 27: Compression and flexural buckling resistance, H-200	126

Chapter 1

1. Introduction

Imperfections in structures is something that must be accepted, as it is impossible to produce a 100% perfect beam or cross-section. An imperfection can be many things, for example a beam that is not perfectly straight will have an out-of-straightness imperfection. Imperfections will usually have a negative effect on the load carrying capacity of a member or a structure, but the actual reduction in load carrying capacity is hard to determine. In most cases, the imperfections found in beams are so small that they can be safely neglected, but what defines a small imperfection?

When a structure is being built, there are different production standards that can help in answering the question above or similar ones. They often use the ratio between the imperfection and the total length of the component, which allows them to determine if the imperfection can be neglected or not. However, these standards give little insight into how these ratios are deemed acceptable or not. Are these **imperfection tolerances** overly conservative or can they be dangerous to follow blindly?

In this thesis, a few simple column models with different degrees of out-of-straightness imperfections will be presented. The flexural buckling behavior of these models will be analyzed, as to better understand the impact of initial imperfections. Aluminum will be used as the structural material and so buckling will be calculated according to Eurocode 9 [1]. The imperfection tolerances will be collected from the fabrication standard for aluminum structures, NS-EN 1090-3:2008 [3]. Hand calculated buckling curves will be determined using the Perry-Robertson equation, which was regarded as the “backbone” for most buckling curves used in national standards [7]. To validate the hand calculations a finite element analysis will be presented, obtained through the software program ANSYS. The ultimate goal being to gain a better understanding of the impact that crookedness can have on a columns strength and check if the present tolerance limit, presented by EN 1090-3, is safe to follow.

In an article named “*Use of Perry formula to represent the new European strut curves*”, on the subject of imperfections, author J.B. Dwight wrote:

“In view of the importance of initial crookedness in strut behavior it is surprising that so little is known statistically about the values which actually occur.”[7]

1.1. Background for thesis

This thesis is written at the request and under the supervision of Marine Aluminium AS. Buckling of beams and columns is something that is calculated regularly and so most structural engineers are comfortable in this area. However, geometrical imperfections, and the effect that these imperfections has on the load carrying capacities, might not be as well known. When beams are ordered, it is expected that they hold a certain standard. If it is not obvious by eyesight that they are not as expected, beams with significant imperfections could be used in a structure. Although Marine Aluminium has not had any previous failures due to imperfections, they are interested in researching the complications that might occur. If the imperfection should prove to be more harmful than expected, mitigating measures can be implemented at an early stage of production.

Marine Aluminium is a company that has specialized itself in offshore constructions and now their two major products are helidecks and telescopic gangways, mainly constructed using aluminium. They also produce living quarters and safety railings, amongst other things. The company started up in 1953 and delivered their first helideck in 1973. Their first offshore telescopic gangway was delivered in 1979. Today Marine Aluminium's main office is located on Karmøy with a production site on Stord. They also have a smaller office with a staff of about 50 people working from Ningbo, China. Although mainly focused on the offshore industry, Marine Aluminium has also delivered some onshore helidecks, perhaps most notably in 2010 when they delivered a helideck to Haukeland Hospital in Bergen. With over 60 years of experience Marine Aluminium is world leading in aluminium access solutions for offshore use.



Picture 1: The main office of Marine Aluminium, Karmøy

1.2. Aluminium as a structural material

Aluminium might not be as common as steel or concrete, but it is still a great structural material. It is a lightweight yet strong material, with excellent corrosion properties. When aluminum was first produced chemically, it was not suitable for structural applications due to the cost. With time, newer and cheaper methods of production were introduced and aluminum structures became an excellent option, especially for the aircraft industry [10]. The lightweight material was perfect for airplane fuselages. Being successfully introduced to the aircraft industry, the development of aluminum boomed and new alloys, with different properties, were discovered. The most common alloys contain Copper, Zinc, Magnesium, Manganese or Silicon or a combination of these. For structural beams the 6000-series of aluminum is often the preferred alloy, this alloy contains Magnesium and Silicon. The 6000-series allows the aluminum to be extruded both easily and economically [10].

One of aluminum's greatest attributes is the fact that beams can be extruded. The extruding process is used to create a fixed cross section profile and it is performed by pressing an aluminum bar through a pre-manufactured die that creates the desired cross-section. The advantages of this is that very complex cross sections can be produced with relative ease. This gives the structural engineers a huge amount of choice in the designing phase. A natural disadvantage to extruding profiles is the size limitations inherent when using a die and extruding machines to create the cross-section.

One of the difficulties when using aluminum is the heat-affected zone (HAZ), which is a phenomenon that occurs where the material is not melted but the microstructure and properties are changed due to the heat. This is unavoidable around welds and can diminish the strength of the material. The most common problem is often reduced tensile strength in the HAZ. This obstacle can be overcome by using extruded beams and bolted connections, thereby reducing the need for welding to a minimum.

Aluminum has many different uses in different industries. In the offshore industry, aluminum is used for the helidecks, gangways, railings, ladders and living quarters, to name a few. Aluminium has also shown promising properties in arctic areas, where structures might be required to withstand temperatures down to minus 60 degrees Celsius. At these temperature, steel will lose a lot of capacity and become brittle. Aluminium does not show these characteristics and will retain its elastic nature.

1.3. Imperfections

When looking at structural beams an imperfection, as the name implies, is an unwanted property. Imperfections are often subcategorized into geometrical imperfections and mechanical imperfections [3].

Mechanical imperfections include residual stress cases. Residual stress is often defined as stress that remains in a material after the initial cause of the stress is removed. Residual stress can be a problem in situations where plastic deformations, large temperature variations or welding has occurred. These residual stresses can lead to failure of the structure.

Geometrical imperfections are a lot easier to visualize than mechanical imperfections. Geometrical imperfections include deformations such as out-of-straightness and variations in the cross-section geometry. A beam with an out-of-straightness imperfection can simply be defined as a beam that is not perfectly straight and the deformation is often idealized as sinusoidal or parabolic expression during calculations, with the maximum displacement located at the midspan. This type of imperfection is present in all beam, as it is impossible to produce a perfectly straight beam. The imperfection is usually larger in rolled sections compared to extruded sections [8].

Another kind of geometrical imperfection is an uneven cross-section. Meaning that for example the width of the web is not constant or that the one of the flanges is slightly tilted. This can lead to local weak zones and an uneven stress distribution. Added material might also cause unexpected weight issues. Tilted flanges can induce difficulties when installing/fastening the beam. A tilted web can cause unexpected moments to arise, which will lower the capacity of the whole beam. These are just some of the dangers when working with uneven cross-sections.

Other kinds of imperfection that occur in structures are loading imperfections. Situations can occur where the force from a load does not go through the centerline as intended, causing unforeseen moments in the structure. This is called loading eccentricities. An eccentrically loaded column will deform similarly to a column with an out-of-straightness imperfection, assuming that the largest deflection is at the middle. The illustration of imperfect loading and the resulting deformation is shown in Figure 1.

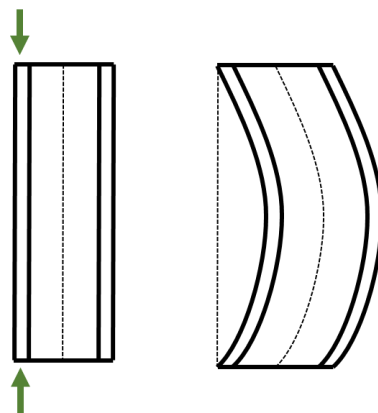


Figure 1: Imperfect loading + deformed shape

1.4. Overview of NS-EN 1090-3:2008

The full name of this standard NS-EN 1090-3:2008 is “Execution of steel structures and aluminium structures, Part 3: Technical requirements for aluminium structures” [3]. This European standard specifies requirements for the execution of aluminium structures, in order to ensure adequate levels of mechanical resistance and stability, serviceability and durability [3]. Among other things, the standard includes a section on geometrical tolerances and an annex that lists permitted deviations for different situations. The annex gives quantitative values for permitted deviations, but these deviations should not be used for elastic deformations. This means that if a given beam unexpectedly becomes elastically deformed while subjected to loading, one cannot argue that this is permitted because the deformation is within the accepted deviations given in the annex.

In this thesis, a lot of attention will be given to the out-of-straightness permitted deviation, which states:

$$\delta = \frac{L}{750}$$

Where:

- L = length of the beam
- δ = largest deflection from centerline

This means that for a 5 meter long beam the largest permitted out-of-straightness deviation will be 6.67 millimeters. According to “Aluminium structural analysis” [8] an analysis of extruded profiles from several European countries showed that the average difference between an extruded industrial bar and a “perfect” bar was $L/2000$. Which means that the average extruded industrial bar is well within the permitted area. Extruded profiles are usually a lot straighter than those that have been straightened by rolling. Extruded aluminium bars are straighter because of the more severe traction process.

Chapter 2

2. Theoretical background

When investigating the effect that an out-of-straightness imperfection has on a column, the flexural buckling resistance of the column must be considered. This chapter will introduce the theoretical background of buckling and show the derivation of some of the formulas used in the calculations. Most of the work that has been done in this field stems from the research done by Leonhard Euler. He discovered a formula, known as Euler's critical load formula, that can be used to find the maximum force a column can withstand before it becomes unstable and buckles. This formula is derived in order to gain a better understanding of buckling. A formula known as the Perry-Robertson equation is also described and derived. This formula is very useful when considering an imperfect column. At the end of the chapter, the flexural buckling resistance calculation method used in Eurocode 9 is introduced.

2.1. Buckling

Buckling is characterized by a structural member suddenly subjected to sideways failure, as a result of compressive stress. The working compressive stress during buckling is lower than the ultimate compressive stress that the material can withstand. Depending on the shape of the cross-section, a member subjected to axial force can buckle in three different ways. These are plane buckling, twist buckling and lateral torsional buckling [8]. Buckling is unique when compared to other structural considerations as it results from an unstable equilibrium state.

Bending and buckling can be easily confused with each other, as their respective deformation shape is very similar. The major difference is that bending is induced by forces acting perpendicular to the beams principle axis and buckling is induced by forces acting through the principle axis. To better illustrate these concepts, examples from everyday life can be useful. Picture a heavy man sitting in the middle of a wooden bench, the bench is in this case subjected to pure bending. Now take a plastic ruler and place the short edge on the desk, apply pressure with a finger on the top, with enough pressure the ruler will buckle.

An axial loaded member will fail by either buckling or crushing. The failure mode is dependent on the slenderness of member. Long and slender member will buckle while short and bulky members will fail by crushing. The most common compressive member is the column and it can be used too easily illustrate the two different failure scenarios, when looking at a "short" and "long" member subjected to a critical axial force. This is illustrated in Figure 4: the short column fails by crushing, while the long column fails by buckling.

Bending:

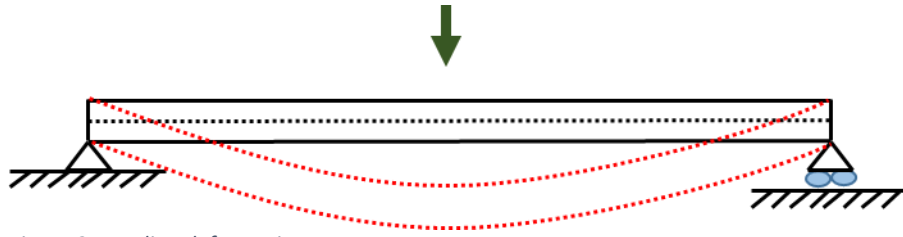


Figure 2: Bending deformation

Buckling:



Figure 3: Buckling deformation

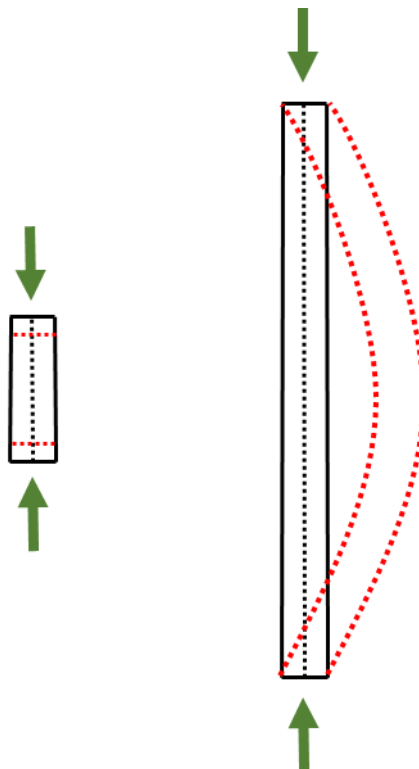


Figure 4: Crushing deformation and buckling deformation

2.2. Euler's critical load

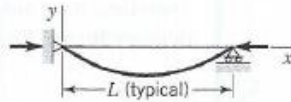





The Euler's critical load formula can be used to determine the maximum axial force that a column can withstand before it fails due to flexural buckling:

$$F = \frac{\pi^2 \cdot EI}{(k \cdot L)^2}$$

- F = Maximum force
- E = Modulus of elasticity
- I = Area moment of inertia
- k = Effective length factor
- L = Length of column

This equation is also known as Euler's buckling formula. From this equation, it is easy to see that the maximum force will increase when the length of the column decreases and *vice versa*. By, for example, doubling the length of a given column, it can now only carry one quarter of the original maximum force. The choice of support (pinned/fixed) is also a very important factor as it directly affects the effective length of the column. For simplicity sake, a chart is often used to identify the effective length factor. The theoretical factor is based on the deformation shape the column will develop during buckling. Standards often use a recommended design value for the effective length factor, which for some supports is more conservative [1]. To gain a better understanding of the impact of this factor two different support situation will be presented:

Table 1: Effective length factor [14]

Boundary conditions	Critical load	Deflected shape	Effective length KL
Simple support–simple support	$\frac{\pi^2 EI}{L^2}$		L
Clamped–clamped	$\frac{4\pi^2 EI}{L^2}$		$\frac{1}{2}L$
Clamped–simple support	$\frac{2.04\pi^2 EI}{L^2}$		0.70L
Clamped–free	$\frac{\pi^2 EI}{4L^2}$		2L
Clamped–guided	$\frac{\pi^2 EI}{L^2}$		L
Simple support–guided	$\frac{\pi^2 EI}{4L^2}$		2L

Two identical columns with different supports:

Drawing

Column 1



Figure 5: Fixed column

Column 2



Figure 6: Free end column

Effective length factor

$$k_1 = 0.5$$

$$k_2 = 2.0$$

Initial formula

$$F_1 = \frac{\pi^2 \cdot EI}{(k_1 \cdot L)^2}$$

$$F_2 = \frac{\pi^2 \cdot EI}{(k_2 \cdot L)^2}$$

Simplification

$$X = \frac{\pi^2 \cdot EI}{L^2}$$

Calculation

$$F_1 = \frac{1}{0.5^2} \cdot X$$

$$F_2 = \frac{1}{2^2} \cdot X$$

$$F_1 = 4 \cdot X$$

$$F_2 = 0.25 \cdot X$$

Result

$$\frac{F_1}{F_2} = \frac{4 \cdot X}{0.25 \cdot X} = 16$$

The example shows that the fixed column can carry a load **16** times larger than the load that the unsupported column can withstand, before failing by flexural buckling. Failure by crushing is now considered in Euler's critical load formula.

Using the Euler's critical load formula with short columns will result in very large maximal forces before failure is assumed to occur. If the resulting stress from this force is higher than the yield stress, the column will already have failed due to material limit. Euler's critical load formula is therefore not applicable for short columns.

2.3. Deriving Euler's critical load equation

In this subchapter, the Euler critical load equation will be derived using two different methods. The first method uses the moment-curvature relationship, while the second method is based on the assumed deformation shape and the criteria that the internal bending moment is equal to the external. The assumed deformation will be exactly the same shape as an out-of-straightness imperfection. The equation is derived in order to gain a better understanding of how buckling occurs.

Assume an ideal pinned column:

- Homogeneous and linear-elastic material
- Load is applied directly through the center, no load eccentricity

When axial loading is applied, the column will begin to bend and gain a curvature. This is shown in the Figure 7.

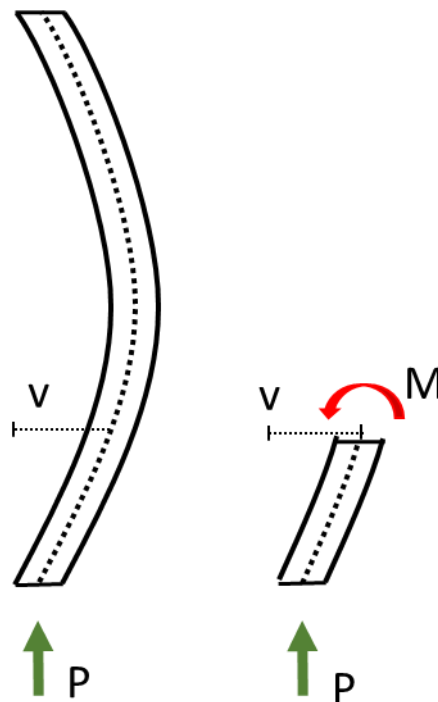


Figure 7: Forces on crooked column

The known moment-curvature relationship is as follows [14]:

$$\frac{d^2v}{dx^2} = \frac{M}{EI}$$

Moment equilibrium for the cut figure gives the following equation:

$$\Sigma M_{cut} = 0 \rightarrow M + P \cdot v = 0$$

$$M = -P \cdot v$$

Substituting this back into the moment-curvature relationship:

$$\frac{d^2 v}{dx^2} = \frac{M}{EI} \rightarrow \frac{d^2 v}{dx^2} = \frac{-P \cdot v}{EI}$$

The result is a second order linear differential equation:

$$\frac{d^2 v}{dx^2} + \frac{P}{EI} \cdot v = 0$$

The general solution of this equation will be [14]:

$$v(x) = A \cdot \sin\left(\sqrt{\frac{P}{EI}} \cdot x\right) + B \cdot \cos\left(\sqrt{\frac{P}{EI}} \cdot x\right)$$

Now the constants A and B can be determined by using the following boundary conditions:

$$v(0) = 0 \quad \text{and} \quad v(L) = 0$$

$$v(0) = 0 \rightarrow A \cdot 0 + B \cdot 1 = 0$$

$$B = 0$$

$$v(L) = 0 \rightarrow A \cdot \sin\left(\sqrt{\frac{P}{EI}} \cdot L\right) = 0$$

$$A = 0$$

Although this is correct, it is a trivial solution and nothing is learned from it. Another solution is found when the sine expression is equal to zero. This is only the case if the core is equal to Pi or an integer multiplied with Pi.

$$\sin\left(\sqrt{\frac{P}{EI}} \cdot L\right) = 0$$

$$\sqrt{\frac{P}{EI}} \cdot L = n \cdot \pi$$

The critical load will be the lowest load that causes the column too buckle, and that load will be found when n=1:

$$\sqrt{\frac{P}{EI}} \cdot L = 1 \cdot \pi$$

$$\frac{P}{EI} \cdot L = \pi^2$$

$$P = \frac{\pi^2 \cdot EI}{L}$$

This is the equation known as Euler's critical load, but this equation is only applicable for a hinged column. In order to make it applicable for all types of supports a modification is needed for the length. This is done by substituting the length for an effective buckling length that is based on the actual length of the column and a factor dependent on the support situation.

The critical load formula can also be found by using an assumed deformed shape and the fact that the internal bending moment is equal to the external bending moment. This method assumes that the column will take the deformation shape of a half-sine wave, so that the largest deformation is always at the middle of the span.

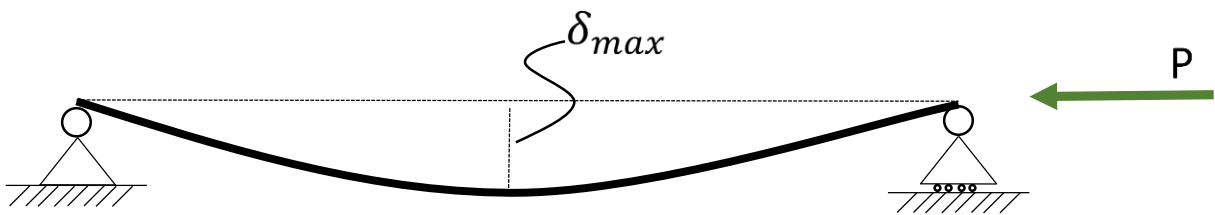


Figure 8: Column with a half sine-wave deflection

When assuming the formula for the deformed shape, the boundary conditions must be satisfied. As this is still a pinned column, the fact that the deflection will be equal to zero for both ends of the column is known:

$$v(0) = 0 \text{ and } v(L) = 0$$

By implementing these boundary conditions, the sine expression for the deflection can be assumed to look like this:

$$v(x) = \sin\left(\frac{\pi \cdot x}{L}\right)$$

This expression satisfies the two initial boundary conditions, but a physical factor is needed to make it applicable for the column in question. It is known that the displacement is largest at the middle of the beam; this gives a third boundary condition:

$$v\left(\frac{L}{2}\right) = \delta_{max}$$

$$X \cdot \sin\left(\frac{\pi \cdot \left(\frac{L}{2}\right)}{L}\right) = \delta_{max}$$

$$X \cdot 1 = \delta_{max}$$

The final expression for the deformed shape becomes:

$$v(x) = \delta_{max} \cdot \sin\left(\frac{\pi \cdot x}{L}\right)$$

Implementing the expression for moment-curvature relationship:

$$\frac{d^2v}{dx^2} = \frac{M}{EI}$$

$$M = EI \cdot v''(x)$$

Finding the derivative using the chain rule:

$$v(x) = \delta_{max} \cdot \sin\left(\frac{\pi \cdot x}{L}\right)$$

$$v'(x) = \frac{\delta_{max} \cdot \pi}{L} \cdot \cos\left(\frac{\pi \cdot x}{L}\right)$$

$$v''(x) = -\frac{\delta_{max} \cdot \pi^2}{L^2} \cdot \sin\left(\frac{\pi \cdot x}{L}\right)$$

The expression for the internal bending moment becomes:

$$M_{int} = -\frac{EI \cdot \delta_{max} \cdot \pi^2}{L^2} \cdot \sin\left(\frac{\pi \cdot x}{L}\right)$$

$$M_{int} = -\frac{EI \cdot \pi^2}{L^2} \cdot v(x)$$

The expression for the external bending moment is much simpler to determine, as it is a common force multiplied by arm expression:

$$M_{ext} = -P \cdot v(x)$$

$$M_{ext} = M_{int}$$

$$-P \cdot v(x) = -\frac{EI \cdot \pi^2}{L^2} \cdot v(x)$$

Removing the displacement expression from both sides of the equation:

$$P = \frac{\pi^2 \cdot EI}{L^2}$$

The exact same formula is obtained as the one Euler found with his more mathematical approach [12]. One of the reason why this “assumed deformed state” model is interesting is that it is very useful when looking at geometric imperfect columns.

2.4. Buckling of imperfect columns:

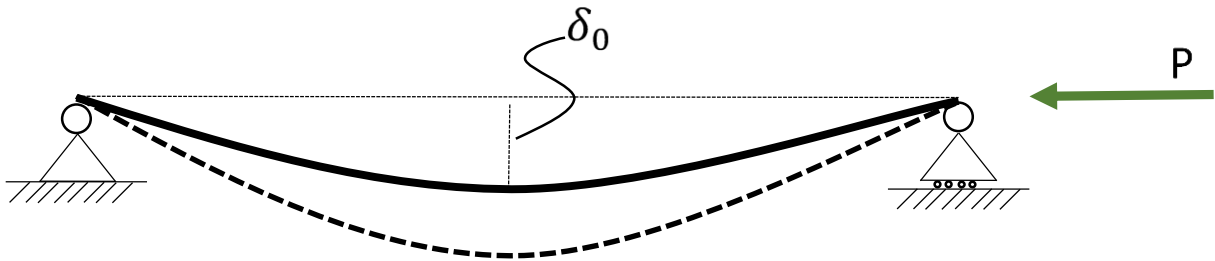


Figure 9: Buckling of imperfect column

The buckling of an imperfect column is similar to buckling of a perfect column, but the Euler critical load formula cannot be used to determine the maximum axial force the column can withstand. When loaded, an imperfect column will have a larger deflection than a perfectly straight column. This will lead to a reduction of the load carrying capacity. An expression for the total deflection of the column must be found in order to investigate how much of a load carrying capacity reduction is present. The expression for the total deflection can be found by using the new governing equilibrium equation [12]:

$$EI \cdot v''(x) + P \cdot v'(x) + P \cdot v_0(x) = 0$$

The form that $v_0(x)$ takes is already known from the previous example with the assumed deformation shape:

$$v_0(x) = \delta_0 \cdot \sin\left(\frac{\pi \cdot x}{L}\right)$$

Implementing this into the equilibrium equation gives the following differential equation:

$$EI \cdot v''(x) + P \cdot v(x) = -P \cdot \delta_0 \cdot \sin\left(\frac{\pi \cdot x}{L}\right)$$

The form of the homogenous solution is already known:

$$v_h = A \cdot \sin\left(\sqrt{\frac{P}{EI}} \cdot x\right) + B \cdot \cos\left(\sqrt{\frac{P}{EI}} \cdot x\right)$$

The particular solution is found by guessing the form and then substituting it into the original governing equilibrium equation:

$$v_p = \alpha \cdot \sin\left(\frac{\pi \cdot x}{L}\right)$$

$$v_p' = \frac{\alpha \cdot \pi}{L} \cdot \cos\left(\frac{\pi \cdot x}{L}\right)$$

$$v_p'' = -\frac{\alpha \cdot \pi^2}{L^2} \cdot \sin\left(\frac{\pi \cdot x}{L}\right)$$

$$EI \cdot \left(-\frac{\alpha \cdot \pi^2}{L^2} \cdot \sin\left(\frac{\pi \cdot x}{L}\right) \right) + P \cdot \left(\alpha \cdot \sin\left(\frac{\pi \cdot x}{L}\right) \right) = -P \cdot \delta_0 \cdot \sin\left(\frac{\pi \cdot x}{L}\right)$$

This equation is true for all values of x, but it is greatly simplified by implementing:

$$x = \frac{L}{2} \rightarrow \sin\left(\frac{\pi \cdot x}{L}\right) = 1$$

$$EI \cdot \left(-\frac{\alpha \cdot \pi^2}{L^2} \right) + P \cdot \alpha = -P \cdot \delta_0$$

This again can be simplified:

$$EI \cdot \left(\frac{\alpha \cdot \pi^2}{P \cdot L^2} \right) - \alpha = \delta_0$$

$$\alpha \cdot \left(\frac{EI \cdot \pi^2}{P \cdot L^2} - 1 \right) = \delta_0$$

$$\alpha = \frac{\delta_0}{\left(\frac{EI \cdot \pi^2}{P \cdot L^2} \right) - 1}$$

This must now be substituted back into the original particular solution:

$$v_p = \frac{\delta_0}{\left(\frac{EI \cdot \pi^2}{P \cdot L^2} \right) - 1} \cdot \sin\left(\frac{\pi \cdot x}{L}\right)$$

The solution to the differential equation becomes:

$$v(x) = v_h + v_p$$

$$v(x) = A \cdot \sin\left(\frac{\pi \cdot x}{L}\right) + B \cdot \cos\left(\frac{\pi \cdot x}{L}\right) + \frac{\delta_0}{\left(\frac{EI \cdot \pi^2}{P \cdot L^2} \right) - 1} \cdot \sin\left(\frac{\pi \cdot x}{L}\right)$$

Now the boundary conditions for a pinned column is introduced:

$$v(0) = 0 \text{ and } v(L) = 0$$

$$x = 0 \rightarrow B \cdot 1 = 0$$

$$B = 0$$

$$x = L \rightarrow A \cdot 0 + \frac{\delta_0}{\left(\frac{EI \cdot \pi^2}{P \cdot L^2} \right) - 1} \cdot 0 = 0$$

$$A = 0$$

With both coefficients equal to zero we are left with the particular solution only:

$$v(x) = \frac{\delta_0}{\left(\frac{EI \cdot \pi^2}{P \cdot L^2}\right) - 1} \cdot \sin\left(\frac{\pi \cdot x}{L}\right)$$

This equation can be simplified by recognizing known equations:

$$P_{cr} = \frac{\pi^2 \cdot EI}{L^2} \quad \text{and} \quad v_0(x) = \delta_0 \cdot \sin\left(\frac{\pi \cdot x}{L}\right)$$

$$v(x) = \frac{v_0(x)}{\frac{P_{cr}}{P} - 1}$$

The total deflection is then:

$$v(x) + v_0(x) = \frac{v_0(x)}{\frac{P_{cr}}{P} - 1} + v_0(x)$$

This can be simplified to the final expression for total deflection, δ :

$$\delta(x) = \frac{v_0(x)}{1 - \frac{P}{P_{cr}}}$$

This equation can be used to find the actual deformation in an imperfect pinned column, being loaded by applied force "P". It will also be important when the Perry-Robertson equation is derived.

2.5. Slenderness ratio

The term “slenderness-ratio” is quite important on the subject of buckling as it helps to classify if a column is considered long or short. As touched upon earlier a short column will most likely not fail by buckling, but a long column might buckle long before the critical load for the material is reached. The slenderness-ratio is defined as follows:

$$\lambda = \frac{k \cdot L}{r}$$

Where:

- λ = The slenderness ratio
- k = Effective length factor
- L = Length of the column
- r = Least radius of gyration

The effective length factor is included to account for different end support situations. The least radius of gyration is defined as:

$$r = \sqrt{\frac{I}{A}}$$

Where:

- I = The second moment of Area
- A = The cross-sectional area

The slenderness ratio is then compared with a “column constant”, which is based on material type, to determine if it shall be considered as a long or short column. When doing buckling calculations in both Eurocode 3 [2] and Eurocode 9 [1] a relative slenderness is used instead. The relative slenderness is in both standards defined as:

$$\bar{\lambda} = \sqrt{\frac{A_{eff} \cdot f_0}{N_{cr}}}$$

Where:

- A_{eff} = Effective cross-sectional area, this is depended on classification of cross-section.
- f_0 = Yield strength of material.
- N_{cr} = elastic critical force or Euler’s critical load.

This relative slenderness will vary depending on which type of buckling that is being considered.

2.6. Different methods of buckling

Failure by buckling can happen in many different ways and to both beams and shells/plates. The most well-known and common failure mode is flexural buckling, often referred to as Euler buckling, strut buckling or just buckling. Torsional buckling, flexural torsional buckling, lateral torsional buckling and plastic buckling are the other most common phenomenon that occurs, and these are known to most structural engineers. In some cases, long columns can even buckle with no other forces than gravity working on it. This phenomenon is known as self-buckling. Some of the buckling types are presented here:

2.6.1 Torsional buckling

Torsional buckling, as the name suggests, happens when a beam or bar is twisted around the longitudinal axis. This type of buckling may occur in members that have a torsional stiffness that is significantly smaller than the flexural stiffness [13]

2.6.2 Flexural torsional buckling

Flexural torsional buckling is a combination between flexural buckling and torsional buckling. Flexural torsional buckling can be very influential in cases where the sections are single symmetry or without symmetry. In these cases, the center of gravity is not in the same place as the shear center, which will lead to new torsional forces created in the cross-section. This occurrence is most prominent in shear loaded beams but can in some cases also occur under axial loading [8]. These forces give the beam/bar a lateral deflection and the cross-section will twist. The shear center will always be located on the axis of symmetry, so for a double symmetric cross-section the shear center will be located on the intersection between the two axes. If the material is homogenous, this will also be the location of the center of gravity. When the center of gravity and the shear center are located in the same spot, no torsional forces will arise in the cross-section. This is the reason why most double symmetric cross-sections are automatically approved where flexural torsional buckling is concerned.

Flexural torsional buckling is most common in members such as channels and structural trees. It is worth noting that due to the many different shapes extruded aluminium members can take, checking for flexural torsional buckling becomes extremely important.

2.6.3 Lateral torsional buckling

When a simply supported beam is loaded in flexure, or normal bending, there exists one compression flange and one tension flange. With large enough compression forces working on the compression flange, it is forced to move away from its original position, in a lateral direction [10]. At the same time, the tension flange tries to keep the member straight. The lateral movement of the compression flange creates restoring forces. These forces combined with the other forces working on the cross-section can cause the member to twist about its longitudinal axis. This means that when the compression flange buckles the cross-section will twist due to torsional forces and the outcome will be member failure due to lateral torsional buckling.

Lateral torsional buckling happens in unrestrained beams. An unrestrained beam is a beam where the compression flange can displace freely in the lateral direction and rotate freely. If a beam is susceptible to lateral torsional buckling steps can be taken to restrain the movement of the compression flange.

2.7. The Perry-Robertson equation

The Perry-Robertson formula has been the background for strut curves, or buckling curves, for many years and unbeknownst to many it is the cornerstone of column design in many countries [7]. The formula helps in determining the maximum stress an imperfect column can withstand. In this context, an imperfect column refers to an initially crooked column. Other imperfections such as residual stress is not accounted for in the formula. Some additional column qualities are assumed when using the formula, such as:

- The column is pinned
- The loading at the ends are perfectly centered
- No residual stress
- Material is linearly elastic
- Failure is assumed to happen when the central stress reaches yield stress levels.

These assumptions are often regarded as the formulas biggest flaws, as they are not realistic in most cases. However, a modified version is still used to find the buckling curves presented in standards such as Eurocode 3 and Eurocode 9.

Many different versions exists of the Perry-Robertson equation, the following will be used in the calculations within this thesis:

$$\sigma = \frac{\sigma_y + \sigma_E \cdot (\eta + 1) - \sqrt{(\sigma_y + \sigma_E \cdot (\eta + 1))^2 - 4 \cdot \sigma_y \cdot \sigma_E}}{2}$$

Where:

- σ = *working stress*
- σ_y = *yield stress*
- σ_E = *Euler stress*
- η = *Imperfection variable*

2.8. Deriving the Perry Robertson equation

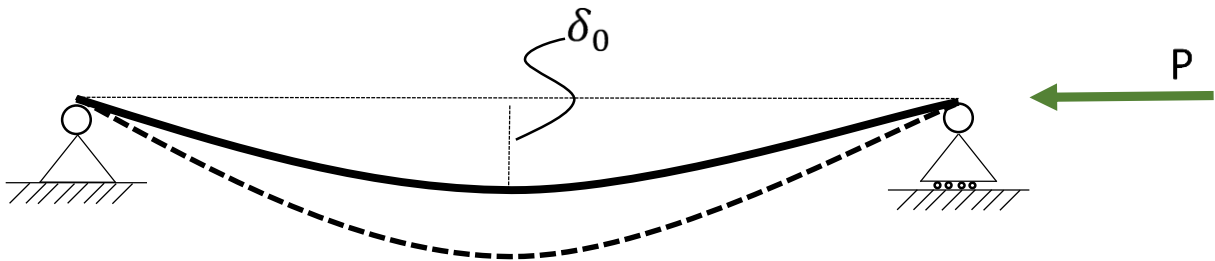


Figure 10: Buckling of imperfect beam

The starting point for deriving the Perry-Robertson formula is to investigate the maximum stress at the midspan of the column [7]. Because of the crooked shape, the maximum stress will be a result of both bending and compression stress. Both the equation for the initial shape and the total deflection were derived earlier and can be used:

$$v_0(x) = \delta_0 \cdot \sin\left(\frac{\pi \cdot x}{L}\right)$$

$$\delta = \frac{v(x)}{1 - \frac{P}{P_{cr}}}$$

The maximum bending moment will occur at the middle of the column, and so the expression for initial deflection is replaced with the actual deflection at the midspan. The moment will be equal to the force times the total deflection at the midspan. The equation becomes:

$$M = \delta \cdot P = \frac{\delta_0}{1 - \frac{P}{P_{cr}}} \cdot P$$

With both moment and axial force working on a member the maximum stress is given by the following equation [14]:

$$\sigma_{max} = \frac{P}{A} + \frac{M \cdot y}{I}$$

Where:

- P = Axial load
- A = Cross-section area
- M = Moment
- y = distance to the neutral axis
- I = Second moment of area

The next step is to introduce the expression for the moment and simplifying the equation with some known expressions for stress due to an axial load and the expression for the radius of gyration:

$$\sigma_{max} = \frac{P}{A} + \frac{\delta_0 \cdot y \cdot P}{\left(1 - \frac{P}{P_{cr}}\right) \cdot I}$$

$$\sigma = \frac{P}{A}$$

$$r^2 = \frac{I}{A}$$

$$\frac{P}{P_{cr}} = \frac{\sigma}{\sigma_E}$$

$$\sigma_{max} = \sigma + \frac{\delta_0 \cdot y \cdot P}{\left(1 - \frac{P}{P_{cr}}\right) \cdot r^2 \cdot A}$$

$$\sigma_{max} = \sigma + \frac{\delta_0 \cdot y \cdot \sigma}{\left(1 - \frac{P}{P_{cr}}\right) \cdot r^2}$$

$$\sigma_{max} = \sigma + \frac{\delta_0 \cdot y \cdot \sigma}{\left(1 - \frac{\sigma}{\sigma_E}\right) \cdot r^2}$$

Where σ_E is the stress associated with Euler's critical load.

At this point one of the assumptions made by Perry-Robertson is implemented, the assumption states that the maximum stress will be equal to the yield stress [7]:

$$\sigma_y = \sigma_{max}$$

$$\eta = \frac{\delta_0 \cdot y}{r^2}$$

$$\sigma_y = \sigma + \frac{\sigma}{\left(1 - \frac{\sigma}{\sigma_E}\right)} \cdot \eta$$

Simplifying the equation:

$$\sigma_y = \sigma + \frac{\sigma \cdot \eta}{\left(1 - \frac{\sigma}{\sigma_E}\right)}$$

$$\sigma \cdot \left(1 - \frac{\sigma}{\sigma_E}\right) + \sigma \cdot \eta - \sigma_y \cdot \left(1 - \frac{\sigma}{\sigma_E}\right) = 0$$

$$\sigma - \frac{\sigma^2}{\sigma_E} + \sigma \cdot \eta - \sigma_y - \frac{\sigma \cdot \sigma_y}{\sigma_E} = 0$$

$$-\sigma \cdot \sigma_E + \sigma^2 - \sigma \cdot \sigma_E \cdot \eta + \sigma_y \cdot \sigma_E - \sigma \cdot \sigma_y = 0$$

$$\sigma^2 - \sigma \cdot (\sigma_E + \sigma_E \cdot \eta + \sigma_y) + \sigma_y \cdot \sigma_E = 0$$

$$\sigma^2 - \sigma \cdot (\sigma_y + \sigma_E \cdot (\eta + 1)) + \sigma_y \cdot \sigma_E = 0$$

This second order equation is solved using the well-known quadratic expression:

$$a \cdot x^2 + b \cdot x + c = 0$$

$$x = \frac{-b \pm \sqrt{b^2 - 4 \cdot a \cdot c}}{2 \cdot a}$$

The answer becomes:

$$\sigma = \frac{\sigma_y + \sigma_E \cdot (\eta + 1) - \sqrt{(\sigma_y + \sigma_E \cdot (\eta + 1))^2 - 4 \cdot \sigma_y \cdot \sigma_E}}{2}$$

This is now the expression known as the Perry- Robertson equation. It is rather simple to derive and the effect of the imperfection has been contained in a single variable, eta. For plotting purposes, the expression can be further simplified by dividing each side with the yield stress, resulting in a stress ratio instead:

$$\frac{\sigma}{\sigma_y} = 0.5 \cdot \left(\left(1 + \frac{\sigma_E}{\sigma_y} \cdot (\eta + 1) \right) - \sqrt{\left(1 + \frac{\sigma_E}{\sigma_y} \cdot (\eta + 1) \right)^2 - 4 \cdot \frac{\sigma_E}{\sigma_y}} \right)$$

$$\frac{P}{P_y} = \frac{\sigma}{\sigma_y}$$

$$\eta = \frac{\delta_0 \cdot y}{r^2}$$

Where:

- P = Maximum axial load for an imperfect column.
- P_y = Axial load associated with yield stress.
- δ_0 = Initial imperfection at midspan.
- y = distance to neutral axis.
- r = radius of gyration.
- σ_E = Euler stress.
- σ_y = Yield stress.

Robertson suggested that the imperfection variable, eta, be set to 0.003 times the beams slenderness [7]. This value was based on tests and it represented an initial out-of-straightness imperfection that is greater than L/1000. Some allowance for residual stress is also included in this theoretical value as the crookedness is exaggerated.

In chapter 4, the Perry-Robertson equation is used to develop buckling curves for different values of an out-of-straightness imperfection. The imperfection variable suggested by Robertson is therefore not used, as it is only applicable for a set value of an out-of-straightness imperfection.

2.9. Eurocode 9 calculation method

To gain a better understanding of the effect that the out-of-straightness imperfections have on Eurocode 9 capacities, the capacities of a regular column must be known. The buckling calculations for aluminium member presented in Eurocode 9 is very similar to the guidelines given in Eurocode 3 for steel members. The same governing equations are used when determining the buckling curves but some of the factors that are used has different values. This is due to the fact that both methods are based on the Perry-Robertson equation.

When a member is subjected to axial compression only, three different design checks has to be made. These are the compression resistance, flexural buckling resistance and torsional-flexural buckling resistance.

The compression resistance is determined by the yield stress of the material and the area of the cross-section, with the inclusion of a safety factor. For a cross-section without any unfilled holes, the following equation is used:

Equation 6.22 [1]

$$N_{C_{Rd}} = \frac{A_{eff} \cdot f_0}{\gamma_{M1}}$$

Where:

- $N_{C_{Rd}}$ = design compression resistance
- A_{eff} = effective area
- f_0 = yield stress
- γ_{M1} = material safety factor

The equation for determining the flexural buckling resistance is very similar:

Equation 6.49 [1]

$$N_{b_{Rd}} = \frac{\kappa \cdot \chi \cdot A_{eff} \cdot f_0}{\gamma_{M1}}$$

Where

- κ = reduction factor allowing for the weakening affect of welding
- χ = reduction factor based on the relevant buckling mode

If it is assumed that no welding has been done, the only difference between the compression resistance and the flexural buckling resistance is then the buckling reduction factor. This buckling reduction factor will therefore be very similar to the maximum stress ratio found when using the Perry-Robertson equation. When the reduction factor is equal to 1 the column will fail in compression, or in other words failure by crushing. If the reduction factor is less than 1, the column will fail by flexural buckling. This is also true for the Perry-Robertson stress ratio. Detailed Eurocode 9 column calculations are performed in Appendix B and presented in chapter 4. The torsional-flexural buckling resistance is not calculated, as this failure type is not considered in the Perry-Robertson equation.

Eurocode 9 also has a dedicated chapter on the subject of imperfections, in case the production tolerance is exceeded. It begins with an important notice:

“Note Geometrical imperfections equal or less than the fundamental geometrical tolerances given in prEN 1090-3 are considered in the resistance formulae, the buckling curves and the γ_m -valued in EN 1999” [1]

Which mean that when doing calculations on a column in accordance with Eurocode 9, it is in practice an imperfect beam that is being considered. This is done as a safety measure and it is the reason that NS-EN 1090-3 automatically approves imperfections lower than its permitted deviation [3]:

$$\delta = \frac{L}{750}$$

As presented earlier this is the permitted deviation given in NS-EN 1090-3, and therefore also the assumed crookedness of the majority of aluminium beams and columns calculated in accordance with Eurocode 9. As touched upon in a previous section the straightness of an extruded aluminium profile is impressive, with some tests finding the average value of the out-of-straightness imperfection to be $L/2000$ [8]. Which means that the calculations according to Eurocode assumes that the imperfection is almost three times larger than the actual average. It is also important to note that these tests were carried out around thirty years ago and production and manufacturing might have improved since then. Rolling, on the other hand, does not yield equally impressive straightness due mostly to the less severe traction process when compared to extruding. Aluminium is also still considered a new structural material, at least when compared to steel, and its behavior is less known than that of steel. This may result in a higher required safety factor.

In the case of a known geometrical imperfection that is larger than the permitted deviation, the Eurocode gives certain guidelines on how these should be handled. In the case of a column with an out-of-straightness imperfection, the situation is simplified by replacing the imperfection with equivalent horizontal forces [1]. These forces are then added to all design calculations for the column. This is not a perfect way to represent the effect of an actual imperfection, but it does offer an alternative method of calculation. A graphical representation of the equivalent horizontal forces is shown in Figure 11. For the out-of-straightness imperfection, or bow imperfection as it is referred to in Eurocode 9, the imperfection is replaced by horizontal forces. These horizontal forces are given as a product of the axial loading and will cause a bending moment to arise in the column. This bending moment will cause a deformation in the column that is similar to the out-of-straightness imperfection.

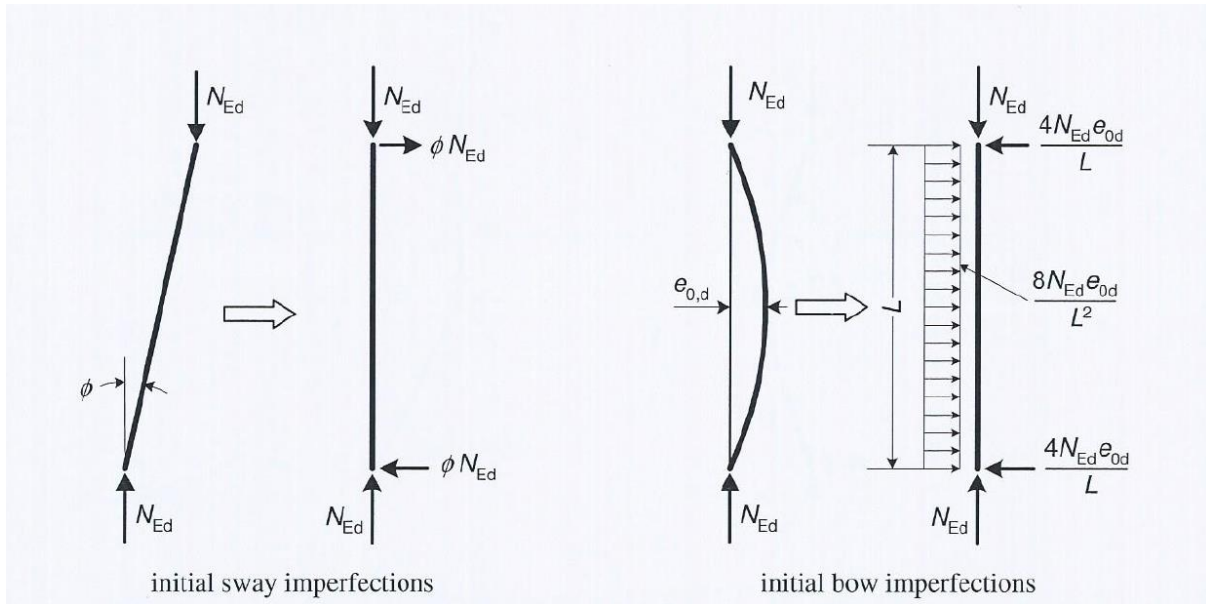


Figure 11: Eurocode 9, equivalent horizontal forces [1]

Out-of-straightness imperfections are not the only imperfection that can be simplified. Initial sway imperfections can also be described by equivalent horizontal forces. Calculations using the equivalent horizontal forces method for a column with an out-of-straightness imperfection is performed in Appendix C and presented in chapter 4. The exact same method for simplifying imperfection calculations is also presented in Eurocode 3 [2].

Chapter 3

3. Previous works

The subject of buckling is very large and papers on the subject are regularly being published. With the large array of different buckling failure modes, different structural elements susceptible to buckling and the different types of material, there is no wonder that new theories and methods are discovered every year. In this chapter, some of the newest findings concerning flexural buckling of columns will be presented and discussed.

3.1. A new design method for stainless steel columns subjected to flexural buckling

In 2014, a paper called “*A new design method for stainless steel columns subjected to flexural buckling*” [4] was written by Ganping Shu, Baofeng Zheng and Lianchun Xin. Their goal was to investigate and possibly improve the method for finding the buckling strength curve for stainless steel members. The present method used by many design codes for finding this strength curve is based on low carbon steel. There are large differences between low carbon steel and stainless steel in material properties. One of the main differences between the two materials is found in the stress-strain curve, and so the materials have different properties in the plastic region. There are also some large differences in material properties found between the different varieties of stainless steel. Different grades of low carbon steel behave more similar to each other, but with different yield stresses. With the goal of making strength curves that are suitable for stainless steel, both gradual yielding and a wide array of mechanical properties must be taken into consideration.

The Perry-type formula for buckling curves presented in Eurocode 3 [2] does not consider different material properties. Five buckling curves are presented in Eurocode 3, which buckling curve that should be used is dependent on cross-section geometry and material grade. However, while there are a choice between several different cross-section geometries only two grades of material strength is presented. A modified Perry formula was presented in 1997, by Rasmussen and Rondal [11]. In this formula, the imperfect parameters were expressed by using the Ramberg-Osgood material model. The Ramberg-Osgood material model is used to express non-linearity in the stress-strain curve. With this modification of the Perry equation, material properties was taken into consideration and method was found to be very accurate.

The proposed method of creating new strength curves related to flexural buckling, by Shu, Zheng and Xin, was based on using the relationship between two known strength curves for different types of stainless steel. It is shown that by using two known strength curves and a slenderness conversion formula, a series of strength curves for different stainless steels can be generated. It is also shown that by using a larger number of known strength curves, a higher accuracy can be achieved. The strength curves that were generated in the paper are suitable for hollow sections with no residual stress and an initial out-of-straightness imperfection equal to $L/1000$.

The resulting strength curves were validated with a finite element analysis using ANSYS, which showed very accurate predictions. When the finite element results were compared to the predictions of the current Eurocode 3 design method, it was revealed that the strength curve used by Eurocode was suitable for high strength stainless steel columns, but not for columns with low proof strength.

4.2. Stability of 6082-T6 aluminium alloy column with H-section and rectangular hollow sections

In 2014, a paper named “*Stability of 6082-T6 aluminium alloy columns with H-section and rectangular hollow sections*” [5] was written by Guy Oyeniran Adeoti, Feng Fan, Yujin Wang and Ximei Zhai. The goal of the paper was to present a column curve formula that could accurately predict the strength of an extruded column failing by flexural buckling. The paper contains an experimental study comprised of fifteen H-sections and fifteen hollow sections of 6082-T6 aluminium alloy. With the use of ANSYS, an analysis of the mechanical and overall buckling of the columns was performed. This analysis considered both geometrical and material non-linear behavior. The materials stress-strain relationship was described by the Ramberg-Osgood equation in this paper as well.

The effect of an initial out-of-straightness imperfection was simplified to be a half sine curve, as is common practice. The imperfections were measured by stretching a metal string between two ends of the sections. However, the imperfections proved to be so small that they were impossible to detect without expensive equipment. Even though the authors of the paper could not detect any imperfections, it was decided that a small imperfection of $L/7500$ should be used in the numerical analysis. This addition of an imperfection is necessary in the numerical analysis as an industrial bar is never perfectly straight, and the analysis would not reflect the real world if the imperfection was entirely neglected. Since all the section were extruded, residual stress could be ignored.

With the test results showing good agreement with the results from the numerical analysis, a calibration of the parameters of the Perry-Robertson formula was proposed:

$$\phi = \left(\frac{1}{2 \cdot \bar{\lambda}^2} \right) \cdot \left((1 + \eta + \bar{\lambda}^2) - \sqrt{(1 + \eta + \bar{\lambda}^2)^2 - 4 \cdot \bar{\lambda}^2} \right) \leq 1.0$$

$$\eta = \alpha \cdot (\bar{\lambda} - \bar{\lambda}_0)$$

Where:

- ϕ = non dimensional column strength
- $\bar{\lambda}$ = non dimensional column slenderness
- η = non dimensional imperfection parameter

This new proposed column curve formula show a larger column strength than Eurocode 9. Which is not surprising when considering the low imperfection value that was used. However, the new proposed column curve also showed very good agreement with both the buckling results of the actual columns that were tested and the finite element analysis.

Chapter 4

4. Calculations of imperfect columns

In this chapter, the results of the Perry-Robertson calculations will be presented and discussed. The calculations are shown in Appendix D. The calculations has been done for different cross-sections and different values for the out-of-straightness imperfection. The Perry-Robertson equation is also used to evaluate the strength of a perfectly straight column. This is done in order to see the difference in load carrying capacity between an imperfect column and a perfect column. The out of straightness production tolerance limit, given by NS-EN 1090-3, is also considered. An ANSYS finite element analysis is presented in order to validate the results from these Perry-Robertson calculations. Eurocode 9 flexural buckling resistance calculations are also performed and presented in order to gain a better understanding of how the out-of-straightness imperfection will affect the capacities. These calculations are presented in Appendix B.

4.1. Buckling curve of an imperfect quadratic hollow section column

To gain a better understanding of the effect that the out-of-straightness imperfection actually has on a column, the Perry-Robertson equation, derived in chapter 2.8, can be very useful. The equation can be used to create buckling curves, which gives a very good indication of how much the load capacity is affected by the length. It also takes the effect of an out-of-straightness imperfection into account. To illustrate this, a pinned column will be presented. The column is made from 6082-T6 aluminium, which has a yield stress of 250 MPa. The cross-section is a 200x10 mm quadratic hollow section, an ideal choice with buckling calculations, as there are no weak or strong axis.

The general cross-section calculations are presented in Appendix A.1.

The column will have a constant initial out-of-straightness imperfection of 10 mm and the length will vary from 0 to 25 m. The choice of this length interval is purely done for illustrative purposes, so that the effect of the imperfection is clear. A pinned column with a length of 25 m and without any extra support is of course not likely to be built. With this version of the Perry-Robertson equation, the results will be given as a ratio of the actual stress in the column to the yield stress of the material. When plotting the results the effective length will be on the x-axis. Note that for this pinned column situation the effective length is equal to the actual length. The resulting buckling curve for this situation is presented in Figure 13:

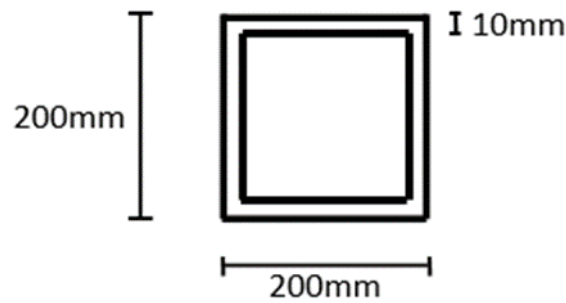


Figure 12: 200x10 mm quadratic hollow section

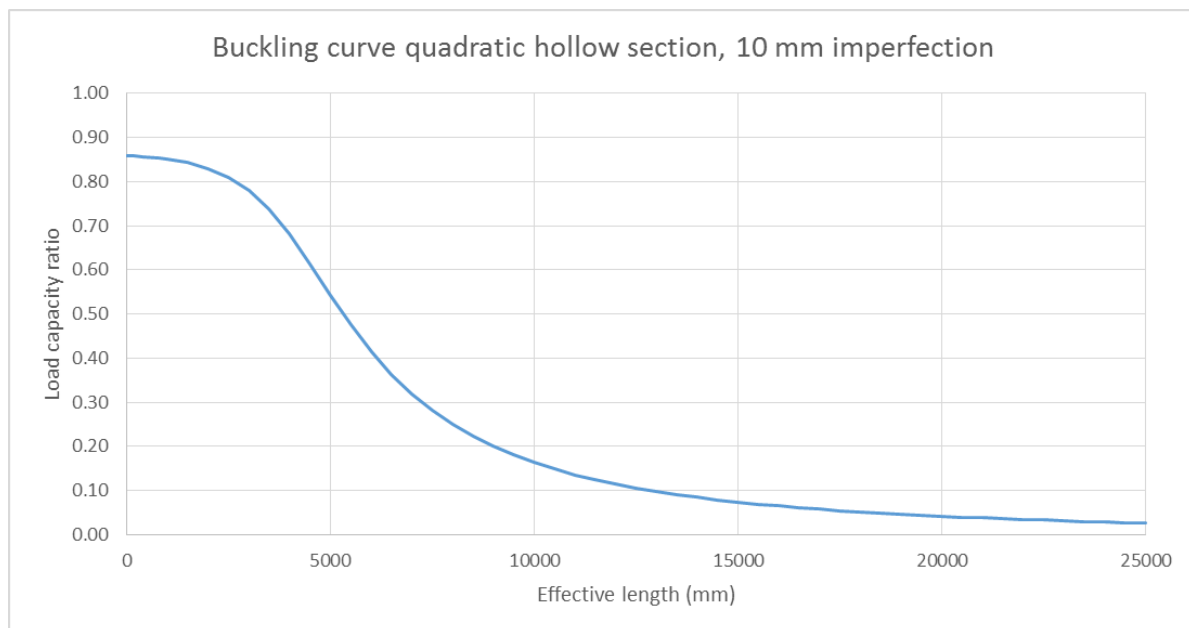


Figure 13: Buckling curve, 10 mm imperfection

As expected, this buckling curve bears some resemblance to the buckling curves found the Eurocode 3 and 9, although those curves are presented with relative slenderness on the x-axis. A clear loss of load capacity is shown as the length of the column increases and it is interesting to note that according to these calculations, the column will never fail by crushing, as the experienced stress does not reach yield stress levels even at the smaller lengths.

For comparison, the same column will also be presented without an initial imperfection. The calculations are done in the same manner as for the imperfect column. The resulting graph is given in Figure 14:

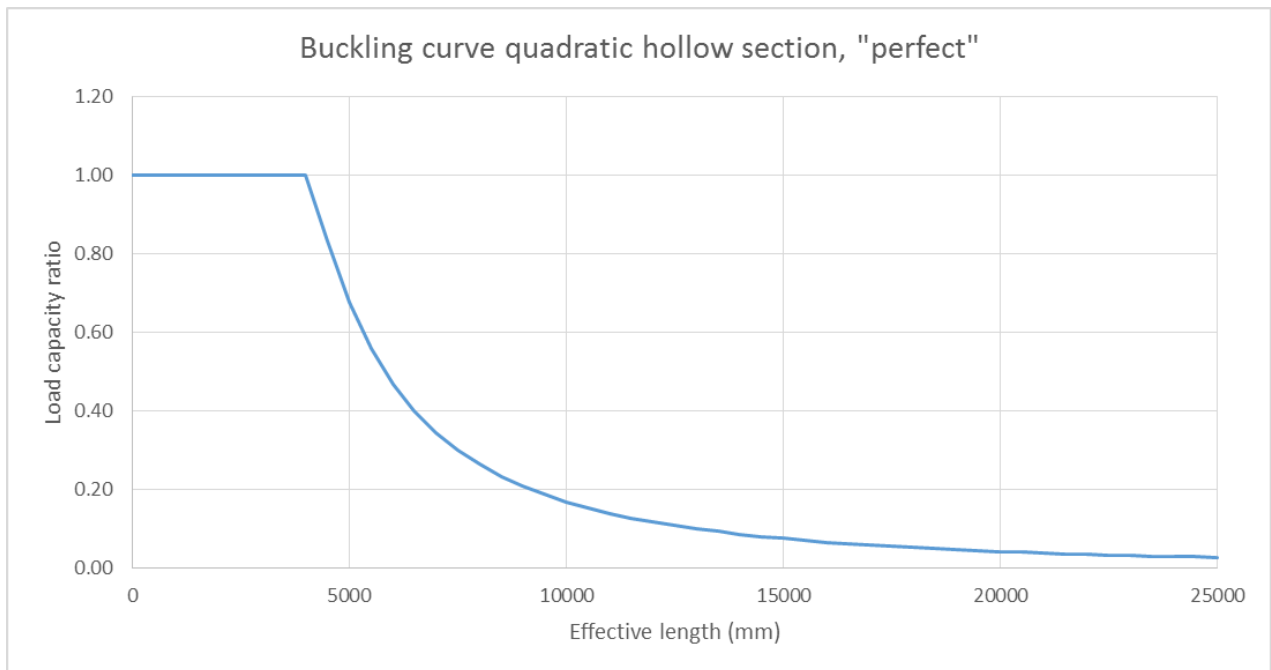


Figure 14: Buckling curve, no imperfection

In this case, a very distinct horizontal plateau can be seen at small column lengths. In this region, the actual stress experienced by the column reaches yield stress levels and the column will fail by crushing, if the load is sufficient. The transition between failure by crushing and failure by buckling is not as clean as the one shown from these results for an actual column. In the transition area where the maximum stress goes from yield stress (plastic behavior) to Euler stress (elastic behavior), the column will fail by inelastic buckling [12]. This phenomenon is not considered in the Perry-Robertson equation. When the length has increased beyond this horizontal plateau, a rapid decrease in capacity is shown. For a better comparison between the two buckling curves, they are plotted together in Figure 15.

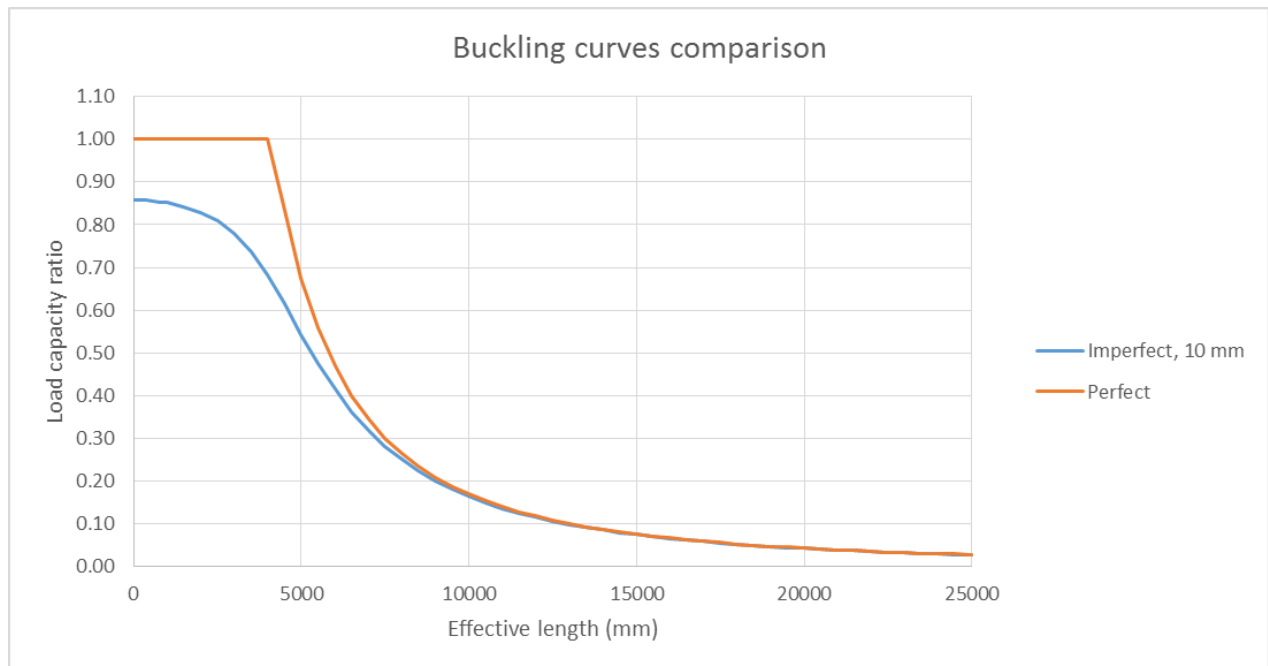


Figure 15: Buckling curve comparison, 10 mm imperfection and no imperfection

With this side-by-side comparison, some large differences between the two curves can be seen. The largest difference in load capacity can be found where the horizontal plateau of the perfect beam ends. At this point, the perfect beam will fail by crushing and therefore utilize its full load capacity, at the same length the imperfect beam can only utilize about 68% of its elastic load capacity before it fails by flexural buckling. A loss of about a third of its capacity can be devastating, if the situation is unforeseen and the column is supposed to be loaded close to its maximum. This situation occurs when the column approaches 4 m and so a 10 mm imperfection can very easily be missed.

At larger lengths, the initial deformation does not seem to have any major effect on the load capacity as the two curves converge. After the end of the horizontal plateau of the perfect column the difference between the two curves becomes smaller and smaller. Which indicates that the initial deformation has its largest effect on short columns that are not expected to fail by flexural buckling.

4.2. NS-EN 1090-3: Permitted deviation

Now that actual buckling curves have been produced using the Perry-Robertson equation it will be interesting to look at the permitted deviation for an out-of-straightness imperfection as listed in NS-EN 1090-3 [3]:

$$\delta \leq \frac{L}{750}$$

A 10 mm imperfection was used in the example, which means that if the column is longer than 7500 mm it is automatically accepted by the NS-EN 1090-3 standard. Assuming of course that the column is approved by the regular Eurocode 9 strength calculations. Below is the same graph as before but with an added tolerance line at 7500 mm, an effective length larger than 7500 mm will be approved. This means that everything to the right of the tolerance line is accepted.

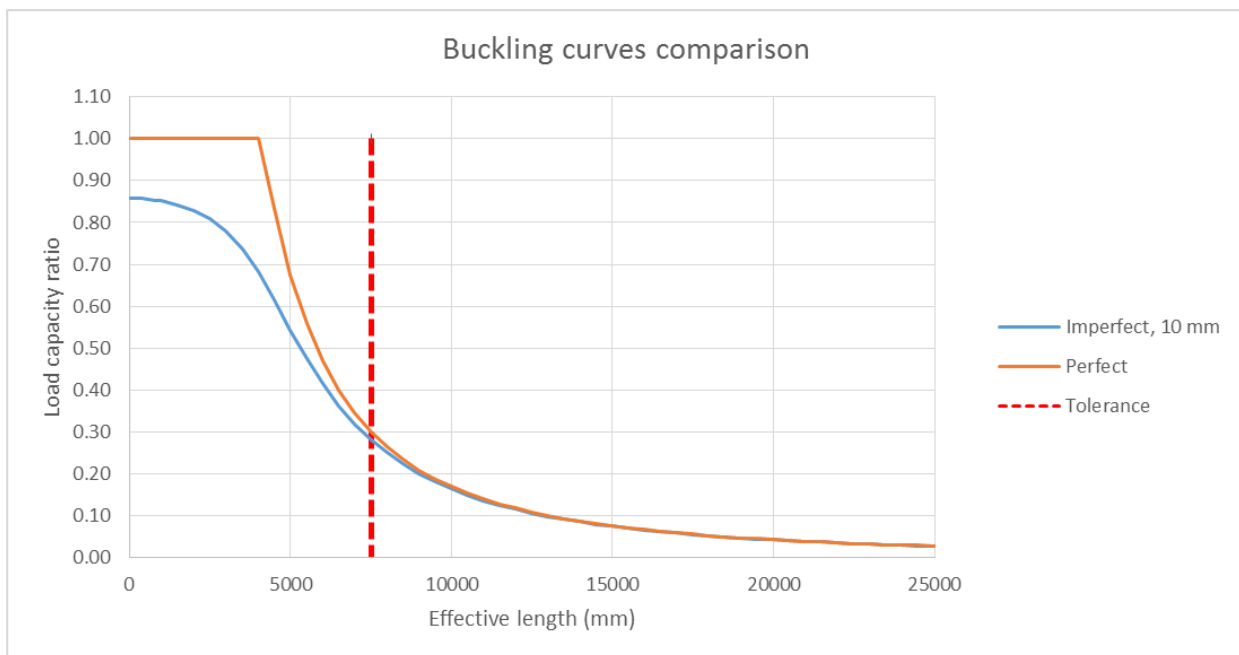


Figure 16: Buckling curve comparison with tolerance line, 10 mm imperfection

As can be seen from the graph the tolerance line seems to be situated perfectly. The area with the highest difference between perfect and imperfect buckling curve is to the left of the line and therefore not accepted. In the area where the tolerance line crosses the curves, the difference is very small and becomes even smaller with larger lengths. With this first test, it must be concluded that the permitted deviation seems very appropriate. To investigate further different values of imperfection will be tested. An imperfection of 15 mm on the same cross-section will be calculated, using the exact same procedure. An imperfection of 15 mm will place the tolerance line at 11250 mm. The results are plotted in the next graph:

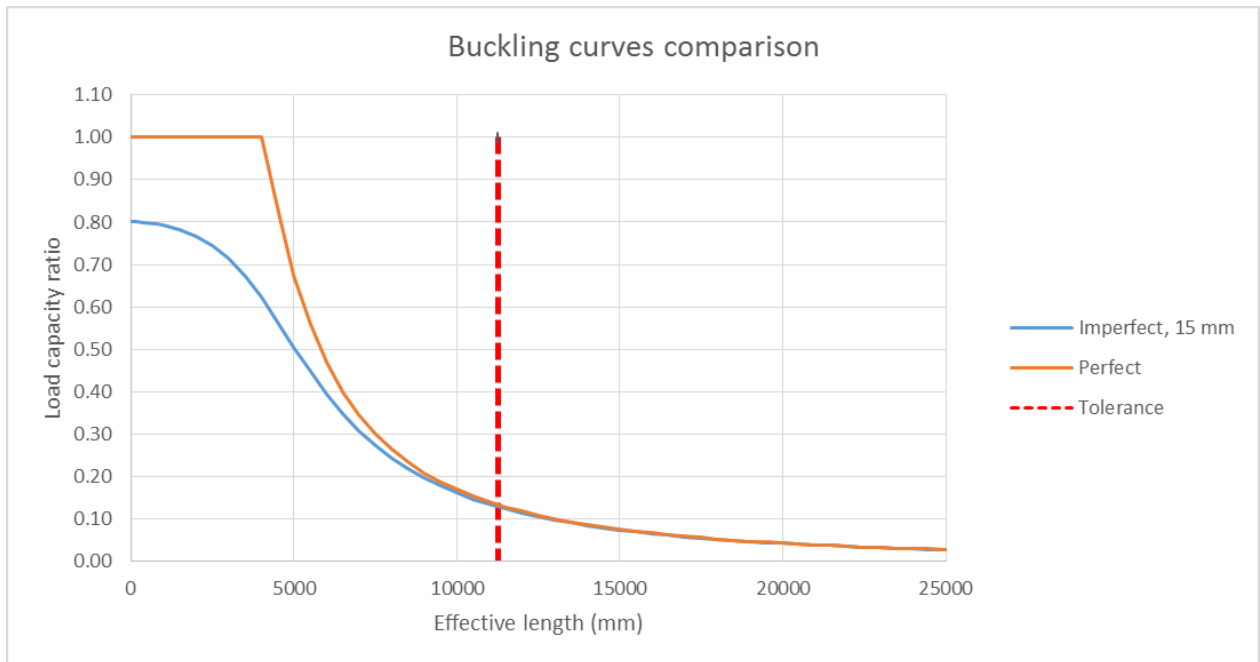


Figure 17: Buckling curve comparison with tolerance line, 15 mm imperfection

This graph and the earlier graph for the 10 mm imperfection are very similar. The shape of the “imperfect” curve is almost identical, but now at lower capacity values. In the accepted area, to the right of the tolerance line, the difference between the perfect and imperfect curves are negligible, further strengthening the guidelines given by NS-EN 1090-3.

The same calculations are performed once more, but now with the smaller imperfection of 5 mm. The corresponding tolerance line will be placed at 3750 mm.

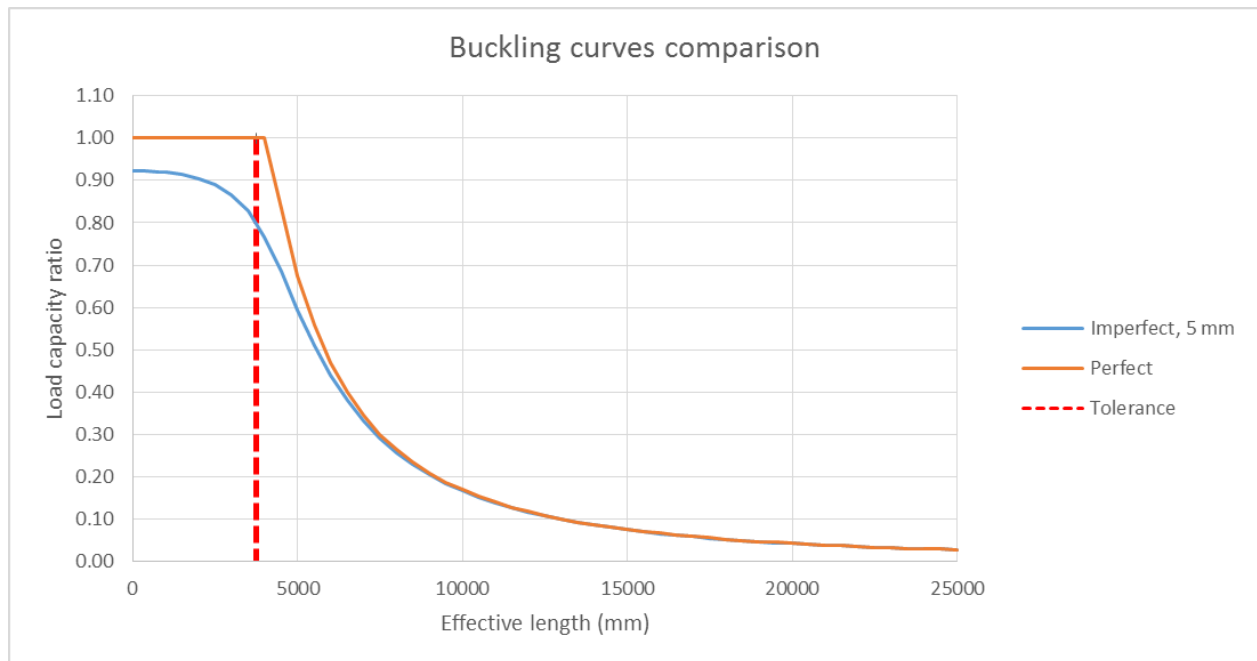


Figure 18: Buckling curve comparison with tolerance line, 5 mm imperfection

In this case, the tolerance line actually intersects with the horizontal plateau of the perfect column. With this smaller imperfection, the imperfect column has a higher load capacity ratio, but the largest loss of capacity compared to the perfect column is still at approximately 4000 m. This area is now in the accepted region and shows that the imperfect column can only withstand 83% of the yield stress before buckling.

It seems that the smaller imperfections are harder for the permitted deviation guideline to handle than larger ones. This can be seen by comparing the three graphs for 5, 10 and 15 mm imperfection. The changes for the imperfect curves are not as dramatic as the changes in the tolerance line, as they retain almost the same shape only at different values. At larger lengths there are almost no difference between the three curves at all.

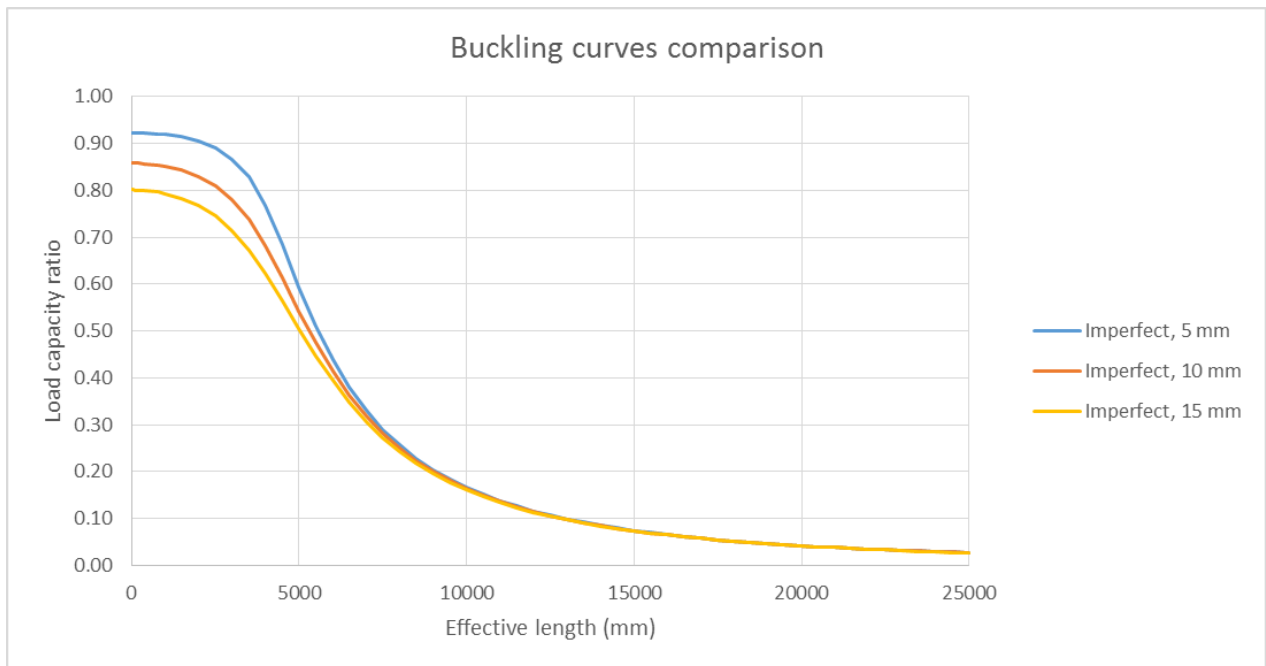


Figure 19: Buckling curve comparison, varying imperfections

One of the reasons that even the small imperfections seems to be so impactful is that it “kick starts” the buckling process. When the column is slightly crooked it is much easier for it to buckle than when it is perfectly straight. As was shown when the Perry-Robertson equation was derived, the crooked shape of an imperfect column under axial loading will cause moment forces to arise in the column. With an initial deformation these moment forces become dominant and forces the column to bend and buckle. This can also be seen from the graph since none of the curves reaches a full load capacity, meaning that they all fail by buckling. In Figure 19, the different imperfections are plotted in the same graph. The size of the imperfection is much more important for small columns. At the larger lengths the flexural buckling resistance of the column is so low that the size of the imperfection hardly matters.

Since the buckling curve for a column with a 5 mm imperfection gave reason to question the guideline from NS-EN 1090-3, the situation will be investigated further.

4.3. Assumptions in the Perry-Robertson equation

To gain a better understanding of the results, the assumptions behind the calculations must be discussed. The assumptions were as follows:

- The column is pinned
- The loading at the ends are perfectly centered
- No residual stress
- Material is linearly elastic
- Failure is assumed to happen when the central stress reaches yield stress levels.

4.3.1. The column is pinned

A pinned column is most likely not the preferred method of supporting a column in real structures. In the calculations the support situation directly affect the effective buckling length. This is due to the deformations shape of the column that the different supports yield when subjected to axial compression. As seen in chapter 2.2 a table is usually used when deciding the effective length factor. For a pinned column the effective length factor is equal to 1, which means that the entire length of the column is considered to be the effective buckling length. By choosing more restraining end supports, such as fixed supports, the effective length factor will be smaller. This will lead to a smaller effective buckling length and a larger load capacity. The effective buckling length is the same for the imperfect and perfect column and it is therefore assumed that the difference seen between them is the same. The pinned situation is chosen because it was the foundation for deriving the Perry-Robertson equation and should in theory give the best results.

4.3.2. The loading at the ends are perfectly centered

This assumption is made to in order to achieve pure buckling and is not realistically achievable. With an eccentricity in the loading the column will experience a bending moment as well, which is not wanted in this simulation. When using this assumption in the calculations the results will be a kind of best-case scenario, since the additional load will cause the column to fail at an earlier stage. This is especially true when combined with an already imperfect column.

The deformation shape of an eccentrically loaded column is very similar to the initial shape of an imperfect column (out-of-straightness imperfection). As the loading is increased, the deflection at the midspan will grow until the column fails. There might exist some scenarios where the eccentricity of the loading will be favorable, as it can counteract the effect of an imperfection to a certain degree. This would require that the loading try to deform the column in the opposite direction of the initial imperfection. This scenario is not very probable and would likely not be intentional from a structural perspective.

4.3.3. No residual stress

The assumption that the column carries no residual stress is done in order to simplify the calculations. Most residual stress cases will lower the maximum capacity of the column. Similar to the load eccentricity discussion, the result when using this assumption will yield the least difference between the perfect and imperfect column. In this example, the effect of the out-of-straightness imperfection is studied. The assumption of no residual stress is therefore acceptable.

4.3.4. Linearly elastic material and failure at yield stress levels

That the material used is linearly elastic is a common assumption to make when doing structural analysis, as calculations are greatly simplified. While doing calculations with a linearly elastic material the stress can never exceed the yield stress levels, hence it is assumed that the material fails when yield stress levels are reached. This is a very conservative assumption to make as the plastic region is ignored and effects such as strain hardening is neglected. When using these assumptions the results can be regarded as being conservative.

With all these assumptions in place, it is highly unlikely that the answer will be true to life. In order to get a better results a modification has to be added to the Perry-type formula as is done in both the “A new design method for stainless steel columns subjected to flexural buckling” [4] and “Stability of 6082-T6 aluminium alloy columns with H-section and rectangular hollow sections” [5] papers, which were discussed in chapter 3. Both of these papers implemented the Ramberg-Osgood parameters for material properties. The Ramberg-Osgood equation is used to describe the stress-strain relationship of a material. It is also used to show how a specific material will behave near its yield stress levels. This method also takes the effect of strain hardening into account. The Ramberg-Osgood equation or law, as it is sometimes called, is now widely used because its predicted behavior is very close to the actual behavior of different aluminium alloys [8] and stainless steels. With these extra parameters, the assumption that the material has to be linearly elastic needs no longer apply. This will result in far more accurate buckling curves, as they are now directly dependent on the material in question.

However, while doing ultimate limit state calculations no plastic deformations are allowed. This means that only the elastic region is utilized. With the objective of the calculations being to see the effect that the imperfection has on capacities from Eurocode 9, the same failure criteria should be used. With this in mind, it seem appropriate that failure is assumed at yield stress levels or when the column becomes unstable.

4.4. ANSYS analysis

Since the Perry-Robertson equation is a simplified method it is important to validate the calculations. A validation of the results can be achieved in many ways, such as a finite element analysis or by conducting actual experiments. A finite element analysis was carried out at Marine Aluminium. The model and results will be presented and compared with the results from the Perry-Robertson equation in order to find out if the method is acceptable.

Multiple models was made of the 200x10 mm quadratic hollow section with a 10 mm out-of-straightness imperfection. The models had varying lengths ranging from 1000 mm to 15000 mm. These columns were loaded until failure by buckling. The maximum stress at the point where the column became unstable is extracted. These results will then be directly comparable to the stress-ratios obtained by the Perry-Robertson calculations.

4.4.1. ANSYS model

All the column models were drawn in Autocad Inventor and then imported to ANSYS for the analysis. The models were drawn with the out-of-straightness imperfection at the midspan. One of these models is shown in Figure 20. The imperfection at the midspan is almost unnoticeable. One complication with the analysis was to create the supports. The original calculations were done for a pinned column. The main reason that the pinned situation was chosen was that the Perry-Robertson equation was derived from the deformation shape of a pinned column, as is shown in chapter 2.8. For a pinned vertical column, the two supports are restrained from horizontal movement and one of the supports are restrained from vertical movement as well. It is also important that each end is free to rotate. In order to create the best possible representation of these end support conditions in the model, some changes had to be implemented. In order to achieve free rotation at the end supports a hole was cut through the cross-section at each end. These holes then became the rotation centers by selecting that the edges of the holes is free to rotate. At the top end, a cylindrical bolt is inserted into the hole and the axial point load is applied on the middle of this bolt. At the lower end only the top half of the edge of the hole was able to freely rotate and the bottom half was restricted from any movement. The configuration is believed to satisfactory represent a pinned situation. The actual length of the beam is measured from center hole to center hole. By applying the axial load to the bolt, a realistic distribution of the load is believed to occur. In the Perry-Robertson equation, one of the assumptions is that the load is applied at the center of the cross-section. This is not possible for the quadratic hollow section. A uniformly distributed load could

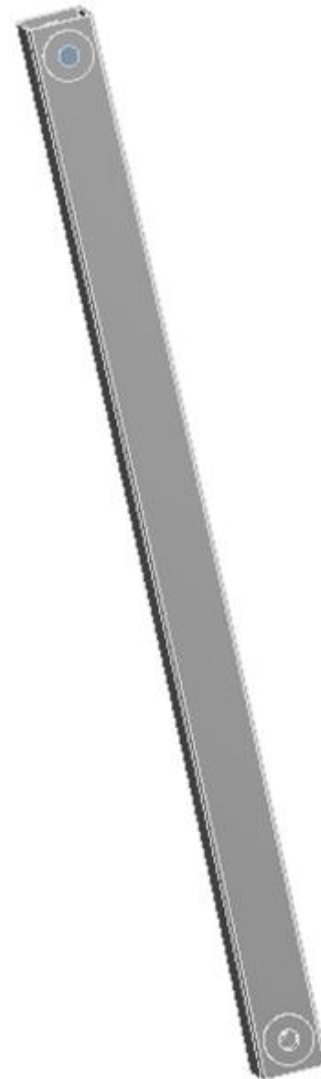


Figure 20: Imperfect column model

have been applied to the edges, but it was assumed that the solution with the bolt was the best method.

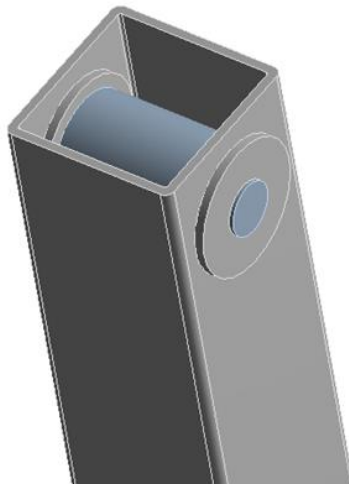


Figure 21: Top end support

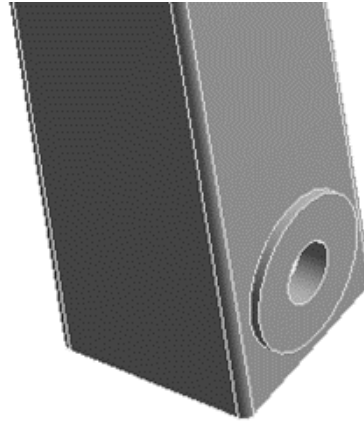


Figure 22: Bottom end support

The goal of the analysis was to decide the maximum axial load that the column could withstand. The axial load was therefore increased in intervals. With an increasing load, the deformation of the column became increasingly larger. At a certain point the load that was required to deform the column further decreased. The peak axial force was extracted and converted into experienced stress.

In the analysis, the stress-strain relationship was described as bilinear. This differs from the Perry-Robertson calculation, as a linear stress-strain relationship was one of the assumptions for the equation. A bilinear stress-strain relationship is used to simplify the actual stress-strain relationship of a material. It uses the regular modulus of elasticity to describe the elastic region and a tangent modulus to describe the plastic region [8]. Most materials are able to withstand more load in the plastic region before ultimate failure occurs. It is therefore suspected that the load capacity ratio found in this analysis will be larger than those found using the Perry-Robertson equation.

The value of the modulus of elasticity was chosen to be 71000 MPa, as it is in the Perry-Robertson equation. The recommended tangent modulus value is sometimes given as:

$$E_T = \frac{E}{100} = 710 \text{ MPa}$$

In the analysis a tangent modulus equal to 500 MPa was chosen, this is believed to be conservative.

4.4.2. Analysis results

With the analysis being run for six different length, an interesting pattern appeared. For columns with a length equal to or less than 3000 mm the failure did not occur at the midspan of the beam. The buckling failure occurred much closer to the lower support. Although this was unexpected, it might be caused by small errors in the modeling of the end supports. Presumably, the failure could also occur closer to the top support. The deformation shape of the longer columns was as expected with buckling occurring at the midspan. The deflection associated with the maximum load was also a lot larger in the longer and more slender columns. This is a good indicator of their more elastic capabilities compared with the short columns. This was also shown with the actual buckling deformation, as the damage to the cross-section was more apparent in the smaller cross-sections.

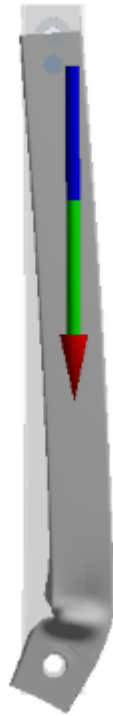


Figure 23: Buckling deformation, $L = 2000$ mm



Figure 24: Buckling deformation, $L = 5000$ mm

It is also interesting to note that all of the columns failed by flexural buckling. Although the deformation of the smaller columns that were analyzed showed some similarities to failure by crushing, it was definitely a case of buckling failure. It seems that it is almost impossible for a column with an out-of-straightness imperfection to fail by crushing. This was also shown by the Perry-Robertson calculations. It should be noted that the 10 mm imperfection could be considered rather large on a column that is 1 meter long. It is also important to note that the deformation occurred in the same direction as the initial imperfection.

The maximum stress at the point where the column became unstable, for all the six columns tested, is tabulated below:

Table 2: ANSYS analysis results

Length of column	Maximum stress at failure
1000 mm	232.5 MPa
2000 mm	232.5 MPa
3000 mm	230 MPa
5000 mm	155 MPa
10000 mm	47.5 MPa
15000 mm	22.5 MPa

These results strengthen the conclusion drawn from the deformation shapes. It is shown that not one of the columns will fail by crushing, as the yield stress is never achieved. The results obtained from the Perry-Robertson equation were presented as a ratio of the yield stress. The yield stress has a value of 250 MPa due to the selection of aluminium alloy. When comparing the different results it is therefore advantageous to list the ANSYS results as stress-ratios as well, this is done in Table 3:

Table 3: ANSYS and Perry-Robertson stress ratio comparison

Length	ANSYS stress ratio	Perry-Robertson stress ratio
1000 mm	0.93	0.86
2000 mm	0.93	0.83
3000 mm	0.92	0.78
5000 mm	0.62	0.54
10000 mm	0.19	0.16
15000 mm	0.09	0.07

As can be seen from these results, the Perry-Robertson calculations seems to be more conservative when compared to the more “real” results from ANSYS. This is expected as the Perry-Robertson equation is a simplified method.

The results can be more easily compared by using the existing graph for the Perry-Robertson results. Please note that due to the limited number of known points for the ANSYS results, a perfect graphical representation cannot be made. However, by drawing a straight line between the known points an idea of the shape that the real buckling curve would take can be formed.

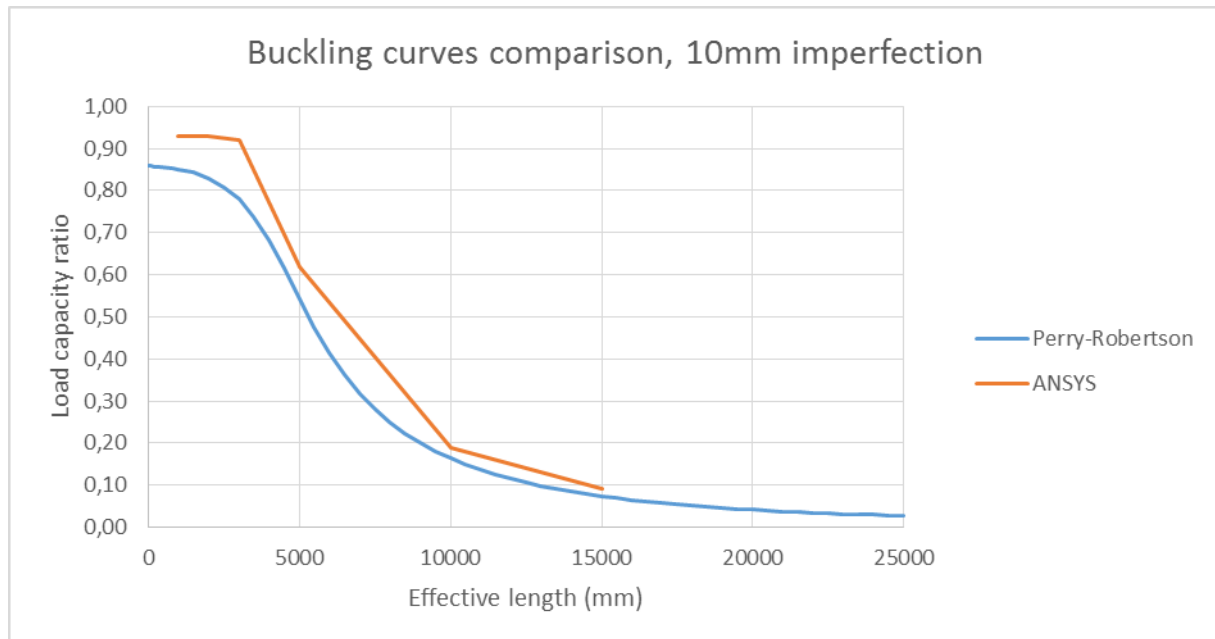


Figure 25: Buckling curve comparison, ANSYS and Perry-Robertson

From this comparison, it can be seen that the two lines are very similar, although the ANSYS line is very crude. By looking closer at both the known points and the graphical comparisons, it would seem that the difference in the results obtained by ANSYS and the Perry-Robertson equation is almost constant. For the values at the known points, the ANSYS results are consistently about 10% larger than the calculated results. Which means that, although the results obtained by the Perry-Robertson equation are conservative, they do grant a better idea of the effect that the imperfection has on the strength of the column. The Perry-Robertson equation therefore seems credible when discussing imperfect columns. The largest discrepancy between the two lines is between lengths of 5000 mm and 10000 mm, this is most likely due to a lack of known points in a crucial region. The region can be considered as crucial because of the rapid loss of load capacity that is shown here. The two lines converge greatly at higher lengths, but this is ultimately pointless as a fifteen meter long unsupported column is not likely to be built. However, it still speaks to the Perry-Robertson equations ability to predict the behavior of this imperfect column.

The analysis was performed in order to validate the results from the Perry-Robertson equation and it was successful, to a certain degree. For a relatively simple method, the Perry-Robertson equation manages to calculate the behavior of an imperfect column with good accuracy. It will certainly give a rough estimate for the load capacity of an imperfect column. In this regard, it might be good that the method is conservative, given the safety factors one must consider. Although only a 10 mm imperfection was modeled, the achieved results is assumed valid for similar situations as well. As is the case for similar cross-sections.

4.5. Eurocode 9 column calculations

As was seen by the Perry-Robertson buckling curve comparisons in chapter 4.2, some large differences between a perfectly straight column and an imperfect column exists. In the example with a 5 mm imperfection, the largest difference in load capacity ratio was found for lengths that would have been approved with the 5 mm imperfection. These results must be compared to some actual calculations, after the rules and regulations given in Eurocode 9 [1], in order to see if this can be dangerous or not.

These calculations are shown in Appendix B.1.

A straight column subjected to axial compression will be considered. In cases with axial forces, three different failure situation must be considered when doing calculations in accordance with Eurocode 9, these being failure by compression, flexural buckling and torsional-flexural buckling. As these results are to be compared with the results from the Perry-Robertson equation, there is no need to calculate torsional-flexural buckling. This is because the results from the Perry-Robertson equation only considers compression and flexural buckling. The calculations were performed for lengths between 1 mm and 10000 mm. The resistances in compression and flexural buckling is presented in the table below:

Table 4: Eurocode 9, compression resistance and flexural buckling resistance

Length	Compression resistance	Flexural buckling resistance
1 mm	1727 kN	1762 kN
500 mm	1727 kN	1720 kN
1000 mm	1727 kN	1676 kN
2000 mm	1727 kN	1572 kN
2500 mm	1727 kN	1502 kN
3000 mm	1727 kN	1412 kN
3750 mm	1727 kN	1234 kN
4500 mm	1727 kN	1024 kN
5000 mm	1727 kN	891 kN
5500 mm	1727 kN	772 kN
6000 mm	1727 kN	671 kN
6500 mm	1727 kN	586 kN
7000 mm	1727 kN	514 kN
7500 mm	1727 kN	455 kN
8000 mm	1727 kN	405 kN
8500 mm	1727 kN	362 kN
9000 mm	1727 kN	326 kN
9500 mm	1727 kN	294 kN
10000 mm	1727 kN	267 kN

As the compression resistance is only dependent on area and the yield stress of the material, it remains constant with varying length. The flexural buckling resistance however, decreases rapidly with the increasing length. For this cross-section, the flexural buckling resistance is usually the critical resistance. The critical resistance is the lesser of compression and flexural buckling, also known as the design resistance or governing resistance. The only time the flexural buckling resistance is not critical is for absurdly short columns, which are included for plotting purposes only.

In order to compare these results with the results from the Perry-Robertson equation, these resistances must be converted into maximum allowable stress. The maximum allowable force is equal to the resistance, if the safety factor for the load is neglected. The relationship between an axial force and the equivalent stress is only dependent on the area. The axial force and stress relationship is as follows:

$$\sigma = \frac{F}{A}$$

Where:

- $\sigma = stress$
- $F = axial\ force$
- $A = area$

The stress ratio is still based on a yield stress of 250 MPa.

Table 5: Eurocode 9, critical resistance and stress ratio

Length	Critical resistance	Stress	Stress ratio
1 mm	1727 kN	232 MPa	0.928
500 mm	1720 kN	226 MPa	0.905
1000 mm	1676 kN	221 MPa	0.882
2000 mm	1572 kN	207 MPa	0.828
2500 mm	1502 kN	198 MPa	0.791
3000 mm	1412 kN	186 MPa	0.743
3750 mm	1234 kN	162 MPa	0.649
4500 mm	1024 kN	135 MPa	0.539
5000 mm	891 kN	117 MPa	0.469
5500 mm	772 kN	102 MPa	0.406
6000 mm	671 kN	88 MPa	0.353
6500 mm	586 kN	77 MPa	0.309
7000 mm	514 kN	68 MPa	0.271
7500 mm	455 kN	60 MPa	0.240
8000 mm	405 kN	53 MPa	0.213
8500 mm	362 kN	48 MPa	0.191
9000 mm	326 kN	43 MPa	0.171
9500 mm	294 kN	39 MPa	0.155
10000 mm	267 kN	35 MPa	0.141

With the conversion of the Eurocode 9 calculation results, they can now be compared to the results from the Perry-Robertson equation. The first comparison will be with the straight Perry-Robertson column.

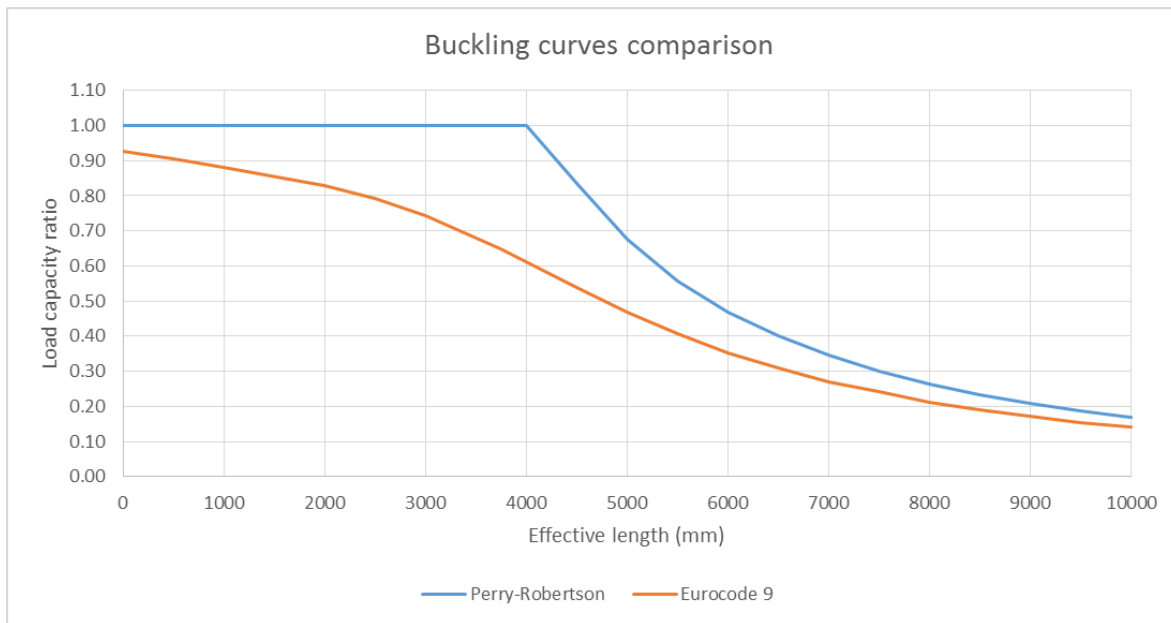


Figure 26: Buckling curve comparison, Perry-Robertson (no imperfection) and Eurocode 9

The two curves shows huge differences. The main reasons for this is the out-of-straightness imperfection imbedded in all Eurocode 9 calculations. At 4000 mm the Eurocode column can only manage a stress ratio of about 60 %, while the perfect column can reach yield stress levels. As mention in chapter 2.9., the permitted deviation found in NS-EN 1090-3 [3] is used as a safety factor in all buckling calculations performed in accordance with Eurocode 9. This means that at 4000 mm the Eurocode column is assumed to have an out-of-straightness imperfection equal to:

$$\delta = \frac{4000 \text{ mm}}{750} = 5.33 \text{ mm}$$

This is a rather large imperfection and will be responsible for a large part of the reduction in load carrying capacity. Although the values found by the Perry-Robertson equation should only be used as an indication of strength, they were proven conservative in the 10 mm imperfection case by the ANSYS analysis. If the results from the perfect column is also conservative, the Eurocode seems to be surprisingly strict with their initial out-of-straightness demand. Even though the two curves converge with the higher lengths, large losses in potential load capacity is shown throughout.

By implementing the permitted deviation from NS-EN 1090-3 into the Perry-Robertson formula, the result should look very similar to the results from Eurocode 9.

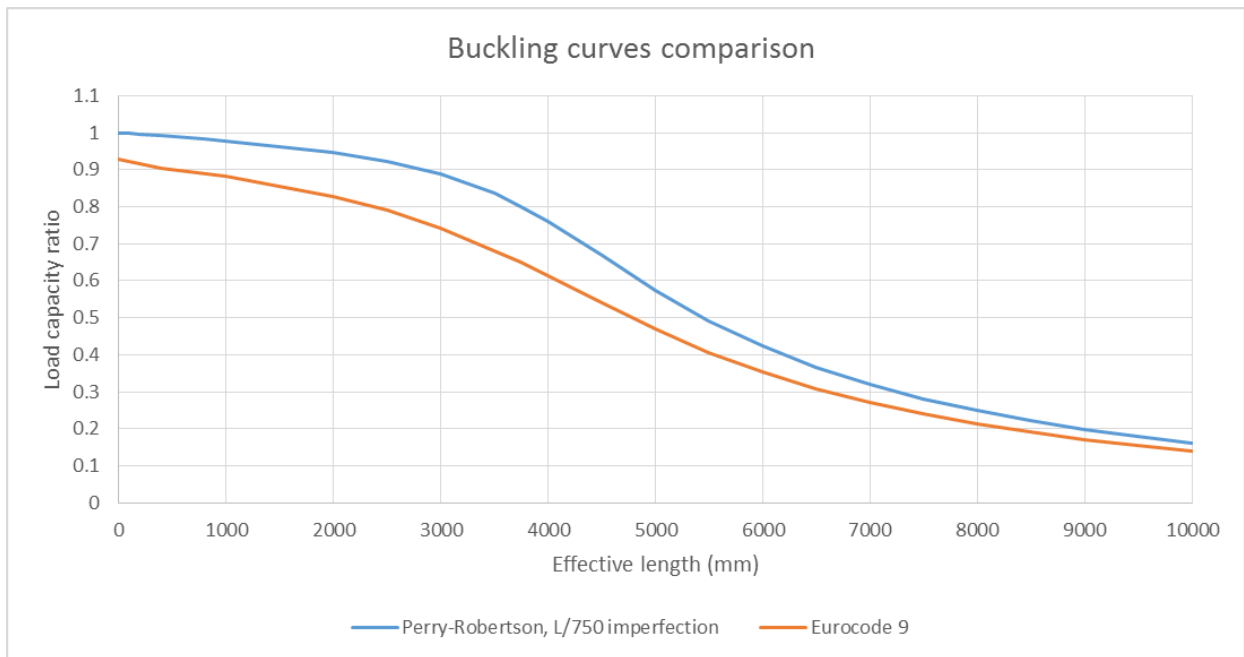


Figure 27: Buckling curve comparison, Perry-Robertson with varying imperfection and Eurocode 9

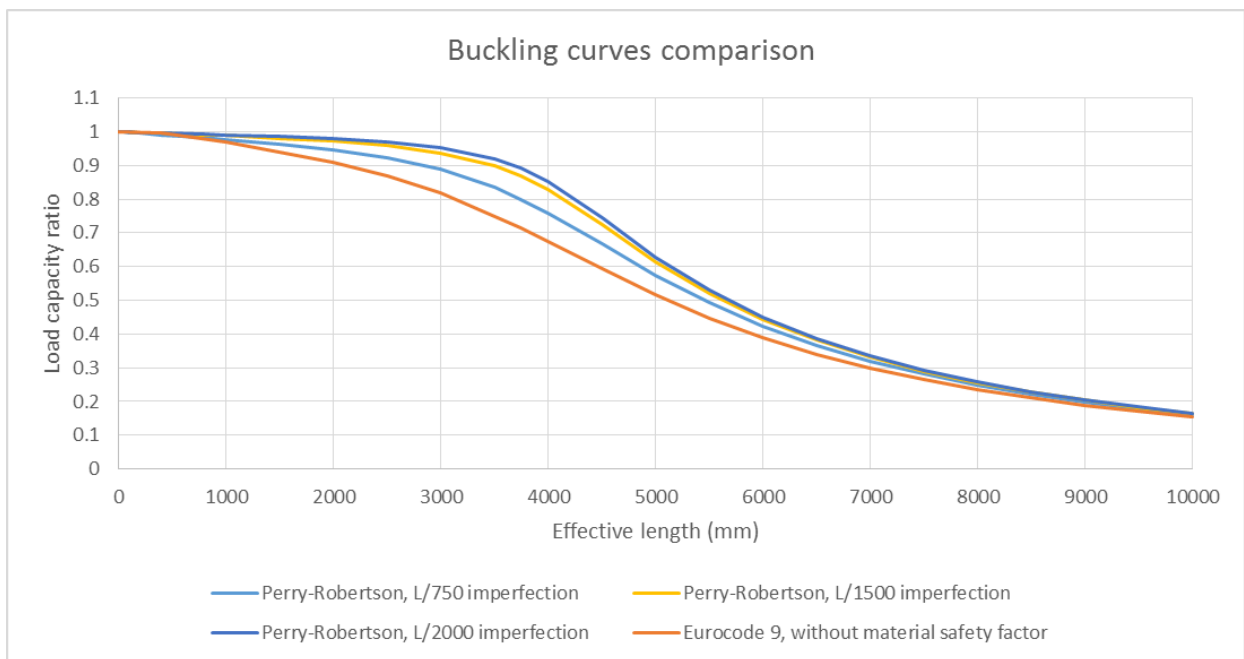


Figure 28: Buckling curve comparison, various imperfections

From the comparison in Figure 27, it is clear that the two graphs are very similar. If the material safety factor used in the Eurocode 9 calculations is removed, the two graphs becomes almost identical. This is shown in Figure 28. In addition, two other Perry-Robertson curves with imperfection $L/1500$ and $L/2000$ is shown. It becomes quite clear that the buckling curves used in Eurocode 9 stems from a Perry-type equation. It is almost surprising how similar they are, as the Eurocode's curve is a variation on the Perry curve strengthen by test results and experiments [7].

In chapter 4.2, a significant difference in the load bearing capacity was found between the perfect and the 5 mm imperfect column. This difference was found to the right of the tolerance line at about 4000 mm. At this length, the 5 mm imperfection would be acceptable according to the permitted deviation from NS-EN 1090-3. This could potentially create a dangerous situation. However, given that the actual Eurocode calculations operates with an imperfection equal to or larger than 5.33 mm in this region, the potentially dangerous situation is averted. This is visualized below:

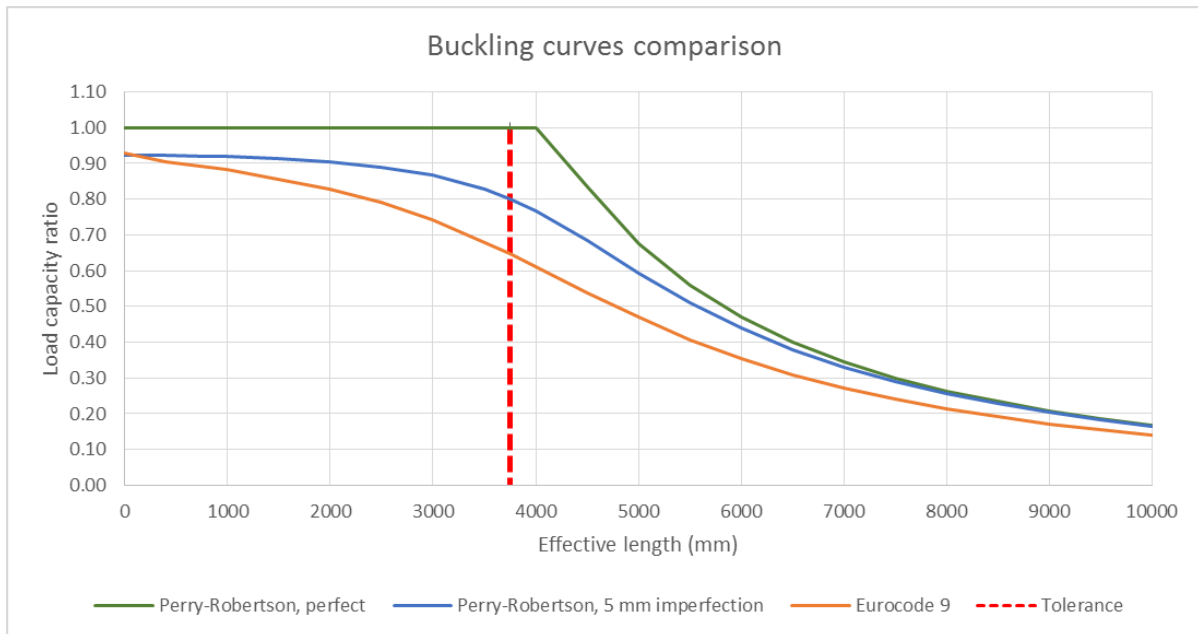
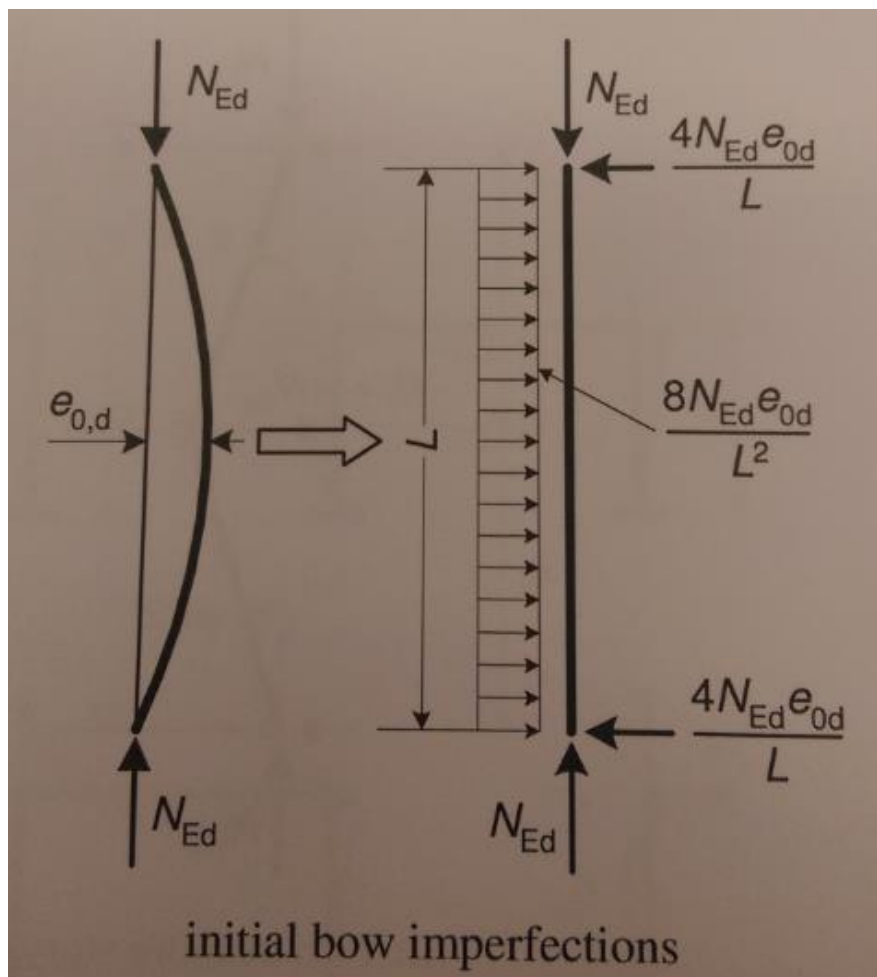


Figure 29: Buckling curve comparison with tolerance line, Perry-Robertson with 5 mm imperfection and Eurocode 9

4.6. Eurocode 9, imperfect column design

A column with a larger imperfection than the permitted deviation given in NS-EN 1090-3 can still be accepted by Eurocode 9, but additional calculations must be performed. By implementing equivalent horizontal forces corresponding to the imperfection, the regular design checks can be made. The equivalent horizontal forces are implemented as shown in the picture below:



Picture 2: Eurocode 9, equivalent horizontal forces method [1]

With the obtained results from the Perry-Robertson buckling curves, the effect of different values of imperfection was shown. It will be interesting to see how this compares to Eurocode's own calculation method. With the equivalent horizontal forces method, new design checks are necessary for shear resistance and bending moment resistance.

The same 200x10 quadratic hollow section, as used in previous calculations, will be utilized. The column will be 5000 mm long with a 10 mm out-of-straightness imperfection and pinned end supports.

The calculations are shown in Appendix C.1., the following resistances were found:

Table 6: Eurocode 9, design resistances and maximum allowable axial force

Check	Resistance	Maximum allowable axial force
Compression	1727 kN	1727 kN
Bending	104.2 kNm	10240 kN
Shear	524.9 kN	65612.5 kN
Flexural buckling	891 kN	891 kN

As can be seen from these results, flexural buckling is still the critical resistance. Since the imperfection does not alter the cross-section in the equivalent horizontal forces method, the resistances will remain constant. A larger imperfection will however yield larger shear forces and in turn, a larger design moment. These forces will directly affect the maximum allowable axial force. The maximum allowable axial force is calculated from the different load types using the relationship between the forces as given in Eurocode 9. Since the shear force is only a fraction of the axial load, the resulting maximum axial force calculated from the shear resistance is very high. From Table 6, it can be seen that the governing design check is still flexural buckling, as it allows for the smallest maximum axial force. With both moment and axial force working on the column, an additional flexural buckling criterion must be met. This is to allow the two forces to work together to buckle the column. It should be noted that the combined effect of shear forces and bending moment should also be checked in accordance with Eurocode 9. However, given the small values for shear force and bending moment compared to the axial force in this example, it is assumed that flexural buckling will be the governing design check.

For members in bending and axial compression:

According to 6.3.3.1 (3): Hollow cross-sections should satisfy the following criterion [1]:

$$\left(\frac{N_{Ed}}{\chi_{min} \cdot \omega_x \cdot N_{Rd}} \right)^{\psi_c} + \frac{1}{\omega_0} \left(\left(\frac{M_{y,Ed}}{M_{y,Rd}} \right)^{1.7} + \left(\frac{M_{z,Ed}}{M_{z,Rd}} \right)^{1.7} \right)^{0.6} \leq 1.00$$

Where:

- $\chi_{min} = 0.714$, reduction factor for flexural buckling found in Appendix B
- $\omega_x = \omega_0 = 1$
- $\psi_c = 0.8$
- $N_{Ed} =$ axial load
- $M_{y,Ed} =$ experienced moment force with regards to the y – axis
- $M_{z,Ed} =$ experienced moment force with regards to the z – axis

In order to check if the criteria is fulfilled for a column, a numeric value for the axial force and bending moment is needed. With the equivalent horizontal forces method and a pinned column, the design value for bending moment and axial force has the following relationship:

$$M_{y,Ed} = \frac{q \cdot L^2}{8}$$

Where q is the uniformly distributed load as is given by the equivalent horizontal forces method:

$$q = \frac{8 \cdot N_{Ed} \cdot e_{0d}}{L^2}$$

By uniting these two equations, a simple relationship between the maximum moment and the maximum allowable axial force can be determined:

$$M_{y,Ed} = \frac{8 \cdot N_{Ed} \cdot e_{0d}}{L^2} \cdot \frac{L^2}{8}$$

$$M_{y,Ed} = N_{Ed} \cdot e_{0d}$$

The resistance calculations revealed that the maximum allowable axial load for the column was 891 kN. By using this value as the design value for the axial load, the criterion for members in bending and axial compression can be checked.

$$\left(\frac{N_{Ed}}{\chi_{min} \cdot \omega_x \cdot N_{Rd}} \right)^{\psi_c} + \frac{1}{\omega_0} \left(\left(\frac{M_{y,Ed}}{M_{y,Rd}} \right)^{1.7} + \left(\frac{M_{z,Ed}}{M_{z,Rd}} \right)^{1.7} \right)^{0.6} \leq 1.00$$

$$\left(\frac{891 \text{ kN}}{0.516 \cdot 1 \cdot 1727 \text{ kN}} \right)^{0.8} + \frac{1}{1} \left(\left(\frac{891 \text{ kN} \cdot 10 \text{ mm}}{104.2 \text{ kNm}} \right)^{1.7} + \left(\frac{0}{104.2 \text{ kNm}} \right)^{1.7} \right)^{0.6} \leq 1.00$$

$$1 + 0.081 \leq 1$$

$$1.081 > 1$$

The criteria is not satisfied. This is not surprising as the column was already loaded to the maximum for flexural buckling due to compression only. With the additional moment forces from the imperfection, the column will buckle. It is interesting to note how small the addition from the bending moment is, as it only contributes to about 8 percent of the capacity. Different values for the applied axial force and the associated contribution from axial compression and bending moment is listed in the table below.

Table 7: Eurocode 9, Bending moment + axial force criteria check

N_{Ed}	Axial contribution	Bending moment contribution	Total utilization	Criteria check
891 kN	1.000	0.081	1.081	Not OK
870 kN	0.981	0.079	1.060	Not OK
850 kN	0.963	0.078	1.040	Not OK
830 kN	0.945	0.076	1.020	Not OK
810 kN	0.926	0.074	1.000	OK

These results show that a reduction of 81 kN, or about 9 %, applied to the axial load is needed for the column to be approved, due to the 10 mm imperfection. It is also shown that the contribution from the bending moment does not vary that much with the decreasing axial load. It must be noted that this 10 mm imperfection is not the “actual” imperfection of the column. A 5000 mm long column will inherently have an out-of-straightness imperfection equal to 6.67 mm, which is the permitted out of

straightness deviation [3]. Since two different imperfections are used in different phases of the calculations, it becomes hard to argue how large the actual imperfection is. However, the L/750 imperfection should be taken as a safety factor and not an actual imperfection, the results from these calculations should therefore be used to represent an imperfection equal to 10 mm.

The effect of the imperfection is better visualized in the Figure 30. The maximum allowable axial load is plotted against increasing imperfection. The calculations were performed in the same manner as for the 5000 mm long column with a 10 mm imperfection. These calculations are presented in Appendix C.2.

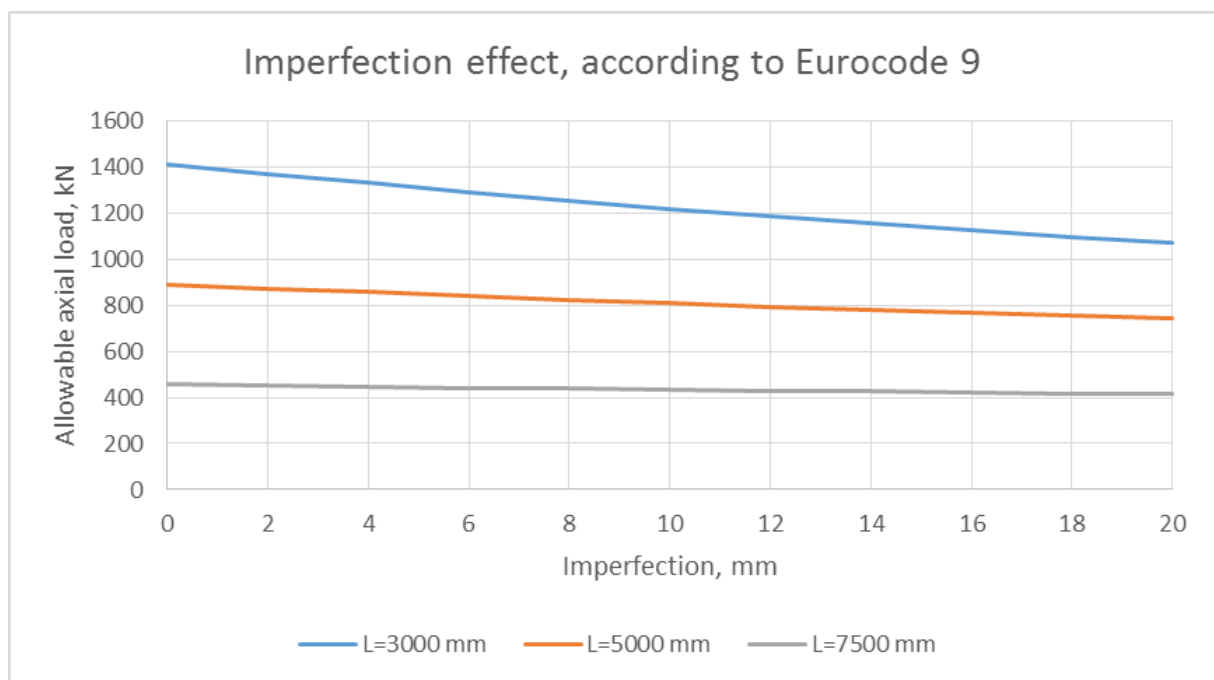


Figure 30: Eurocode 9, imperfection effect

From the graph, it is clear to see that the effect of the imperfection is much more important in short columns. This is logical since the longer column already operates with a sizeable imperfection and the effect of the “extra” imperfection is less noticeable. A similar conclusion was shown with the Perry-Robertson calculations, where the difference between the perfect and imperfect column was much larger at short lengths and negligible at longer lengths.

To compare these results with results found earlier, the maximum stress must be determined. The stress contribution from axial force and bending moment can be combined with the following formula:

$$\sigma_{max} = \frac{P}{A} + \frac{M \cdot y}{I}$$

Where:

- P = Axial load
- A = Cross-section area
- M = Moment
- y = distance to the neutral axis
- I = moment of inertia

Table 8: Eurocode 9, imperfection effect on design resistances

Length (mm)	Imperfection (mm)	Design axial force (kN)	Design bending moment (kNm)	Maximum stress (MPa)
3000	10	1218.00	12.2	186.63
5000	10	809.00	8.09	124.10
7500	10	433.00	4.33	66.42

The maximum stress for the imperfect beam found by Eurocode equivalent horizontal force can now be compared to the result from both the ANSYS analysis and the Perry-Robertson equation. One of the ANSYS values are approximates found by linear interpolation, as there were no known values at this length.

Table 9: Stress comparison: Eurocode 9, Perry-Robertson and ANSYS

Length (mm)	Imperfection (mm)	Max stress (MPa)		
		Eurocode 9	Perry-Robertson	ANSYS analysis
3000	10	173.65	195.00	230.00
5000	10	124.10	135.00	155.00
7500	10	66.42	70.00	Ca. 101.25

With this comparison, it is shown that the use of equivalent horizontal forces instead of the imperfection works well. There is a good fit between the results from Eurocode and Perry-Robertson. Although the value from ANSYS is a bit higher than expected for the 7500 mm long column, it is most likely due to the lack of known values between 5000 and 10000 mm.

It is also shown that Eurocode retains its safety factor, as it is more conservative than the Perry-Robertson results and much more conservative than the ANSYS results. This was the expected results as Eurocode 9 calculates with a larger imperfection and a material safety factor. The method of equivalent horizontal forces can therefore be said to be an acceptable calculation method for dealing with out-of-straightness imperfections. The method does require a precise measurement of the imperfection, which can be very difficult to obtain. In cases where there are no other choice than to use a column with a larger imperfection than the permitted deviation, then this method can safely be used to interpret the effect of the imperfection. In certain modeling programs, it can be quite difficult to create the shape of an out-of-straightness imperfection, this method offers an acceptable solution to that problem.

4.7. H-400 calculations

As the previous calculations were all done for a quadratic hollow cross-section, some additional calculations will be done for an I-type cross-section. This is done in order to determine that the effect that the out-of-straightness imperfection had on the quadratic hollow section is not unique to that type of cross-section. One major difference when using the I-section in flexural buckling calculations is that these types of cross-sections has a major and a minor buckling axis. In other words, two different values for the moment of inertia exists. Flexural buckling occurs about the axis with the largest slenderness ratio, and the smallest radius of gyration. The moment of inertia is directly used to calculate the radius of gyration and an increase in moment of inertia will result in an increase of the radius of gyration. Flexural buckling will therefore occur more easily about the axis with the lowest moment of inertia.

In Figure 31, both the minor and major axes are drawn on a sketch of an I-type cross-section. The moment of inertia is based on the slenderness of each component and its location compared to the neutral axis. A component with a large height and low thickness is considered slender and will have a large contribution to the moment of inertia. The web of the I-section will therefore be considered slender about the y-axis and not slender about the x-axis. This is illustrated by rotating the sketch of the I-section, this is shown in Figure 32. In most I-sections, this will result in the x-axis being considered the minor axis and the most critical for buckling concerns. However, it is not uncommon practice to reinforce the buckling resistance about the minor axis, in beams or columns susceptible to buckling. With this in mind, it will be interesting to investigate the effect of the out-of-straightness imperfection for both the minor and major axis.

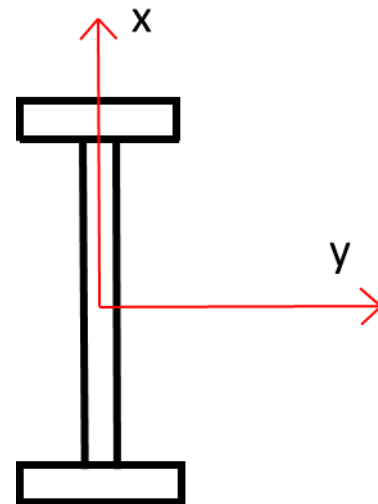


Figure 31: H-400 cross-section

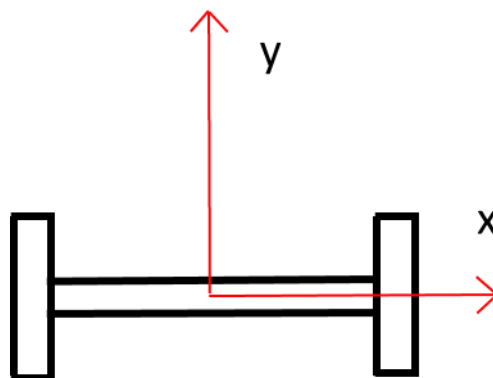


Figure 32: Rotated H-400 cross-section

The H-400 cross-section, which will be considered in the calculations, is presented in Figure 33. The cross-sectional properties is calculated in Appendix A.2. With the moment of inertia calculations, it is shown that the x-axis was indeed the minor axis. It was also shown that, according to Eurocode 9, the web is so slender that it is susceptible to local buckling. This will result in a reduction of flexural buckling resistance in the Eurocode 9 calculation; this reduction is applicable for both minor and major axis. As the Perry-Robertson equation does not take local buckling into consideration, a larger difference between the results from the Perry-Robertson calculations compared to Eurocode 9 is expected for the H-400 cross-section when compared with those found for the 200x10 mm quadratic hollow section. Local buckling and its impact on the Eurocode 9 capacities is discussed more in chapter 5.

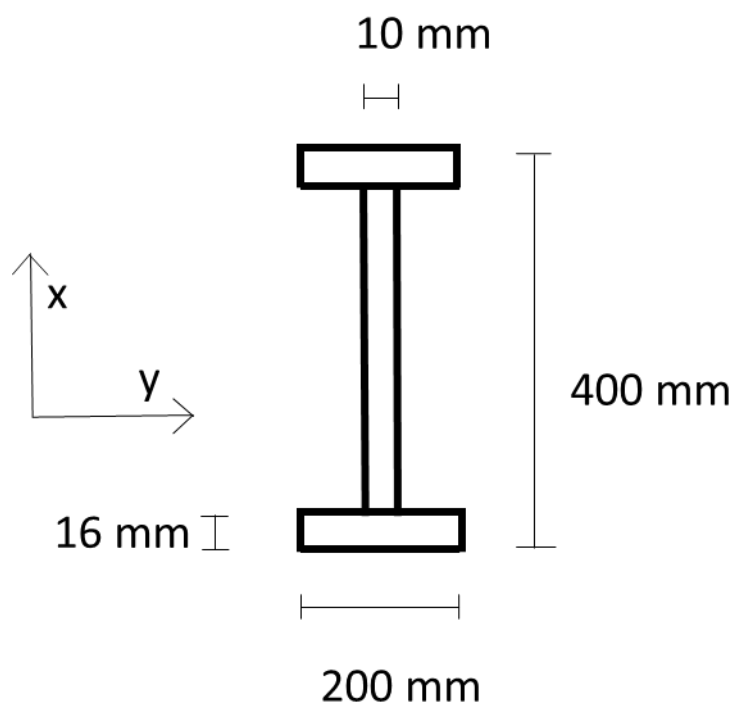


Figure 33: H-400 cross-section dimensions

The calculations will be done in much the same manner as for the 200x10 mm quadratic hollow section. Both a column with a constant imperfection and a “perfect” column will be calculated with the Perry-Robertson equation, so that the effect of the imperfection can be decided. This result will then be compared to regular Eurocode 9 calculations. In the Perry-Robertson equation, the out of straightness imperfection is on the axis about which buckling is considered. In other words when buckling about the x-axis is considered, the deflection at the midpoint of the column will be along the y-axis. In the Eurocode 9 calculations, the imperfection safety factor is present in all buckling calculations, which should give a comparable answer when both the minor and major axis is considered.

The Perry-Robertson calculations for the H-400 cross-section is performed in Appendix D5 to D8. The imperfection was set at 10 mm for both the x- and y-axis. The results are plotted with maximum stress-ratio against length of the column. As with the previous Perry-Robertson calculations, the column is assumed to be pinned. Although a pinned column might not be the most realistic support configuration, it allows the deformation shape to take the form of a half sine wave. Different end supports can be used with the addition of a buckling length factor, as discussed in chapter 2.2. The same factor would be used in both the Perry-Robertson and the Eurocode 9 calculation, which should therefore not be important to the comparison.

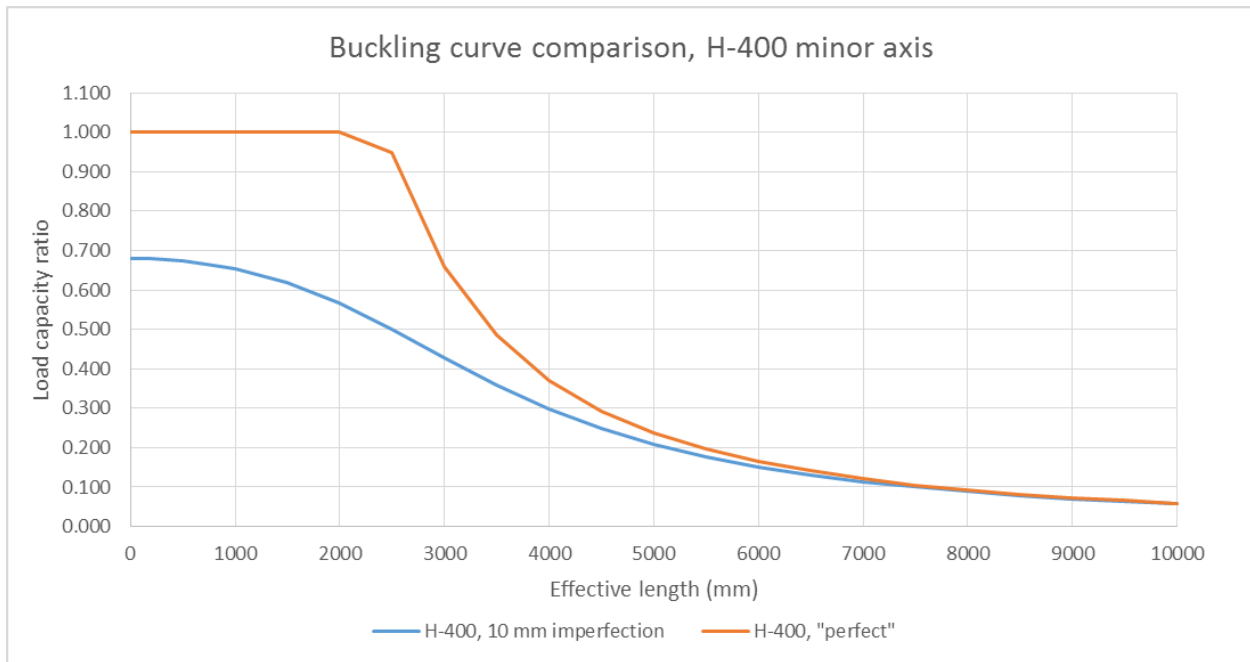


Figure 34: Buckling curve comparison, H-400 minor axis

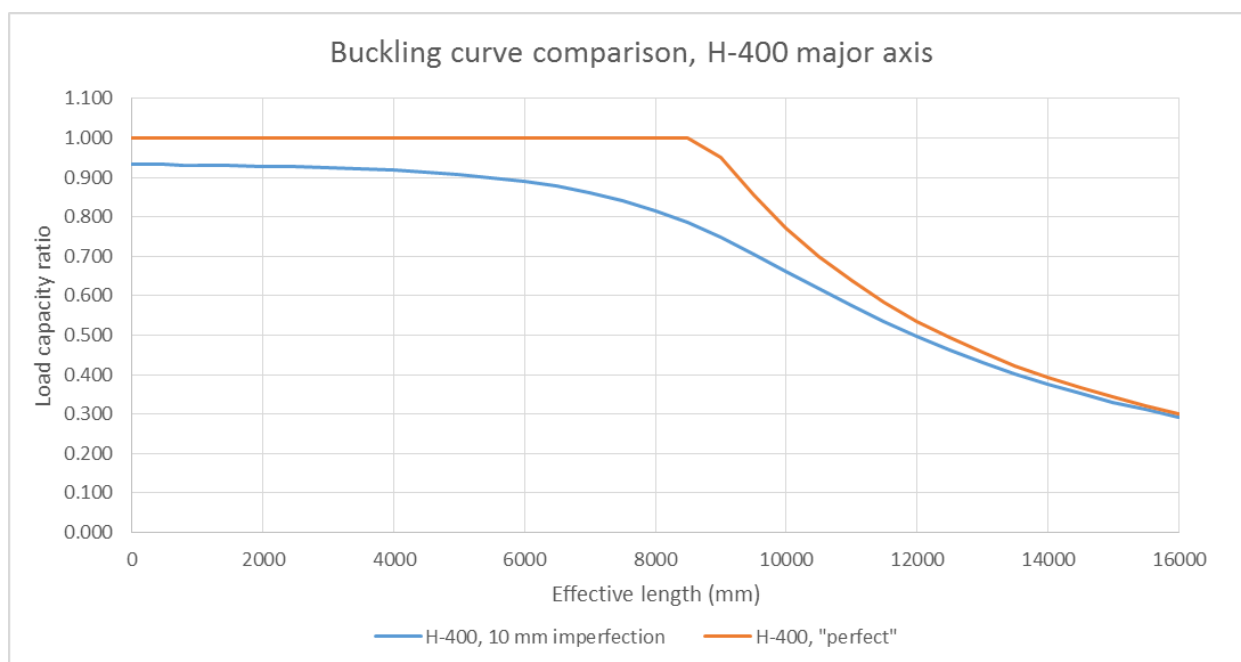


Figure 35: Buckling curve comparison, H-400 major axis

The comparison between Figure 34 and Figure 35 shows very large differences between the flexural buckling resistance for the minor and major axis. The “perfect” column buckles about the x-axis at 2000 mm. If buckling about this axis is restrained the column could be up to 8000 mm before buckling about the y-axis would occur. This also illustrates how much more effective an I-section is at resisting bending moment about its major axis. From the plots, it can also be seen that the 10 mm imperfection has a much larger effect on the minor axis. At certain lengths, this relatively weak axis loses about 30 % -40 % of its load capacity with this imperfection. Comparably the strong axis only loses about 20 % of its capacity and this is at a larger length as well. This indicates that the effect of the imperfection is not only based on the imperfection size, as the effect is not the same for these two axes. With a 10 mm imperfection, the maximum load capacity reduction is definitely largest for the minor axis of the H-400 column compared to the major axis and the 200x10 mm quadratic hollow section. The minor axis has the lowest moment of inertia of the three. An axis or cross-section with a low moment of inertia will also have a low resistance to flexural buckling or bending. It would therefore seem that “weak” columns are much more affected by the initial out-of-straightness imperfection, than columns that are more resistant. This is also shown by the major axis, as it has the largest moment of inertia and the lowest capacity reduction.

With the quadratic hollow section calculations, it was found that the Eurocode 9 calculations has enough safety factors to warrant the permitted deviation stated in NS-EN 1090-3. For this 10 mm imperfection, the column must be at least 7500 mm long to be approved by NS-En 1090-3. For the minor axis the largest difference between perfect and imperfect is at lower lengths than 7500 mm and would therefore not be approved. For the major axis on the other hand, the largest difference is found at about 8500 mm, which would be approved. By comparing with Eurocode calculations performed in Appendix B.2., it can be seen that the maximum flexural buckling resistance for the major axis at 8500 mm is 1458.3 kN, which can be converted to a load capacity ratio of 0.579. The Perry-Robertson equation gave a load capacity ratio of 0.785 at this length. It can be concluded that the Eurocode 9 calculations are conservative enough that there will be no dangerous situations when following the tolerance limits given by NS-EN 1090-3. At least when flexural buckling of column is

considered. This is the same conclusion that was offered from the quadratic hollow section calculations. To illustrate this further two more graphs are presented, showing the “perfect” column calculations, the Eurocode 9 calculations and a Perry-Robertson column with varying imperfection. This imperfection is equal to $L/750$, which is the assumed imperfection value that Eurocode 9 uses in its buckling calculations. A graph is presented for both the minor and major axis. As with the quadratic hollow section calculations, the Eurocode 9 calculations are always the most conservative. By comparing the two graphs, it is shown again that an out-of-straightness imperfection has a larger effect on the minor axis, strengthening the conclusion.

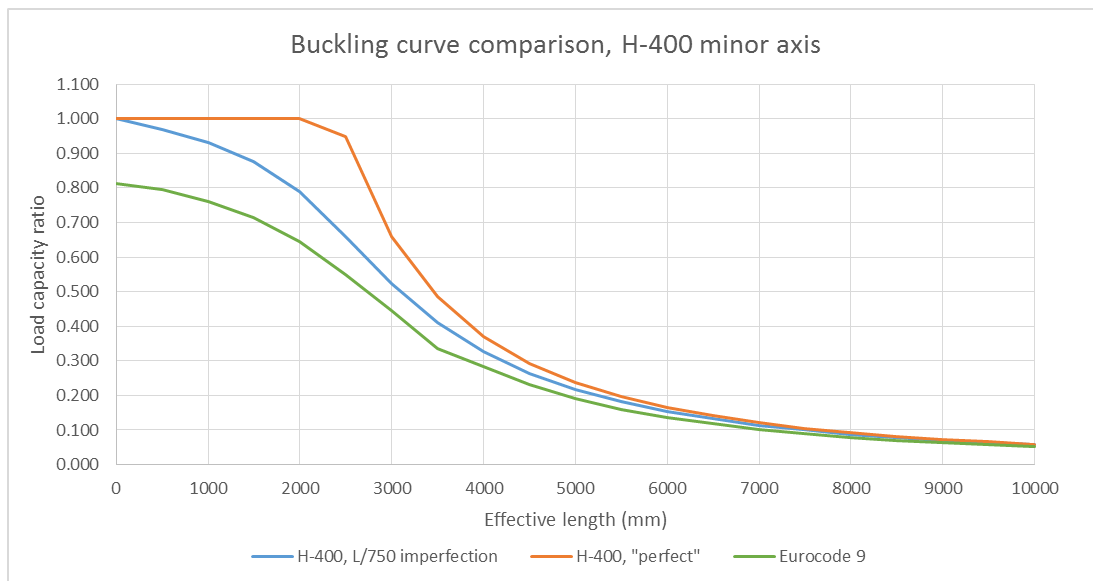


Figure 36: Buckling curve comparison, varying imperfection, H-400 minor axis and Eurocode 9

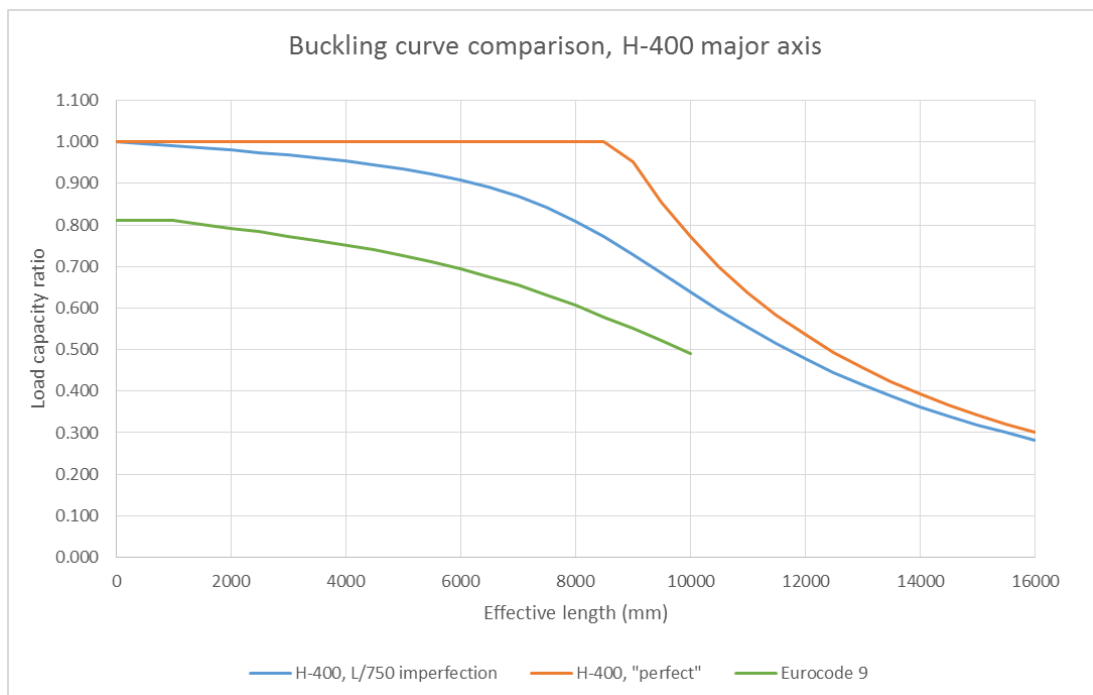


Figure 37: Buckling curve comparison, varying imperfection, H-400 major axis and Eurocode 9

4.8. Result discussion

The main objective behind these calculations was to gain a better understanding of how the tolerance limits given by NS-EN 1090-3 affect the capacity of the column. It has been shown that the Perry-Robertson gives a good representation of the buckling curves presented by Eurocode 9. Since the out-of-straightness tolerance limit is used as a safety factor in all the buckling calculations done in accordance with Eurocode 9, it comes as no surprise that the permitted deviation is not dangerous to follow. If an out-of-straightness imperfect column is approved by Eurocode 9 with the regular calculations and the imperfection is smaller than the permitted deviation, there will be no problems. At least not with regards to flexural buckling and compression.

The results from the “original” Perry-Robertson equation showed large differences between a perfect and an imperfect column and the difference between those curves and the Eurocode results were larger still. This indicates a rather large loss in potential load capacity due to safety factors. The tolerance limit of $L/750$ seems to be very large when compared to the actual crookedness of most produced beams. As mentioned chapter 2.9, measurement from tests performed 30 years ago, show an average crookedness of $L/2000$ for extruded industrial bars. During the test performed in “*Stability of 6082-T6 aluminium alloy columns with H-section and rectangular hollow sections*” [5] no initial crookedness was discovered in any of the 30 beams tested, that could be measured without high cost equipment. With the comparison between the $L/750$, $L/1500$ and $L/2000$ imperfection, the Perry-Robertson equation showed a large difference at certain lengths.

It should be noted that one of the reasons why the permitted deviation is so strict is to take into account any additional reduction in the capacity that can be caused by residual stress [6]. The residual stress in an extruded aluminium member is very low. It has in fact been deemed insignificant by European studies [9]. Residual stresses can also occur as a direct result of welding, but this is considered in heat affected zone calculations. This is yet another indication that the out-of-straightness tolerance limit is very strict for extruded members. However, only flexural buckling and compression was considered in the Perry-Robertson formula. The out-of-straightness production tolerance is not specifically stated for a column and it will be applicable for beams subjected to shear forces and bending moments as well. Since the effect of the imperfection was only considered for a column subjected to axial loading, a recommendation for a less restrictive production tolerance cannot be based on the obtained results.

However, the results can be used to discuss the optimization of the buckling curves presented in Eurocode 9. In Eurocode 9, all aluminium alloys are divided into one of only two different buckling classes based on material properties. Similar to the discussion presented in “*A new design method for stainless steel columns subjected to flexural buckling*” [4], where the differences in material properties between different stainless steel alloys was highlighted, and the effect that these properties has on the flexural buckling resistance. The same argument can be made for different aluminium alloys. Dividing them all into only two different buckling classes, will most likely prove to be inefficient for some alloys.

In addition, the buckling curves for flexural buckling presented by Eurocode 9 are independent of cross-section geometry. The buckling curves for torsional and torsional-flexural buckling separates different cross-section geometry into either a general cross-section or a cross-sections composed entirely out of radiating outstands [1]. In comparison, Eurocode 3 presents five different buckling

curves for flexural buckling. With these buckling curves the geometry of the cross-section is taken into account and large differences between the buckling curves are shown, see Figure 38. The methods for calculating flexural buckling resistance for steel and aluminium is very similar and so one would assume that the similar differences would occur for aluminium cross-sections. The geometry of the aluminium cross-section is considered during calculation of the moment of inertia and implemented into the buckling curve via the relative slenderness, but this is also true for steel cross-sections.

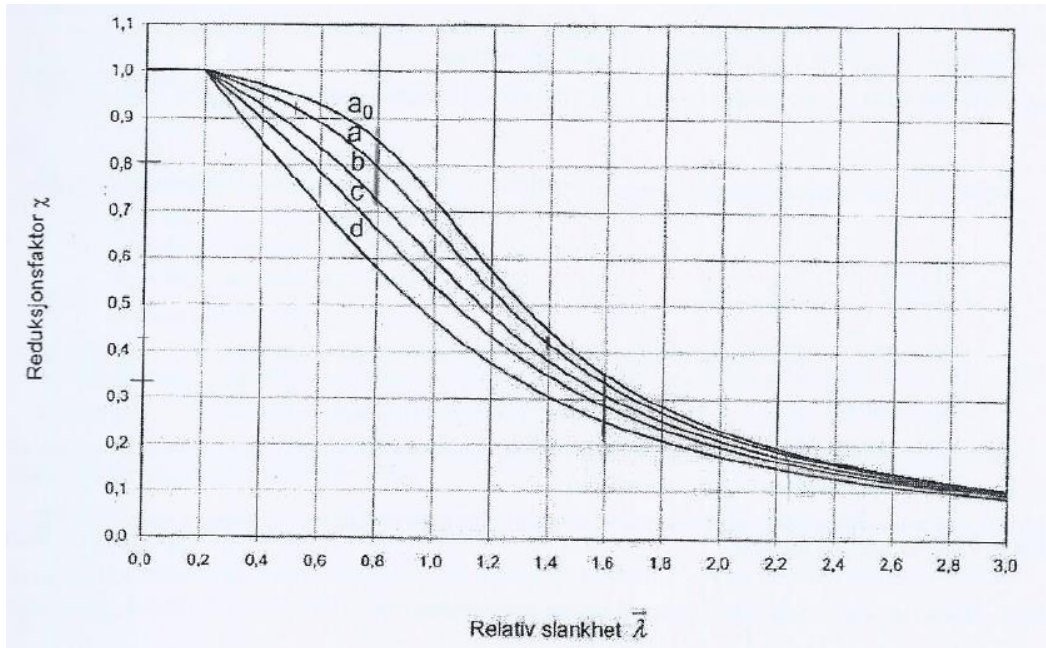


Figure 38: Eurocode 3, buckling curves [2]

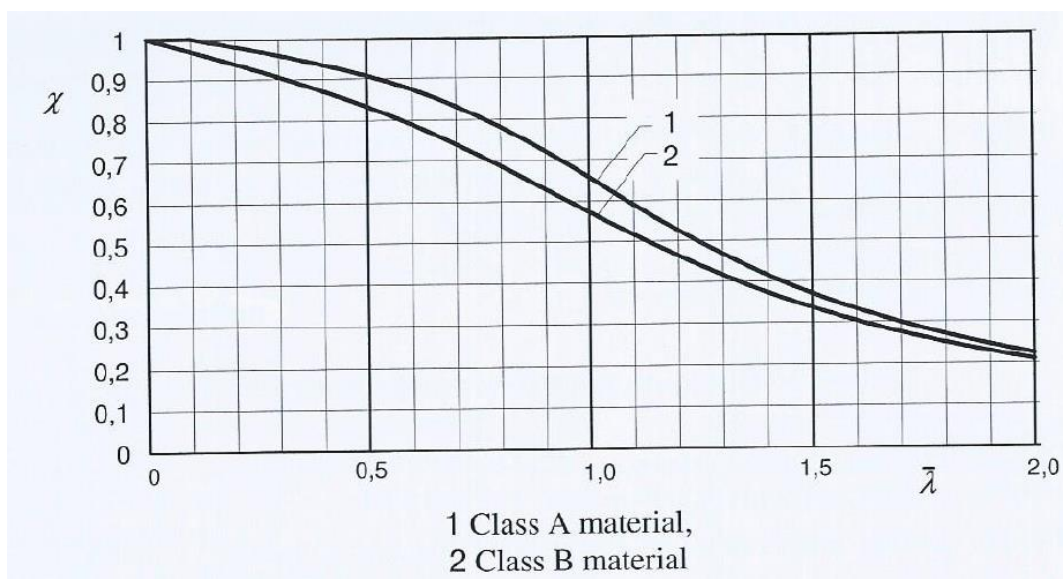


Figure 39: Eurocode 9, buckling curves [1]

Both Eurocode 3 and Eurocode 9 describes their buckling curves using relative slenderness on the x-axis and reduction factor on the y-axis. The reduction factor is used with the compression resistance in order to determine the flexural buckling resistance. The compression resistance is directly linked to the yield stress. This means that this reduction factor is very comparable with the stress-ratio used in the Perry-Robertson equation.

As is shown by figure 37 and 38, Eurocode 3 presents 5 different buckling curves while Eurocode 9 only presents 2. In Eurocode 3 some very large differences exists in the buckling curve for the strongest and the weakest class. Differences is also seen between the two aluminium buckling curves, but these differences are much smaller. As mentioned, the buckling class for steel is determined using both cross-section type and steel grade. While the aluminium buckling class is only determined by the aluminium alloy that is used. The main difference in the reduction factor between the different classes is the imperfection factor that is used in the calculations. The strongest steel class uses an imperfection factor of 0.13 [2] while the strongest aluminium class uses an imperfection factor of 0.20 [1]. A low imperfection factor leads to a higher flexural buckling resistance.

With the argument that extruded beams are straighter and without residual stress, the calculation method in Eurocode 9 seems to be inefficient with regards to the actual flexural buckling capacity. Buckling curves based on production method, as well as aluminium alloy used, could create more efficient flexural buckling resistance calculations. The introduction of more buckling classes should also be considered. The material properties and the behavior of different aluminium alloys varies greatly [5] and it seems unlikely that two buckling curves can be used to represent them all efficiently.

Safety factors are very important and it is not the goal of this discussion to remove them. With more precise calculations however, the actual behavior of a member can be better understood. This can lead to savings in material costs while still having a good level of safety.

Chapter 5

5. Cross-section imperfection and local buckling

Although the focus of this thesis has been the out-of-straightness imperfections and its effect on flexural buckling, it is far from the only production tolerance listed in NS-EN 1090-3. In this chapter, the effect that an imperfect cross-section has on both local and global buckling will be discussed briefly.

5.1. Imperfect cross-section

There are many different permitted deviations, concerning the cross-section geometry, listed in NS-EN 1090-3. Among these are width of flange, position of web and depth of the cross-section. Unexpected deviations in cross-section geometry can be unfortunate as it can lead to less resistance to local buckling and a lower flexural buckling resistance. With alterations in the geometry of the different cross-section components, their respective slenderness parameters will also be altered. With a higher slenderness, the probability of local buckling is increased.

While the buckling of a beam is known as global buckling, the buckling of cross-sectional components are known as local buckling. Local buckling can be seen as its own limit state, as it can in some cases lead to failure of the member. Local buckling is very similar to global buckling, as it affects slender components in compression. In slender components, local buckling may occur long before the material strength is reached and the cross-section will become distorted. Normal cross-sections, such as an I-section, consists of an assembly of thin plates and the slenderness parameter of each of these thin plates is a function of width divided by thickness. Slender components have a high width to thickness ratio, while a component with a low width to thickness ratio is known as compact. A compact component is not susceptible to buckling and failure for such components will come at higher stresses than for slender components [10].

The components in a cross-section, such as flanges and webs, can be either stiffened against buckling or unstiffened. For example, the web of a regular I-section is stiffened by the flanges, while the flanges themselves are unstiffened. A stiffened component will show a larger resistance to buckling than an unstiffened component. In rectangular hollow sections, all the plates that compose the section is stiffened.

The stress distribution in the cross-section is very important when considering local buckling. While global buckling only occurs with the inclusion of axial loading, local buckling can happen for almost all loading scenarios. With the exception of uniformly distributed tension forces working on the cross-section. A regular I-section experiencing bending about its major axis will for instance experience compression forces in one of its flanges and tension forces in the other. The compression flange can therefore be susceptible to local buckling. It is also important to note that local buckling does not only occur for slender members. Short column can also be affected by local buckling, if any of the components in the cross-section is considered slender.

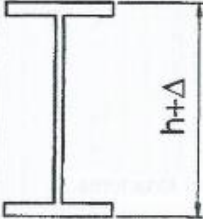

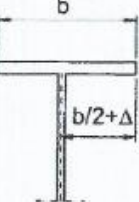
To check if a cross-section is susceptible to local buckling, Eurocode 9 utilizes the cross-section classification method. A cross-section is categorized from class 1 to class 4, based on the slenderness parameter. The classes are defined as follows:

From 6.1.4.2 Classification, Eurocode 9 [1]:

- *Class 1 cross-sections are those that can form a plastic hinge with the rotation capacity required for plastic analysis without reduction of the resistance.*
- *Class 2 cross-sections are those that can develop their plastic moment resistance, but have limited rotation capacity because of local buckling.*
- *Class 3 cross-sections are those in which the calculated stress in the extreme compression fibre of the aluminium member can reach its proof strength, but local buckling is liable to prevent development of the full plastic moment resistance.*
- *Class 4 cross-sections are those in which local buckling will occur before the attainment of proof stress in one or more parts of the cross-section.*

With elastic calculations, it is only class 4 cross-sections that are susceptible to local buckling, as local buckling occurs at a lower stress level than yield stress for these sections. To allow for a class 4 cross-sections in the design calculations, a reduction to the thickness is needed. This reduction is done in order to create an effective cross-section that is assumed not to experience local buckling before yield stress levels are reached. This effective cross-section is then used in the resistance calculations.

Table G.1 — Permitted deviations for welded I-sections

Case	Type of deviation	Dimensional parameter	Permitted deviation
A	Depth: 	Depth of section: $h < 900 \text{ mm}$ $900 < h \leq 1\,800 \text{ mm}$ $h > 1\,800 \text{ mm}$	$\Delta = \pm 3 \text{ mm}$ $\Delta = \pm 5 \text{ mm}$ $\Delta = + 8 \text{ mm or } - 5 \text{ mm}$
B	Flange width: 	Width b_1 or b_2 : $b < 300 \text{ mm}$ $b \geq 300 \text{ mm}$	$\Delta = \pm 3 \text{ mm}$ $\Delta = \pm 5 \text{ mm}$
C		Position of web:	$\Delta = b/50$ but not less than 2 mm

Picture 3: Table G.1 from NS-EN 1090-3 [3]

Table G.1 from NS-EN 1090-3 [3] shows the permitted deviations for a welded I-section. Please note that the table presented here is not the complete table. By increasing the width of the flange, two differences are immediately noticeable. Both the moment of inertia and the slenderness of the flange is increased. With the increase in moment of inertia, the sections resistance to both bending and buckling is increased as well. With an increase in the slenderness of the flange, it becomes more susceptible to local buckling. This results in a larger resistance to global buckling and less resistance to local buckling or vice versa if the width of the flange is decreased. The same will be true for the height of the web.

The production tolerances in 1090-3 offers little leeway in terms of the permitted flange width deviation and web height deviation, by only allowing for +/- 3 mm on the smaller cross-sections. As the changes will bring both positive and negative effects, the overall impact on the load capacity is assumed small. Calculations of the flexural buckling resistance for two different cross-sections with varying width of flange and height of web were performed for two different I-sections; these calculations are shown in Appendix E. A worst-case scenario is considered where both the width of

the flanges and height of the web is increased or decreased simultaneously. A graphical comparison is given in Figure 40 for the H-400 cross-section and in Figure 41 for the H-200 cross-section.

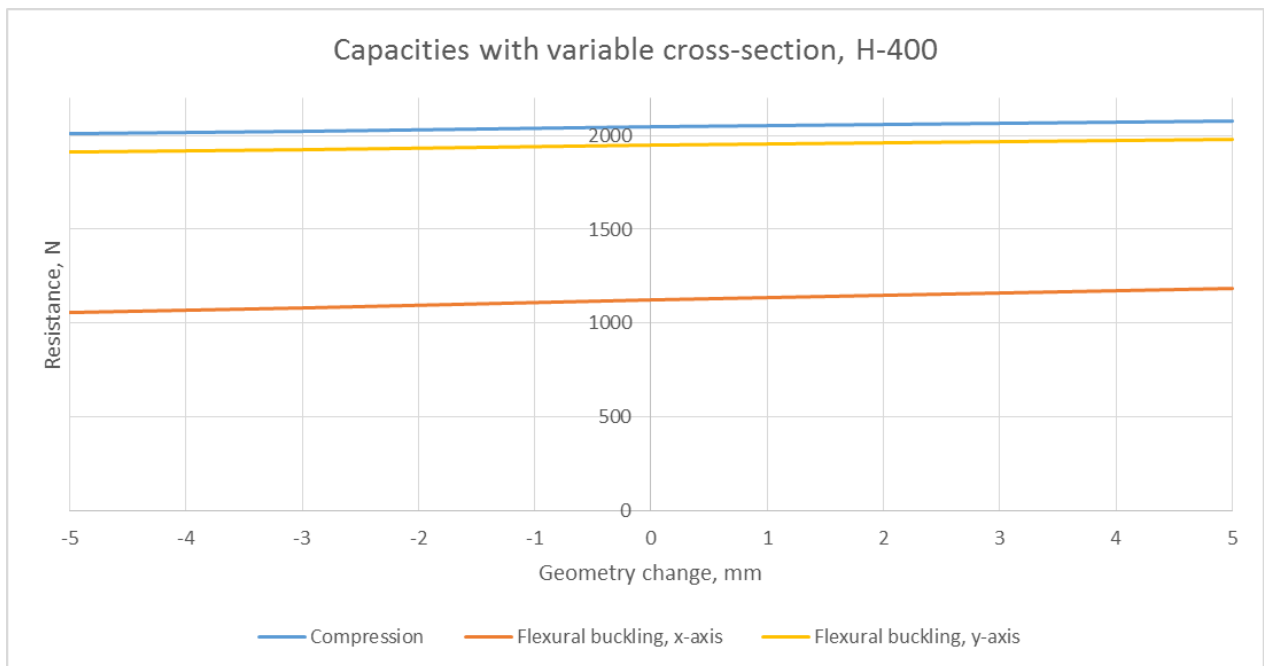


Figure 40: Capacities with variable cross-section, H-400

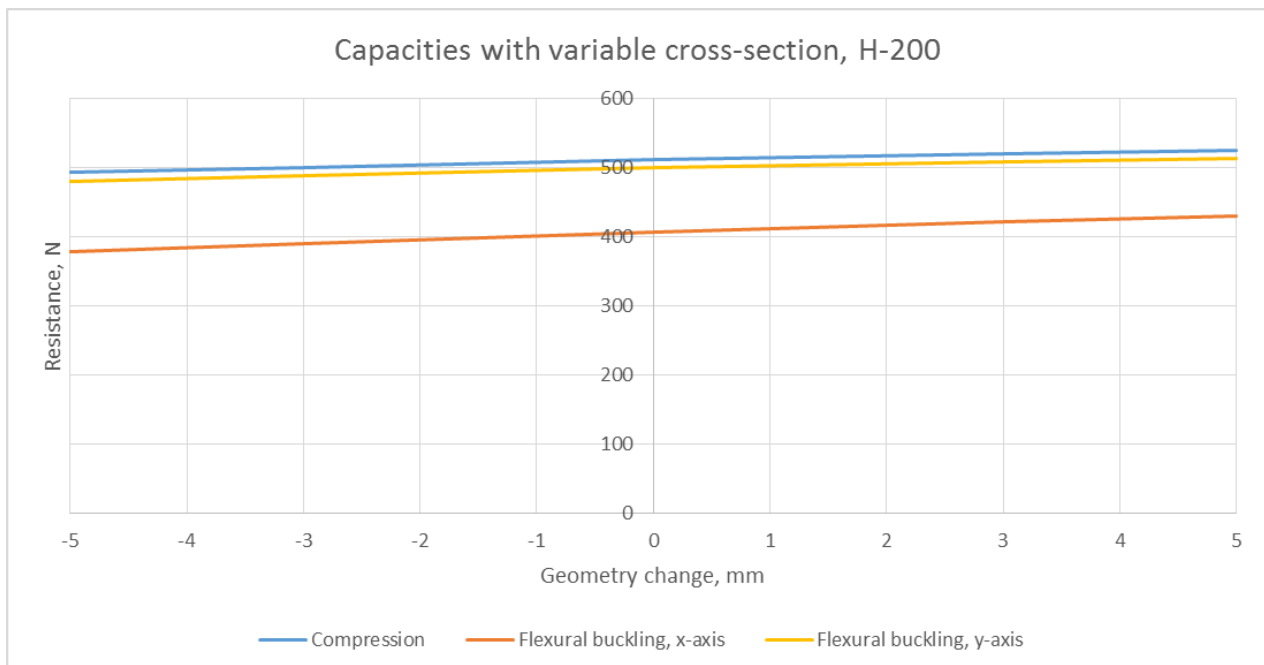


Figure 41: Capacities with variable cross-section, H-200

In its original state both the H-400 and H-200 cross-sections have a class 4 web and class 3 flanges, when subjected to axial compression. With the increase of flange width, the classification for the flanges changed to class 4. A reduction to the thickness is therefore required. In Eurocode 9 the required reduction is based on the actual slenderness of the component. Since the slenderness was barely categorized as class 4, the required reduction to the thickness became very small. Comparably, the web is considered very slender and the thickness was reduced with about 30 %.

The calculations of these cross-sections showed that the increase in moment of inertia was more influential than the required reduction of thickness. This is shown by the increase in flexural buckling resistance with increasing geometry dimensions. Since the permitted deviations are set as a constant value and not a function of width or height, the effect will be largest in small cross-sections. This was confirmed by the calculations. The overall change in flexural resistance was noticeable but not large, especially between -3 mm and 3 mm. As was discussed in chapter 4.8, the flexural buckling calculations done in accordance with Eurocode 9 are conservative. With the relative small differences in flexural buckling resistance while including the permitted deviations, and the knowledge that Eurocode 9 calculations are already conservative, it seems highly unlikely that a dangerous situation can occur when following the guidelines given by NS-EN 1090-3. The strict tolerance limits is most likely based on installation concerns, as uneven cross-sections may cause problems during installation of the member.

It should be noted that these permitted deviations are specified for a welded I-section and the calculations were performed for a cross-section without welds. This was done in order to ignore the effects of HAZ-softening (HAZ = heat affected zone) and focus on the impact of the changes in geometry. The results are still applicable for this discussion.

Chapter 6

6. Conclusion

With the calculations performed in this thesis, it is safe to say that initial imperfections definitely has a negative effect on the capacities of a member. A column with an initial out-of-straightness imperfection will not be able to withstand the same axial load as a perfectly straight column. The largest difference between a perfectly straight column and an imperfect column was in this thesis found for flexural buckling about the minor axis of the H-400 cross-section. With a 10 mm imperfection and a length of 2000 mm, the imperfect column could only carry 60% of the load that the perfect column could carry. A 40% loss in load carrying capacity is very large and a 10 mm imperfection could very easily go unnoticed. The largest difference between the perfect and the imperfect column always occurred for the lengths at which the perfect column would fail by crushing and the imperfect column would fail by flexural buckling. The effect of the imperfection was therefore more impactful on the short columns. The initial bend in the column makes the column much more susceptible to flexural buckling and a noticeable drop in load capacity can be seen. Effects such as inelastic buckling and loading imperfections are not considered in the Perry-Robertson formula. The results from the perfectly straight Perry-Robertson column is not likely to be applicable for real columns.

Since a 100% perfectly straight column is impossible to produce, it means that all columns will have an initial out-of-straightness imperfection. This imperfection will be very small in most cases. The imperfection is assumed to be at the midspan of the column, this will both simplify and be conservative with regards to the calculations. As discussed earlier, Eurocode 9 simplifies it further by using an imperfection of $L/750$ for all beams and columns regardless of production method. This is not an optimized solution. In chapter 4.5, both the imperfections $L/1500$ and $L/2000$ were compared with $L/750$ for the 200x10 mm quadratic hollow section. The largest difference between the $L/750$ and $L/1500$ imperfection was equal to 10% of the total load capacity at certain lengths. This difference is larger still between the $L/750$ and $L/2000$ imperfections.

Argument can be made against the efficiency of the Eurocode 9 flexural buckling resistance calculation method. In the result discussion from chapter 4, several point were brought up that might indicate poor optimization of the design capacity. The imperfection safety factor used by Eurocode 9 seems to be very conservative. If this factor were to be reduced, more efficient column design could be achieved.

The Perry-Robertson equation that was used to investigate the effect of the out-of-straightness imperfection is a simplified method. This means that the results will not be accurate when compared with a real column, but it gives a good indication of the columns capacity. By implementing the $L/750$ imperfection into the Perry-Robertson equation, the results were very similar to Eurocode 9 calculations. This indicates that the Perry-Robertson equation can be used to predict the effect that the out-of-straightness imperfections will have on Eurocode 9 capacities with good accuracy.

An extruded member is on average much straighter than the out-of-straightness tolerance limit [8] and the residual stress in the member will be insignificant [9]. An extruded column should then be close to the perfect column used in the Perry-Robertson equation. Eurocode 9 does not take production method of a member into consideration and so the same imperfection safety factor is used for all members. As seen throughout the calculations performed in this thesis, the difference between Eurocode 9 results and a perfect Perry-Robertson column is significant.

The imperfection safety factor cannot be removed completely, but it can be optimized. Buckling curves for the most common production methods, with their respective imperfection safety factor, could be presented in Eurocode 9. This choice between different production methods would most likely increase the flexural buckling resistance of an extruded column. The respective imperfection safety factor would have to be determined based on actual out-of-straightness measurements, with an allowance for other imperfection concerns and a safety factor.

As a conclusion to this investigation into the effect of the out-of-straightness imperfection, it must be said that the effect is significant. Relatively low imperfections were shown to have a large impact on the flexural buckling resistance. With the relatively large imperfection safety factor used in Eurocode 9 today, it is believed that the potential load capacity is heavily reduced in flexural buckling. Changes to this assumed crookedness cannot be based on the results given in this thesis, as the Perry-Robertson equation is a simplified method. A recommendation for further research into the optimization of the Eurocode 9 flexural buckling calculation method is given instead.

Chapter 7

7. Future work

The effect that imperfections and other tolerance limits will have on capacity calculations is a rather large field. Only a small part of it was discussed in this thesis. An out-of-straightness imperfection does not only affect the flexural buckling resistance, and its effect on other failure modes could be interesting to investigate.

The Perry-Robertson equation that were used in the calculations is a simplified method. The method was chosen to investigate the effect that the out-of-straightness imperfection has on Eurocode 9 capacities. The effect that the imperfection would have on a real column is therefore not precisely given from these calculations. The ANSYS results is a better representation of a real column, as it uses a bilinear stress-strain relationship. However, the ANSYS analysis has not been validated. A good way to validate an analysis is through laboratory experiments. In this case, it can be done by creating multiple columns, measuring their initial out-of-straightness imperfection and then apply an increasing axial load until failure. This will give the best possible indication off the actual effect that the imperfection has on flexural buckling resistance. The results can be used to validate both the ANSYS analysis and the Perry-Robertson calculations. The analysis result seem to interpret the effect of the imperfection similarly to the Perry-Robertson calculations, but an actual experiment might reveal a different effect.

Investigating other types of imperfections and their effect on the Eurocode 9 calculations should also be done. For a column, imperfections such as load eccentricity and support displacement can also cause a loss of load capacity. Support displacement will cause a column to have an initial unwanted sway. This inclined column will not experience the same loading situation as a perfectly straight column would. This type of imperfection can be especially impactful in buildings with a row of columns or multi-story buildings, as the imperfection might be applicable for all the columns. This will without doubt enhance the capacity loss for the columns. NS-EN 1090-3 includes permitted deviations for the sway of both a single column and columns that are part of a larger structure. It would be interesting to investigate these permitted deviations to make sure that they are sufficient. Imperfections of this sort is handled very similarly to the out-of-straightness imperfections by Eurocode 9. The imperfection is substituted with equivalent horizontal forces in order to simplify the calculations. The calculations in this thesis showed that this method was acceptable for the out-of-straightness imperfection and it would be interesting to find out if this is also true for the sway imperfection.

The Eurocode 9 buckling guidelines and calculations method showed poor optimization, when compared to the results from ANSYS and the Perry-Robertson equation. Conservative calculations is needed so that the finished structure has the required level of safety. Overly conservative calculation will however lead to wasted load carrying potential, which in turn will lead to material waste. To optimize the flexural buckling calculation method used in the present Eurocode 9, a lot of research and experiments must be performed. These must include the actual buckling behavior of columns with different types of cross-section and different aluminium alloys. As of today, the flexural buckling calculations in Eurocode 3 has more options for types of cross-section and material grade than Eurocode 9, this in turn is assumed to lead to a better optimization of steel columns than aluminium columns.

References

- [1] *NS-EN 1999-1-1:2007+A1:2009+NA:2009. Eurocode 9: Design of aluminium structures. Part 1-1: General structural rules.* Standard Norge, 2009.
- [2] *NS-EN 1993-1-1:NA:2008. Eurocode 3: Design of steel structures. Part 1-1: General rules and rules for buildings.* Standard Norge, 2008.
- [3] *NS-EN 1090-3:2008. Execution of steel structures and aluminium structures. Part 3: Technical requirements for aluminium structures.* Standard Norge, 2008.
- [4] Ganping Shu, Baofeng Zheng, Lianchun Xin. (2014). *A new design method for stainless steel columns subjected to flexural buckling.* Thin-Walled Structures, volume 83, p 43-51. Elsevier.
- [5] Guy Oyeniran Adeoti, Feng Fan, Yujin Wang, Ximei Zhai. (2015). *Stability of 6082-T6 aluminium alloy columns with H-section and rectangular hollow sections.* Thin-Walled Structures, vol. 89, p 1-16. Elsevier.
- [6] Petr Hradil, Ludovic Fülöp, Asko Talja. (2012). *Global stability of thin-walled ferritic stainless steel members.* Thin-Walled Structures, vol. 61, p 106-114. Elsevier.
- [7] J.B. Dwight. (1975). *Use of Perry formula to represent the new European strut curves.* IABSE reports of the working commissions, vol. 23, p 399-411.
- [8] P.S. Bulson (1992). *Aluminium Structural Analysis, Recent European Advances.* Elsevier Applied Science. Essex, England.
- [9] Theodore V. Galambos (1998). *Guide to Stability Design Criteria for Metal Structures, fifth edition.* John Wiley & Sons, inc. New York.
- [10] John Dwight (1999). *Aluminium Design and Construction.* E & FN SPON. New York.
- [11] K.J.R. Rasmussen, J. Rondal (1997). *Strength curves for metal columns.* Journal of Structural Engineering, vol 123, p 721-728. ASCE
- [12] Pål G. Bergan, Tor G. Syvertsen (1978). *Knekking av søyler og rammer.* Tapir
- [13] Rekha Bhoi, L.G. Kalurkar (2014). *Study of buckling behaviour of beam and column subjected to axial loading for various rolled I-sections.* IJIRSET, vol.3, issue 11, November 2014.
- [14] Arthur P. Boresi, Richard J. Schmidt (2003). *Advanced Mechanics of Materials, 6th edition.* John Wiley & Sons inc. Hoboken.

Appendix A: Cross-section properties and classification

A.1. The 200x10 mm quadratic hollow section

For a buckling analysis it is proficient to use a quadratic hollow section as it removes much of the concern for lateral-torsional buckling. During the analysis in this thesis, this is an advantage as flexural buckling is the main consideration. The 200x10 quadratic hollow section is widely used at Marine Aluminium and its properties are well known. However, for this thesis a slightly simplified version of the cross-section is used so the properties will be calculated using well-known formulas.

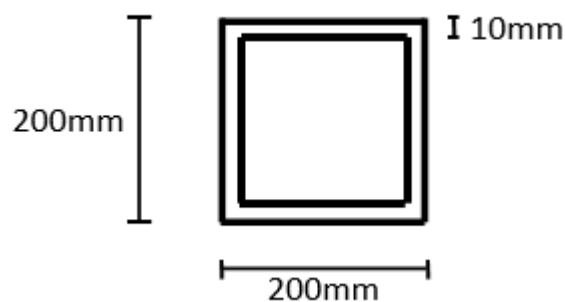


Figure 42: 200x10 mm quadratic hollow section

Area:

$$A = 2 \cdot 200\text{mm} \cdot 10\text{mm} + 2 \cdot 180\text{mm} \cdot 10\text{mm} = 7600\text{mm}^2$$

Second moment of inertia:

Since the cross-section is symmetric, there is no weak or strong axis. There exists only one second moment of inertia for this cross-section, Steiner's formula is used to find it:

$$I = 2 \cdot \left(\frac{1}{12} \cdot 200 \cdot 10^3 \right) + 2 \cdot (200 \cdot 10) \cdot (100 - 5)^2 + 2 \cdot \left(\frac{1}{12} \cdot 10 \cdot 180^3 \right) + 2 \cdot (180 \cdot 10) \cdot 0$$

$$I = 45853333.33 \text{ mm}^4$$

Cross-section classification, according to Eurocode 9 [1]:

6.1.4.3 Slenderness parameter:

$$\beta = \frac{b'}{t}$$

Where

- β = slenderness parameter
- b' = internal width
- t = thickness

$$\beta = \frac{(200 - 2 \cdot 10)}{10} = 18$$

6.1.4.4 Classification of cross-section parts

Table 10: Table 6.2 from Eurocode 9 [1]

Material classification according to Table 3.2	Internal part			Outstand part		
	β_1/ϵ	β_2/ϵ	β_3/ϵ	β_1/ϵ	β_2/ϵ	β_3/ϵ
Class A, without welds	11	16	22	3	4,5	6
Class A, with welds	9	13	18	2,5	4	5
Class B, without welds	13	16,5	18	3,5	4,5	5
Class B, with welds	10	13,5	15	3	3,5	4
$\epsilon = \sqrt{250/f_0}$, f_0 in N/mm ²						

According to Table 3.2b, the aluminium alloy 6082-T6 has buckling class A and has a yield strength of 250 MPa. For the use in this thesis the material is also without welds.

$$\epsilon = \sqrt{\frac{250}{f_0}} = \sqrt{\frac{250}{250}} = 1$$

This quadratic hollow section has a cross-section classification of **class 3**. Which means that there is no reduced thickness to allow for local buckling resistance in further calculations.

$$A = A_{eff}$$

A.2. The H-400 cross-section

The H-400 cross-section is a typical aluminium cross-section, consisting of very slender plates. This means that local buckling must be considered when using this type of cross-section. This cross-section may also be susceptible to lateral torsional buckling. It is made from 6082-T6 aluminium alloy, which gives it a yield strength of 250 MPa and buckling class A.

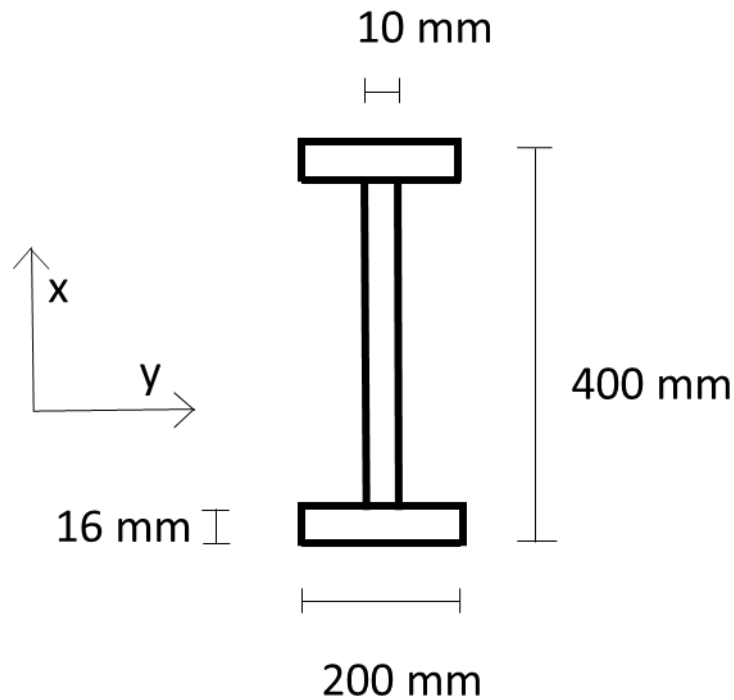


Figure 43: H-400 cross-section

Area:

$$A = 2 \cdot 200 \text{ mm} \cdot 16 \text{ mm} + (400 \text{ mm} - 2 \cdot 16 \text{ mm}) \cdot 10 \text{ mm}$$

$$A = 10080 \text{ mm}^2$$

Moment of inertia

This cross-section will have one minor and one major axis. Flexural buckling will normally happen with regards to the axis with the lowest moment of inertia.

$$\begin{aligned}
 I_y = & 2 \cdot \left(\frac{1}{12} \cdot 200 \text{ mm} \cdot (16 \cdot \text{mm})^3 \right) + 2 \cdot 200 \text{ mm} \cdot 16 \text{ mm} \cdot \left(\frac{400 \text{ mm}}{2} - \frac{16 \text{ mm}}{2} \right)^2 \\
 & + \left(\frac{1}{12} \cdot 10 \text{ mm} \cdot (368 \text{ mm})^3 \right) + 10 \text{ mm} \cdot 368 \text{ mm} \cdot 0^2
 \end{aligned}$$

$$I_y = 277596160 \text{ mm}^4$$

$$I_x = 2 \cdot \left(\frac{1}{12} \cdot 16 \text{ mm} \cdot (200 \text{ mm})^3 \right) + \left(\frac{1}{12} \cdot 368 \text{ mm} \cdot (10 \text{ mm})^3 \right)$$

$$I_x = 21364000 \text{ mm}^4$$

Cross-section classification, according to Eurocode 9 [1]:

6.1.4.3 Slenderness parameter:

The slenderness calculation is based on axial compression forces acting on the cross-section.

Slenderness flange:

$$\beta_f = \frac{\left(\frac{200 \text{ mm}}{2} - \frac{10 \text{ mm}}{2} \right)}{16 \text{ mm}} = 5.93$$

The flange has a cross-section classification of class 3. There will be no need for a reduced thickness.

Slenderness web:

$$\beta_w = \frac{(400 \text{ mm} - 2 \cdot 16 \text{ mm})}{10 \text{ mm}} = 36.8$$

The web has a cross-section classification of class 4. A reduced thickness is needed.

The reduced thickness is calculated in accordance with 6.1.5 [1]:

$$t'_w = t_w \cdot p_c$$

$$p_c = \frac{C_1}{\left(\frac{\beta_w}{\epsilon} \right)} - \frac{C_2}{\left(\frac{\beta_w}{\epsilon} \right)^2}$$

Where:

- $C_1 = 32$ for internal part
- $C_2 = 220$ for internal part
- $\epsilon = \sqrt{\frac{250}{f_0}} = 1$

$$p_c = \frac{32}{36.8} - \frac{220}{36.8^2} = 0.707$$

$$t'_w = 10 \text{ mm} \cdot 0.707 = 7.07 \text{ mm}$$

With this new web thickness, a new effective area must be calculated:

$$A_{eff} = 2 \cdot 200 \text{ mm} \cdot 16 \text{ mm} + 368 \text{ mm} \cdot 7.07 \text{ mm} = 9001.8 \text{ mm}^2$$

Appendix B: Eurocode 9 design calculations

B.1. 200x10 mm quadratic hollow section

In chapter 3, a pinned column with a 5 mm out-of-straightness imperfection was presented. Using the Perry-Robertson equation, it was found that this column had a load capacity ratio of 83% when it was 3750 mm long. In order to see the true effect of these calculation, the strength of this column will be calculated using the Eurocode 9 rules and guidelines.

6.2.4 Compression

Equation 6.20:

$$\frac{N_{Ed}}{N_{cRd}} \leq 1.0$$

Equation 6.22:

$$N_{cRd} = \frac{A_{eff} \cdot f_0}{\gamma_{M1}}$$

$$N_{cRd} = \frac{7600 \text{ mm}^2 \cdot 250 \text{ N/mm}^2}{1.10} = 1727 \text{ kN}$$

6.3.1.1 Buckling Resistance

Equation 6.48:

$$\frac{N_{Ed}}{N_{bRd}} \leq 1.0$$

Equation 6.49:

$$N_{bRd} = \frac{\kappa \cdot \chi \cdot A_{eff} \cdot f_0}{\gamma_{M1}}$$

Where:

- κ = factor to allow for the weakening effect of welding
- χ = reduction factor for the relevant buckling mode

Equation 6.50:

$$\chi = \frac{1}{\phi + \sqrt{\phi^2 - \bar{\lambda}^2}} \text{ but } \chi < 1.0$$

$$\phi = 0.5 \cdot (1 + \alpha \cdot (\bar{\lambda} - \bar{\lambda}_0) + \bar{\lambda}^2)$$

$$\bar{\lambda} = \sqrt{\frac{A_{eff} \cdot f_0}{N_{cr}}}$$

Where:

- $\alpha = \text{imperfection factor}$
- $\bar{\lambda} = \text{limit of horizontal plateau}$
- $N_{cr} = \text{Elastic critical force}$

For a member in compression, buckling must be checked for both flexural buckling and torsional-flexural buckling. However, for this situation only flexural buckling is considered.

Flexural buckling:

From table 6.6:

$$\alpha = 0.20$$

$$\bar{\lambda}_0 = 0.10$$

Slenderness for flexural buckling is defined in 6.3.1.3:

Equation 6.52:

$$\bar{\lambda} = \sqrt{\frac{A_{eff} \cdot f_0}{N_{cr}}} = \frac{L_{cr}}{i} \cdot \frac{1}{\pi} \cdot \sqrt{\frac{A_{eff}}{A} \cdot \frac{f_0}{E}}$$

Where:

- $L_{cr} = \text{buckling length or effective length}$
- $i = \text{radius of gyration about the relevant axis}$

Since this is a pinned situation the effective length will be equal to the actual length of the column. The cross-section was found to be a class 3 cross-section in appendix A, which means that the effective area is equal to the actual area. The radius of gyration is calculated using the following formula:

$$i = \sqrt{\frac{I_x}{A}} = \sqrt{\frac{45853333.33 \text{ mm}^4}{7600 \text{ mm}^2}} = 77.675 \text{ mm}$$

$$\bar{\lambda} = \frac{3750 \text{ mm}}{77.675 \text{ mm}} \cdot \frac{1}{\pi} \cdot \sqrt{\frac{7600 \text{ mm}^2}{7600 \text{ mm}^2} \cdot \frac{250 \text{ N/mm}^2}{71000 \text{ N/mm}^2}}$$

$$\bar{\lambda} = 0.912$$

Every variable for determining the buckling resistance for flexural buckling is now known, and the resistance can be found:

$$\phi = 0.5 \cdot (1 + 0.20 \cdot (0.912 - 0.10) + 0.912^2) = 0.997$$

$$\chi = \frac{1}{0.997 + \sqrt{0.997^2 - 0.912^2}} = 0.714$$

$$N b_{Rd} = \frac{0.714 \cdot 7600 \text{ mm}^2 \cdot 250 \text{ N/mm}^2}{1.10} = 1234 \text{ kN}$$

This is the maximum resistance for the flexural buckling case.

These calculations were repeated with different lengths to obtain the following table:

Table 11: Eurocode 9 resistances, 200x10 mm quadratic hollow section

Length	Compression resistance	Reduction factor, χ	Flexural buckling resistance
1 mm	1727 kN	1.000	1727 kN
500 mm	1727 kN	0.996	1720 kN
1000 mm	1727 kN	0.544	1676 kN
2000 mm	1727 kN	0.910	1572 kN
2500 mm	1727 kN	0.870	1502 kN
3000 mm	1727 kN	0.818	1412 kN
3750 mm	1727 kN	0.714	1234 kN
4500 mm	1727 kN	0.593	1024 kN
5000 mm	1727 kN	0.516	891 kN
5500 mm	1727 kN	0.447	772 kN
6000 mm	1727 kN	0.389	671 kN
6500 mm	1727 kN	0.339	586 kN
7000 mm	1727 kN	0.298	514 kN
7500 mm	1727 kN	0.264	455 kN
8000 mm	1727 kN	0.234	405 kN
8500 mm	1727 kN	0.210	362 kN
9000 mm	1727 kN	0.189	326 kN
9500 mm	1727 kN	0.170	294 kN
10000 mm	1727 kN	0.155	267 kN

B.2. H-400 cross-section

Eurocode 9 calculations will be performed once more, but this time with the H-400 cross-section. This is done in order to check if the results found in chapter 4 is applicable for other types of cross-sections as well. A check for both compression resistance and flexural buckling resistance must be done. The H-400 cross-section has slender elements, which means that a reduction in the thickness of the web is implemented in the calculations.

6.2.4 Compression

The maximum compression resistance is given as:

Equation 6.22

$$N_{cRd} = \frac{A_{eff} \cdot f_0}{\gamma_{M1}}$$

Where:

- $A_{eff} = \text{Effective Area} = 9001.8 \text{ mm}^2$
- $f_0 = \text{yield stress} = 250 \text{ MPa}$
- $\gamma_{M1} = \text{Material safety factor} = 1.10$

$$N_{cRd} = \frac{9001.8 \text{ mm}^2 \cdot 250 \text{ N/mm}^2}{1.10} = 2045.9 \text{ kN}$$

6.3.1.1. Buckling resistance

From Table 6.6

$$\alpha = \text{imperfection factor} = 0.20$$

$$\bar{\lambda}_0 = \text{limit of horizontal plateua} = 0.10$$

Equation 6.51:

$$\bar{\lambda} = \sqrt{\frac{A_{eff} \cdot f_0}{N_{cr}}}$$

Where:

- $\bar{\lambda}$ = relative slenderness
- N_{cr} = elastic critical force

For flexural buckling the relative slenderness can be found with another equation as well.

Equation 6.52:

$$\bar{\lambda} = \frac{L_{cr}}{i} \cdot \frac{1}{\pi} \cdot \sqrt{\frac{A_{eff}}{A} \cdot \frac{f_0}{E}}$$

Where:

- L_{cr} = buckling length = $k \cdot L$
- k = buckling length factor = 1
- E = Modulus of elasticity = 71000 MPa
- A = Gross area = 10080 mm²
- i = radius of gyration about the relevant axis

The column is assumed to be pinned, which results in the buckling length factor being 1. These calculations will be repeated different lengths varying from 0 mm to 10000 mm. The calculations will be shown for a length of 3000 mm. The calculations will be performed with regards to both axes. The radius of gyration can be determined using the following equation:

$$i_x = \sqrt{\frac{I_x}{A}} = \sqrt{\frac{21364000 \text{ mm}^4}{10080 \text{ mm}^2}} = 46.04 \text{ mm}$$

$$i_y = \sqrt{\frac{I_y}{A}} = \sqrt{\frac{277596160 \text{ mm}^4}{10080 \text{ mm}^2}} = 165.95 \text{ mm}$$

The moment of inertia was calculated in Appendix A.2. The rest of the calculations must be done twice, on time for each axis. Flexural buckling usually occurs about the axis with the lowest radius of gyration, in this case the x-axis.

Equation 6.52:

$$\bar{\lambda}_x = \frac{L_{cr}}{i_x} \cdot \frac{1}{\pi} \cdot \sqrt{\frac{A_{eff}}{A} \cdot \frac{f_0}{E}} = \frac{3000 \text{ mm}}{46.04 \text{ mm}} \cdot \frac{1}{\pi} \cdot \sqrt{\frac{9001.8 \text{ mm}^2}{10080 \text{ mm}^2} \cdot \frac{250 \text{ N/mm}^2}{71000 \text{ N/mm}^2}}$$

$$\bar{\lambda}_x = 1.16$$

$$\bar{\lambda}_y = \frac{L_{cr}}{i_y} \cdot \frac{1}{\pi} \cdot \sqrt{\frac{A_{eff}}{A} \cdot \frac{f_0}{E}} = \frac{3000 \text{ mm}}{165.95 \text{ mm}} \cdot \frac{1}{\pi} \cdot \sqrt{\frac{9001.8 \text{ mm}^2}{10080 \text{ mm}^2} \cdot \frac{250 \text{ N/mm}^2}{71000 \text{ N/mm}^2}}$$

$$\bar{\lambda}_y = 0.323$$

A huge difference can be seen between the two values of relative slenderness. A large relative slenderness will result in a large reduction factor.

Equation 6.50

$$\chi = \frac{1}{\phi + \sqrt{\phi^2 - \bar{\lambda}^2}} \text{ but } \chi < 1$$

Where:

- $\chi = \text{reduction factor}$

$$\phi = 0.5 \cdot (1 + \alpha \cdot (\bar{\lambda} - \bar{\lambda}_0) + \bar{\lambda}^2)$$

$$\phi_x = 0.5 \cdot (1 + \alpha \cdot (\bar{\lambda}_x - \bar{\lambda}_0) + \bar{\lambda}_x^2) = 0.5 \cdot (1 + 0.2 \cdot (1.16 - 0.10) + 1.16^2)$$

$$\phi_x = 1.28$$

$$\phi_y = 0.5 \cdot (1 + \alpha \cdot (\bar{\lambda}_y - \bar{\lambda}_0) + \bar{\lambda}_y^2) = 0.5 \cdot (1 + 0.2 \cdot (0.323 - 0.10) + 0.323^2)$$

$$\phi_y = 0.574$$

$$\chi_x = \frac{1}{\phi_x + \sqrt{\phi_x^2 - \bar{\lambda}_x^2}} = \frac{1}{1.28 + \sqrt{1.28^2 - 1.16^2}}$$

$$\chi_x = 0.55$$

$$\chi_y = \frac{1}{\phi_y + \sqrt{\phi_y^2 - \bar{\lambda}_y^2}} = \frac{1}{0.574 + \sqrt{0.574^2 - 0.323^2}}$$

$$\chi_y = 0.95$$

A large difference is seen here. For this 5000 mm column, the reduction factor is simply huge for the x-axis. The actual flexural resistance can now be calculated:

Equation 6.49

$$Nb_{Rd} = \frac{\kappa \cdot \chi \cdot A_{eff} \cdot f_0}{\gamma_{M1}}$$

Where:

- κ = factor to allow for the weakening effect of welding = 1

$$Nb_{Rd-x} = \frac{\kappa \cdot \chi_x \cdot A_{eff} \cdot f_0}{\gamma_{M1}} = \frac{1 \cdot 0.55 \cdot 9001.8 \text{ mm}^2 \cdot 250 \frac{\text{N}}{\text{mm}^2}}{1.10}$$

$$Nb_{Rd-x} = 1125.2 \text{ kN}$$

$$Nb_{Rd-y} = \frac{\kappa \cdot \chi_y \cdot A_{eff} \cdot f_0}{\gamma_{M1}} = \frac{1 \cdot 0.95 \cdot 9001.8 \text{ mm}^2 \cdot 250 \frac{\text{N}}{\text{mm}^2}}{1.10}$$

$$Nb_{Rd-y} = 1943.6 \text{ kN}$$

The calculations are repeated for different lengths, the results are tabulated below:

Table 12: Eurocode 9 resistances, H-400

Length	Compression resistance	Reduction factor		Flexural buckling resistance	
		χ_x	χ_y	Nb_{Rd-x}	Nb_{Rd-y}
1 mm	2045.9 kN	1.000	1.000	2045.9 kN	2045.9 kN
500 mm	2045.9 kN	0.981	1.000	2006.7 kN	2045.9 kN
1000 mm	2045.9 kN	0.937	0.998	1917.4 kN	2042.7 kN
1500 mm	2045.9 kN	0.879	0.988	1799.2 kN	2020.4 kN
2000 mm	2045.9 kN	0.795	0.976	1625.4 kN	1997.7 kN
2500 mm	2045.9 kN	0.677	0.965	1384.7 kN	1974.2 kN
3000 mm	2045.9 kN	0.550	0.950	1125.2 kN	1943.6 kN
3500 mm	2045.9 kN	0.437	0.940	849.2 kN	1923.2 kN
4000 mm	2045.9 kN	0.351	0.926	717.3 kN	1849.8 kN
4500 mm	2045.9 kN	0.285	0.911	583.8 kN	1863.9 kN
5000 mm	2045.9 kN	0.236	0.894	482.6 kN	1829.7 kN
5500 mm	2045.9 kN	0.198	0.876	404.8 kN	1791.8 kN
6000 mm	2045.9 kN	0.168	0.855	344.0 kN	1749.5 kN
6500 mm	2045.9 kN	0.145	0.832	295.8 kN	1702.1 kN
7000 mm	2045.9 kN	0.126	0.806	256.9 kN	1649.3 kN
7500 mm	2045.9 kN	0.110	0.778	225.1 kN	1590.7 kN
8000 mm	2045.9 kN	0.097	0.746	198.9 kN	1526.8 kN
8500 mm	2045.9 kN	0.087	0.713	177.0 kN	1458.3 kN
9000 mm	2045.9 kN	0.077	0.678	158.5 kN	1386.4 kN
9500 mm	2045.9 kN	0.070	0.642	142.7 kN	1312.7 kN
10000 mm	2045.9 kN	0.063	0.606	129.2 kN	1238.8 kN

Appendix C: Eurocode 9 imperfect column design

C.1. Equivalent horizontal forces method.

The column will be 5000 mm long and have an initial out-of-straightness imperfection equal to 10 mm. This imperfection will be larger than $L/750$ and so it must be calculated using Eurocode's equivalent horizontal forces. The horizontal forces is in the form of an evenly distributed load. With these horizontal forces working on the column, shear and moment forces will arise as well as the existing axial forces. The design resistance of the column will be the lowest of the bending resistance, shear resistance, compression resistance and flexural buckling resistance.

The length and imperfection was chosen to coincide with a known point from the ANSYS analyses. The cross-section will be a 200x10 quadratic hollow section; the cross-sectional properties are shown in Appendix A.1.

Compression resistance:

Compression resistance is only dependent on area and yield stress, it was calculated in Appendix B.1.

$$N_{C_{Rd}} = \frac{A_{eff} \cdot f_0}{\gamma_{M1}}$$

$$N_{C_{Rd}} = \frac{7600 \text{ mm}^2 \cdot 250 \text{ N/mm}^2}{1.10} = 1727 \text{ kN}$$

Bending resistance:

6.2.5.1: The bending moment resistance is to be taken as the lesser of:

Equation 6.24:

$$M_{u_{Rd}} = \frac{W_{net} \cdot f_u}{\gamma_{M2}}$$

And:

Equation 6.25:

$$M_{c_{Rd}} = \frac{\alpha \cdot W_{el} \cdot f_0}{\gamma_{M1}}$$

W_{net} is the elastic modulus of the net section allowing for holes and HAZ softening. As the cross-section used has neither holes nor have been welded, the net section is equal to the elastic modulus for the gross section.

$$W_{net} = W_{el}$$

$$W_{el} = \frac{I_x}{y} = \frac{45853333.33 \text{ mm}^4}{100 \text{ mm}} = 458533.33 \text{ mm}^3$$

$$Mu_{Rd} = \frac{458533.33 \text{ mm}^3 \cdot 290 \text{ N/mm}^2}{1.25} = 106.4 \text{ kNm}$$

According to Table 6.4:

$$\alpha = \alpha_{3,u} = 1$$

$$Mc_{Rd} = \frac{\alpha \cdot W_{el} \cdot f_0}{\gamma_{M1}} = \frac{1 \cdot 458533.33 \text{ mm}^3 \cdot 250 \text{ N/mm}^2}{1.10} = 104.2 \text{ kNm}$$

The bending moment resistance is equal to 104.2 kNm.

$$M_{y,Rd} = 104.2 \text{ kNm}$$

Corresponding maximum axial load is found using the relationship between bending moment and axial force, as it is given in the equivalent horizontal forces method:

$$M_{y,Ed} = N_{Ed} \cdot \delta_0$$

$$N_{Ed} = \frac{104.2 \text{ kNm}}{10 \text{ mm}} = 10420 \text{ kN}$$

Shear:

Equation 6.29:

$$V_{Rd} = A_v \cdot \frac{f_0}{\sqrt{3} \cdot \gamma_{M1}}$$

Where:

- $A_v = \text{Shear area}$

$$V_{Rd} = 2 \cdot 200 \text{ mm} \cdot 10 \text{ mm} \cdot \frac{250 \text{ N/mm}^2}{\sqrt{3} \cdot 1.10}$$

$$V_{Rd} = 524.9 \text{ kN}$$

Corresponding maximum axial load:

$$V_{Ed} = \frac{4 \cdot N_{Ed} \cdot e_{0d}}{L^2}$$
$$N_{Ed} = \frac{524.9 \text{ kN} \cdot 5000 \text{ mm}}{4 \cdot 10 \text{ mm}} = 65612.5 \text{ kN}$$

Flexural buckling:

The new horizontal forces does not have any impact on flexural resistance due to axial load, the result is therefore the same as in Appendix B.1.

$$N_{bRd} = \frac{0.516 \cdot 7600 \text{ mm}^2 \cdot 250 \text{ N/mm}^2}{1.10} = 891.2 \text{ kN}$$

C.2: Imperfection effect

The effect that different values of imperfection has on the capacities of an imperfect Eurocode 9 column will be considered. Three columns with different lengths will be used: 3000 mm, 5000 mm and 7500 mm. The 200x10 mm quadratic hollow section will be used. The maximum allowable axial load with no imperfection has been calculated for these lengths in Appendix B.1. Imperfections ranging from 0 mm to 20 mm will be considered.

The out-of-straightness imperfection will be described using the equivalent horizontal force method. In chapter 4.6, it was determined that the flexural buckling criteria for members in bending and axial compression is the governing design criteria for these columns. The following relationship exists between the bending moment and the axial load:

$$M_{y,Ed} = N_{Ed} \cdot e_{0d}$$

The governing criteria:

Equation 6.62 [1]:

$$\left(\frac{N_{Ed}}{\chi_{min} \cdot \omega_x \cdot N_{Rd}} \right)^{\psi_c} + \frac{1}{\omega_0} \left(\left(\frac{M_{y,Ed}}{M_{y,Rd}} \right)^{1.7} + \left(\frac{M_{z,Ed}}{M_{z,Rd}} \right)^{1.7} \right)^{0.6} \leq 1.00$$

$$\left(\frac{N_{Ed}}{\chi_{min} \cdot \omega_x \cdot N_{Rd}} \right)^{\psi_c} + \frac{1}{\omega_0} \left(\left(\frac{N_{Ed} \cdot e_{0d}}{M_{y,Rd}} \right)^{1.7} + \left(\frac{0}{M_{z,Rd}} \right)^{1.7} \right)^{0.6} \leq 1.00$$

The bending moment resistance and compression resistance is determined in Appendix C.1. The flexural buckling reduction factor is determined in Appendix B.1., this factor is dependent on length and will be different for the columns at are going to be tested.

From Appendix B.1.:

- $L = 3000 \text{ mm} \rightarrow \chi_{min} = 0.818 \rightarrow N_{Ed} = 1412 \text{ kN}$
- $L = 5000 \text{ mm} \rightarrow \chi_{min} = 0.516 \rightarrow N_{Ed} = 891 \text{ kN}$
- $L = 7500 \text{ mm} \rightarrow \chi_{min} = 0.264 \rightarrow N_{Ed} = 455 \text{ kN}$

From Appendix C.1.:

- $N_{Rd} = 1727 \text{ kN}$
- $M_{y,Rd} = 104.2 \text{ kNm}$

From Eurocode 9:

- $\psi_c = 0.8$
- $\omega_x = \omega_0 = 1$

To determine the maximum axial load that satisfies the criteria, the value will be guessed. The results are shown in Table 13.

Table 13: Eurocode 9, imperfection effect

Imperfection (mm)	$L = 3000 \text{ mm}$		$L = 5000 \text{ mm}$		$L = 7500 \text{ mm}$	
	N_{Ed}	M_{Ed}	N_{Ed}	M_{Ed}	N_{Ed}	M_{Ed}
0	1412 kN	0.00 kNm	891 kN	0.00 kNm	455 kN	0.00 kNm
2	1370 kN	2.74 kNm	873 kN	1.75 kNm	451 kN	0.90 kNm
4	1328 kN	5.31 kNm	856 kN	3.42 kNm	446 kN	1.78 kNm
6	1290 kN	7.74 kNm	840 kN	5.04 kNm	442 kN	2.65 kNm
8	1252 kN	10.0 kNm	824 kN	6.59 kNm	438 kN	3.05 kNm
10	1218 kN	12.2 kNm	809 kN	8.09 kNm	433 kN	4.33 kNm
12	1185 kN	14.2 kNm	794 kN	9.53 kNm	429 kN	5.15 kNm
14	1153 kN	16.1 kNm	780 kN	10.92 kNm	425 kN	5.95 kNm
16	1125 kN	18.0 kNm	767 kN	12.27 kNm	421 kN	6.74 kNm
18	1096 kN	19.3 kNm	754 kN	13.57 kNm	417 kN	7.50 kNm
20	1069 kN	23.4 kNm	741 kN	14.82 kNm	413 kN	8.26 kNm

Appendix D: Perry-Robertson calculations

To gain a better understanding of the effect that an initial out-of-straightness imperfection has on the flexural buckling resistance, the buckling curve for a member with a constant imperfection will be presented. As can be seen from the Figure 44, a pinned situation will be considered. The deformation will then take the shape of a sinusoidal curve. The Perry-Robertson equation that was derived in chapter 2.8 will be used to determine the buckling curve. The results from using this equation will be given as a stress ratio at failure. If the ratio is equal to 1, it means that column has failed by crushing. Ratios lower than 1 indicates failure by flexural buckling. The stress ratio is based on experienced stress at failure divided by the yield stress. The test will be repeated for different values of imperfection and different cross-sections.

D.1. 10 mm imperfection, 200x10 mm quadratic hollow section

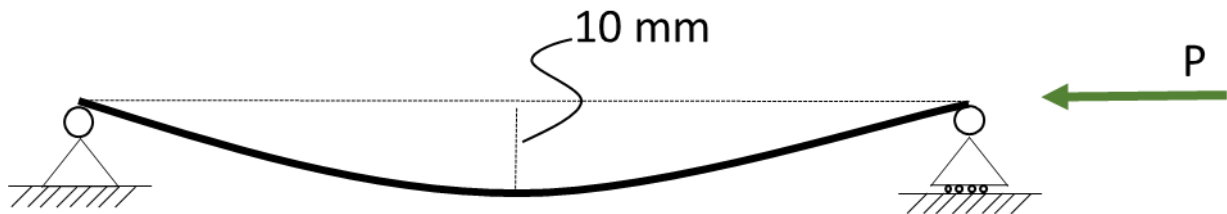


Figure 44: Imperfect column model, 10 mm imperfection

For the first test, a 200x10 mm quadratic hollow section will be used. This cross-section is an ideal choice for investigating the flexural buckling resistance, as this cross-section type is not as likely to fail due to torsional-flexural buckling and it is not susceptible to lateral torsional buckling. The basic cross-sectional properties is given in Appendix A.1. As the 200x10 mm quadratic hollow section is symmetric about both axes, there is no major or minor axis about which buckling can occurs.

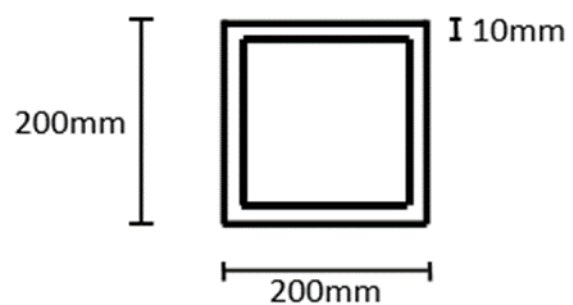


Figure 45: 200x10 mm quadratic hollow section

Imperfection at midspan:

$$\delta_0 = 10 \text{ mm}$$

Effective buckling length factor:

$$k = 1$$

Area of cross-section:

$$A = 7600 \text{ mm}^2$$

Moment of inertia:

$$I = 45853333.33 \text{ mm}^4$$

Distance to neutral axis:

$$y = 100 \text{ mm}$$

Modulus of elasticity:

$$E = 71000 \text{ MPa}$$

Yield stress:

$$\sigma_y = 250 \text{ MPa}$$

Radius of gyration:

$$r = \sqrt{\frac{I}{A}} = \sqrt{\frac{45853333.33 \text{ mm}^4}{7600 \text{ mm}^2}} = 77.67 \text{ mm}$$

Imperfection variable:

$$\eta = \frac{\delta_0 \cdot y}{r^2} = \frac{10 \text{ mm} \cdot 100 \text{ mm}}{(77.67 \text{ mm})^2} = 0.166$$

Euler's critical load:

$$P_E = \frac{\pi^2 \cdot E \cdot I}{(k \cdot L)^2}$$

Euler's critical stress:

$$\sigma_E = \frac{P_E}{A} = \frac{\pi^2 \cdot E \cdot I}{(k \cdot L)^2 \cdot A}$$

Perry-Robertson stress ratio:

$$\frac{\sigma}{\sigma_y} = 0.5 \cdot \left(\left(1 + \frac{\sigma_E}{\sigma_y} \cdot (\eta + 1) \right) - \sqrt{\left(1 + \frac{\sigma_E}{\sigma_y} \cdot (\eta + 1) \right)^2 - 4 \cdot \frac{\sigma_E}{\sigma_y}} \right)$$

Table 14: Perry-Robertson results, 10 mm imperfection, 200x10 mm quadratic hollow section

Length (mm)	Euler's stress, σ_E (MPa)	Stress ratio, $\frac{\sigma}{\sigma_y}$	Length (mm)	Euler's stress, σ_E (MPa)	Stress ratio, $\frac{\sigma}{\sigma_y}$
1	4.22e^9	0.858	10500	38.31	0.149
500	16894.10	0.856	11000	34.91	0.136
1000	4223.52	0.851	11500	31.94	0.125
1500	1877.12	0.843	12000	29.33	0.11
2000	1055.88	0.829	12500	27.03	0.11
2500	675.76	0.809	13000	24.99	0.10
3000	469.28	0.779	13500	23.17	0.09
3500	344.78	0.737	14000	21.55	0.08
4000	263.97	0.681	14500	20.09	0.08
4500	208.57	0.614	15000	18.77	0.07
5000	168.94	0.543	15500	17.58	0.07
5500	139.62	0.475	16000	16.50	0.07
6000	117.32	0.414	16500	15.51	0.06
6500	99.97	0.362	17000	14.61	0.06
7000	86.19	0.318	17500	13.79	0.05
7500	75.08	0.281	18000	13.04	0.05
8000	65.99	0.249	18500	12.34	0.05
8500	58.46	0.223	19000	11.70	0.05
9000	52.14	0.200	19500	11.11	0.04
9500	46.80	0.180	20000	10.56	0.04
10000	42.24	0.163			

D.2. 15 mm imperfection, 200x10 mm quadratic hollow section

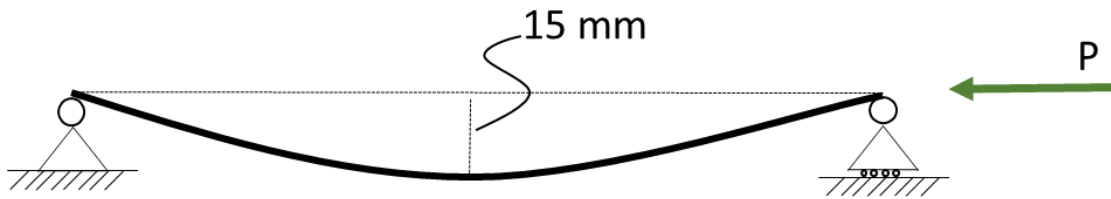


Figure 46: Imperfect column model, 15 mm imperfection

The calculations are repeated for an imperfection of 15 mm.

Imperfection at midspan:

$$\delta_0 = 15 \text{ mm}$$

Effective buckling length factor:

$$k = 1$$

Area of cross-section:

$$A = 7600 \text{ mm}^2$$

Moment of inertia:

$$I = 45853333.33 \text{ mm}^4$$

Distance to neutral axis:

$$y = 100 \text{ mm}$$

Modulus of elasticity:

$$E = 71000 \text{ MPa}$$

Yield stress:

$$\sigma_y = 250 \text{ MPa}$$

Radius of gyration:

$$r = \sqrt{\frac{I}{A}} = \sqrt{\frac{45853333.33 \text{ mm}^4}{7600 \text{ mm}^2}} = 77.67 \text{ mm}$$

Imperfection variable:

$$\eta = \frac{\delta_0 \cdot y}{r^2} = \frac{15 \text{ mm} \cdot 100 \text{ mm}}{(77.67 \text{ mm})^2} = 0.249$$

Euler's critical load:

$$P_E = \frac{\pi^2 \cdot E \cdot I}{(k \cdot L)^2}$$

Euler's critical stress:

$$\sigma_E = \frac{P_E}{A} = \frac{\pi^2 \cdot E \cdot I}{(k \cdot L)^2 \cdot A}$$

Perry-Robertson stress ratio:

$$\frac{\sigma}{\sigma_y} = 0.5 \cdot \left(\left(1 + \frac{\sigma_E}{\sigma_y} \cdot (\eta + 1) \right) - \sqrt{\left(1 + \frac{\sigma_E}{\sigma_y} \cdot (\eta + 1) \right)^2 - 4 \cdot \frac{\sigma_E}{\sigma_y}} \right)$$

Table 15: Perry-Robertson results, 15 mm imperfection, 200x10 mm quadratic hollow section

Length (mm)	Euler's stress, σ_E (MPa)	Stress ratio, $\frac{\sigma}{\sigma_y}$	Length (mm)	Euler's stress, σ_E (MPa)	Stress ratio, $\frac{\sigma}{\sigma_y}$
1	4.22e^9	0.801	10500	38.31	0.147
500	16894.10	0.799	11000	34.91	0.134
1000	4223.52	0.793	11500	31.94	0.123
1500	1877.12	0.783	12000	29.33	0.114
2000	1055.88	0.767	12500	27.03	0.105
2500	675.76	0.745	13000	24.99	0.097
3000	469.28	0.714	13500	23.17	0.090
3500	344.78	0.673	14000	21.55	0.084
4000	263.97	0.623	14500	20.09	0.079
4500	208.57	0.565	15000	18.77	0.074
5000	168.94	0.505	15500	17.58	0.069
5500	139.62	0.446	16000	16.50	0.065
6000	117.32	0.394	16500	15.51	0.061
6500	99.97	0.347	17000	14.61	0.058
7000	86.19	0.307	17500	13.79	0.054
7500	75.08	0.272	18000	13.04	0.051
8000	65.99	0.243	18500	12.34	0.049
8500	58.46	0.218	19000	11.70	0.046
9000	52.14	0.196	19500	11.11	0.044
9500	46.80	0.177	20000	10.56	0.042
10000	42.24	0.161			

D.3. 5 mm imperfection, 200x10 mm quadratic hollow section

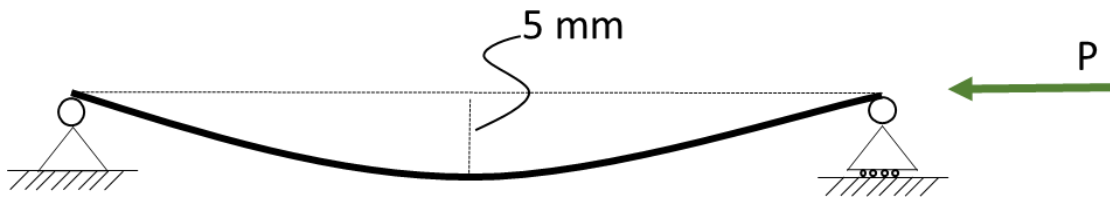


Figure 47: Imperfect column model, 5 mm imperfection

The calculations are repeated for an imperfection for an imperfection of 5 mm.

Imperfection at midspan:

$$\delta_0 = 5 \text{ mm}$$

Effective buckling length factor:

$$k = 1$$

Area of cross-section:

$$A = 7600 \text{ mm}^2$$

Moment of inertia:

$$I = 45853333.33 \text{ mm}^4$$

Distance to neutral axis:

$$y = 100 \text{ mm}$$

Modulus of elasticity:

$$E = 71000 \text{ MPa}$$

Yield stress:

$$\sigma_y = 250 \text{ MPa}$$

Radius of gyration:

$$r = \sqrt{\frac{I}{A}} = \sqrt{\frac{45853333.33 \text{ mm}^4}{7600 \text{ mm}^2}} = 77.67 \text{ mm}$$

Imperfection variable:

$$\eta = \frac{\delta_0 \cdot y}{r^2} = \frac{5 \text{ mm} \cdot 100 \text{ mm}}{(77.67 \text{ mm})^2} = 0.0829$$

Euler's critical load:

$$P_E = \frac{\pi^2 \cdot E \cdot I}{(k \cdot L)^2}$$

Euler's critical stress:

$$\sigma_E = \frac{P_E}{A} = \frac{\pi^2 \cdot E \cdot I}{(k \cdot L)^2 \cdot A}$$

Perry-Robertson stress ratio:

$$\frac{\sigma}{\sigma_y} = 0.5 \cdot \left(\left(1 + \frac{\sigma_E}{\sigma_y} \cdot (\eta + 1) \right) - \sqrt{\left(1 + \frac{\sigma_E}{\sigma_y} \cdot (\eta + 1) \right)^2 - 4 \cdot \frac{\sigma_E}{\sigma_y}} \right)$$

Table 16: Perry-Robertson results, 5 mm imperfection, 200x10 mm quadratic hollow section

Length (mm)	Euler's stress, σ_E (MPa)	Stress ratio, $\frac{\sigma}{\sigma_y}$	Length (mm)	Euler's stress, σ_E (MPa)	Stress ratio, $\frac{\sigma}{\sigma_y}$
1	4.22e^9	0.923	10500	38.31	0.151
500	16894.10	0.922	11000	34.91	0.138
1000	4223.52	0.919	11500	31.94	0.126
1500	1877.12	0.914	12000	29.33	0.116
2000	1055.88	0.905	12500	27.03	0.107
2500	675.76	0.890	13000	24.99	0.099
3000	469.28	0.867	13500	23.17	0.092
3500	344.78	0.828	14000	21.55	0.086
4000	263.97	0.767	14500	20.09	0.080
4500	208.57	0.684	15000	18.77	0.075
5000	168.94	0.594	15500	17.58	0.070
5500	139.62	0.510	16000	16.50	0.066
6000	117.32	0.439	16500	15.51	0.062
6500	99.97	0.380	17000	14.61	0.058
7000	86.19	0.331	17500	13.79	0.055
7500	75.08	0.290	18000	13.04	0.052
8000	65.99	0.256	18500	12.34	0.049
8500	58.46	0.228	19000	11.70	0.047
9000	52.14	0.204	19500	11.11	0.044
9500	46.80	0.184	20000	10.56	0.042
10000	42.24	0.166			

D.4. No imperfection, 200x10 mm quadratic hollow section

The calculations are performed once more for a column without any imperfection. This is done in order to compare the results for this “perfect” column, with the results found for imperfect columns. Although a “perfect” column does not exist, the buckling curve will still be interesting to develop.

Imperfection at midspan:

$$\delta_0 = 0 \text{ mm}$$

Effective buckling length factor:

$$k = 1$$

Area of cross-section:

$$A = 7600 \text{ mm}^2$$

Moment of inertia:

$$I = 45853333.33 \text{ mm}^4$$

Distance to neutral axis:

$$y = 100 \text{ mm}$$

Modulus of elasticity:

$$E = 71000 \text{ MPa}$$

Yield stress:

$$\sigma_y = 250 \text{ MPa}$$

Radius of gyration:

$$r = \sqrt{\frac{I}{A}} = \sqrt{\frac{45853333.33 \text{ mm}^4}{7600 \text{ mm}^2}} = 77.67 \text{ mm}$$

Imperfection variable:

$$\eta = \frac{\delta_0 \cdot y}{r^2} = \frac{0 \text{ mm} \cdot 100 \text{ mm}}{(77.67 \text{ mm})^2} = 0.00$$

Euler's critical load:

$$P_E = \frac{\pi^2 \cdot E \cdot I}{(k \cdot L)^2}$$

Euler's critical stress:

$$\sigma_E = \frac{P_E}{A} = \frac{\pi^2 \cdot E \cdot I}{(k \cdot L)^2 \cdot A}$$

Perry-Robertson stress ratio:

$$\frac{\sigma}{\sigma_y} = 0.5 \cdot \left(\left(1 + \frac{\sigma_E}{\sigma_y} \cdot (\eta + 1) \right) - \sqrt{\left(1 + \frac{\sigma_E}{\sigma_y} \cdot (\eta + 1) \right)^2 - 4 \cdot \frac{\sigma_E}{\sigma_y}} \right)$$

Table 17: Perry-Robertson results, no imperfection, 200x10 mm quadratic hollow section

Length (mm)	Euler's stress, σ_E (MPa)	Stress ratio, $\frac{\sigma}{\sigma_y}$	Length (mm)	Euler's stress, σ_E (MPa)	Stress ratio, $\frac{\sigma}{\sigma_y}$
1	4.22e^9	1.000	10500	38.31	0.153
500	16894.10	1.000	11000	34.91	0.140
1000	4223.52	1.000	11500	31.94	0.128
1500	1877.12	1.000	12000	29.33	0.117
2000	1055.88	1.000	12500	27.03	0.108
2500	675.76	1.000	13000	24.99	0.100
3000	469.28	1.000	13500	23.17	0.093
3500	344.78	1.000	14000	21.55	0.086
4000	263.97	1.000	14500	20.09	0.080
4500	208.57	0.834	15000	18.77	0.075
5000	168.94	0.676	15500	17.58	0.070
5500	139.62	0.558	16000	16.50	0.066
6000	117.32	0.469	16500	15.51	0.062
6500	99.97	0.400	17000	14.61	0.058
7000	86.19	0.345	17500	13.79	0.055
7500	75.08	0.300	18000	13.04	0.052
8000	65.99	0.264	18500	12.34	0.049
8500	58.46	0.234	19000	11.70	0.047
9000	52.14	0.209	19500	11.11	0.044
9500	46.80	0.187	20000	10.56	0.042
10000	42.24	0.169			

D.5. 10 mm imperfection, H-400 cross-section - Minor axis

Buckling curves will also be developed for the H-400 cross-section. This is done in order to compare the buckling curves for H-400 and the 200x10 mm quadratic hollow section. The H-400 cross-section is very slender and the web is susceptible to local buckling. This is not accounted for in the Perry-Robertson equation and so it is expected that the differences between the Perry-Robertson results and Eurocode 9 results will be larger for the H-400 cross-section compared with the 200x10 mm quadratic hollow section. Lateral torsional buckling might also be a problem for this I-section.

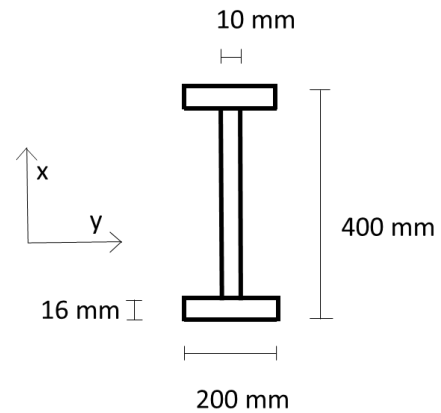


Figure 48: H-400 cross-section

Calculations of the capacity for this section will be performed with regards to flexural buckling about both major and minor axis. The cross-sectional properties was calculated in Appendix A.2. The differences between the major and minor axes is the moment of inertia and the radius of gyration, as well as the distance to the neutral axis. Flexural buckling occurs about the axis with the largest slenderness ratio and the smallest radius of gyration. This is then called the minor axis. This means that buckling must be suppressed with regards to the minor axis if buckling is ever to occur about the major axis. This is however common practice and the results for the major axis will be equally interesting. The following calculations is for the minor axis, while the calculations for the major axis is performed in Appendix D.7.

Imperfection at midspan:

$$\delta_0 = 10 \text{ mm}$$

Effective buckling length factor:

$$k = 1$$

Area of cross-section:

$$A = 10080 \text{ mm}^2$$

Moment of inertia:

$$I_x = 21364000 \text{ mm}^4$$

Distance to neutral axis:

$$y_x = 100 \text{ mm}$$

Modulus of elasticity:

$$E = 71000 \text{ MPa}$$

Yield stress:

$$\sigma_y = 250 \text{ MPa}$$

Radius of gyration:

$$r = \sqrt{\frac{I_x}{A}} = \sqrt{\frac{21364000 \text{ mm}^4}{10080 \text{ mm}^2}} = 46.04 \text{ mm}$$

Imperfection variable:

$$\eta = \frac{\delta_0 \cdot y}{r^2} = \frac{10 \text{ mm} \cdot 100 \text{ mm}}{(46.04 \text{ mm})^2} = 0.472$$

Euler's critical load:

$$P_E = \frac{\pi^2 \cdot E \cdot I_x}{(k \cdot L)^2}$$

Euler's critical stress:

$$\sigma_E = \frac{P_E}{A} = \frac{\pi^2 \cdot E \cdot I_x}{(k \cdot L)^2 \cdot A}$$

Perry-Robertson stress ratio:

$$\frac{\sigma}{\sigma_y} = 0.5 \cdot \left(\left(1 + \frac{\sigma_E}{\sigma_y} \cdot (\eta + 1) \right) - \sqrt{\left(1 + \frac{\sigma_E}{\sigma_y} \cdot (\eta + 1) \right)^2 - 4 \cdot \frac{\sigma_E}{\sigma_y}} \right)$$

Table 18: Perry-Robertson results, 10 mm imperfection, H-400 minor axis

Length (mm)	Euler's stress, σ_E (MPa)	Stress ratio, $\frac{\sigma}{\sigma_y}$
1	1.48e^9	0.679
500	5934.71	0.673
1000	1483.68	0.654
1500	659.41	0.619
2000	370.92	0.567
2500	237.39	0.501
3000	164.85	0.427
3500	121.12	0.357
4000	92.73	0.297
4500	73.27	0.248
5000	59.35	0.208
5500	49.05	0.176
6000	41.21	0.151
6500	35.12	0.131
7000	30.28	0.114
7500	26.38	0.100
8000	23.18	0.088
8500	20.54	0.079
9000	18.32	0.071
9500	16.44	0.064
10000	14.84	0.058

D.6. No imperfection, H-400 cross-section - Minor axis

The following calculations are done for a “perfect” H-400 column, with regards to the minor axis.

Imperfection at midspan:

$$\delta_0 = 0 \text{ mm}$$

Effective buckling length factor:

$$k = 1$$

Area of cross-section:

$$A = 10080 \text{ mm}^2$$

Moment of inertia:

$$I_x = 21364000 \text{ mm}^4$$

Distance to neutral axis:

$$y_x = 100 \text{ mm}$$

Modulus of elasticity:

$$E = 71000 \text{ MPa}$$

Yield stress:

$$\sigma_y = 250 \text{ MPa}$$

Radius of gyration:

$$r = \sqrt{\frac{I_x}{A}} = \sqrt{\frac{21364000 \text{ mm}^4}{10080 \text{ mm}^2}} = 46.04 \text{ mm}$$

Imperfection variable:

$$\eta = \frac{\delta_0 \cdot y}{r^2} = \frac{0 \text{ mm} \cdot 100 \text{ mm}}{(46.04 \text{ mm})^2} = 0$$

Euler’s critical load:

$$P_E = \frac{\pi^2 \cdot E \cdot I_x}{(k \cdot L)^2}$$

Euler’s critical stress:

$$\sigma_E = \frac{P_E}{A} = \frac{\pi^2 \cdot E \cdot I_x}{(k \cdot L)^2 \cdot A}$$

Perry-Robertson stress ratio:

$$\frac{\sigma}{\sigma_y} = 0.5 \cdot \left(\left(1 + \frac{\sigma_E}{\sigma_y} \cdot (\eta + 1) \right) - \sqrt{\left(1 + \frac{\sigma_E}{\sigma_y} \cdot (\eta + 1) \right)^2 - 4 \cdot \frac{\sigma_E}{\sigma_y}} \right)$$

Table 19: Perry-Robertson results, no imperfection, H-400 minor axis

Length (mm)	Euler's stress, σ_E (MPa)	Stress ratio, $\frac{\sigma}{\sigma_y}$
1	1.48e^9	1.000
500	5934.71	1.000
1000	1483.68	1.000
1500	659.41	1.000
2000	370.92	1.000
2500	237.39	0.950
3000	164.85	0.659
3500	121.12	0.484
4000	92.73	0.371
4500	73.27	0.293
5000	59.35	0.237
5500	49.05	0.196
6000	41.21	0.165
6500	35.12	0.140
7000	30.28	0.121
7500	26.38	0.106
8000	23.18	0.093
8500	20.54	0.082
9000	18.32	0.073
9500	16.44	0.066
10000	14.84	0.059

D.7. 10 mm imperfection, H-400 cross-section - Major axis

The calculations are repeated for the major axis:

Imperfection at midspan:

$$\delta_0 = 10 \text{ mm}$$

Effective buckling length factor:

$$k = 1$$

Area of cross-section:

$$A = 10080 \text{ mm}^2$$

Moment of inertia:

$$I_y = 277596160 \text{ mm}^4$$

Distance to neutral axis:

$$y_y = 200 \text{ mm}$$

Modulus of elasticity:

$$E = 71000 \text{ MPa}$$

Yield stress:

$$\sigma_y = 250 \text{ MPa}$$

Radius of gyration:

$$r = \sqrt{\frac{I_y}{A}} = \sqrt{\frac{277596160 \text{ mm}^4}{10080 \text{ mm}^2}} = 165.95 \text{ mm}$$

Imperfection variable:

$$\eta = \frac{\delta_0 \cdot y}{r^2} = \frac{10 \text{ mm} \cdot 200 \text{ mm}}{(165.95 \text{ mm})^2} = 0.073$$

Euler's critical load:

$$P_E = \frac{\pi^2 \cdot E \cdot I_y}{(k \cdot L)^2}$$

Euler's critical stress:

$$\sigma_E = \frac{P_E}{A} = \frac{\pi^2 \cdot E \cdot I_y}{(k \cdot L)^2 \cdot A}$$

Perry-Robertson stress ratio:

$$\frac{\sigma}{\sigma_y} = 0.5 \cdot \left(\left(1 + \frac{\sigma_E}{\sigma_y} \cdot (\eta + 1) \right) - \sqrt{\left(1 + \frac{\sigma_E}{\sigma_y} \cdot (\eta + 1) \right)^2 - 4 \cdot \frac{\sigma_E}{\sigma_y}} \right)$$

Table 20: Perry-Robertson results, 10 mm imperfection, H-400 major axis

Length (mm)	Euler's stress, σ_E (MPa)	Stress ratio, $\frac{\sigma}{\sigma_y}$
1	1.93e ¹⁰	0.932
500	77113.53	0.932
1000	19278.38	0.932
1500	8568.17	0.931
2000	4819.60	0.929
2500	3084.54	0.927
3000	2142.04	0.925
3500	1573.75	0.922
4000	1204.90	0.918
4500	952.02	0.913
5000	771.14	0.907
5500	637.30	0.899
6000	535.51	0.890
6500	456.29	0.877
7000	393.44	0.862
7500	342.73	0.842
8000	301.22	0.816
8500	266.83	0.785
9000	238.00	0.747
9500	213.61	0.706
10000	192.78	0.662
10500	174.86	0.617
11000	159.33	0.575
11500	145.77	0.534
12000	133.88	0.497
12500	123.38	0.463
13000	114.07	0.431
13500	105.78	0.402
14000	98.36	0.376
14500	91.69	0.352
15000	85.68	0.330
15500	80.24	0.310
16000	75.31	0.292

D.8. No imperfection, H-400 cross-section - Major axis

Imperfection at midspan:

$$\delta_0 = 0 \text{ mm}$$

Effective buckling length factor:

$$k = 1$$

Area of cross-section:

$$A = 10080 \text{ mm}^2$$

Moment of inertia:

$$I_y = 277596160 \text{ mm}^4$$

Distance to neutral axis:

$$y_y = 200 \text{ mm}$$

Modulus of elasticity:

$$E = 71000 \text{ MPa}$$

Yield stress:

$$\sigma_y = 250 \text{ MPa}$$

Radius of gyration:

$$r = \sqrt{\frac{I_y}{A}} = \sqrt{\frac{277596160 \text{ mm}^4}{10080 \text{ mm}^2}} = 165.95 \text{ mm}$$

Imperfection variable:

$$\eta = \frac{\delta_0 \cdot y}{r^2} = \frac{0 \text{ mm} \cdot 200 \text{ mm}}{(165.95 \text{ mm})^2} = 0.0$$

Euler's critical load:

$$P_E = \frac{\pi^2 \cdot E \cdot I_y}{(k \cdot L)^2}$$

Euler's critical stress:

$$\sigma_E = \frac{P_E}{A} = \frac{\pi^2 \cdot E \cdot I_y}{(k \cdot L)^2 \cdot A}$$

Perry-Robertson stress ratio:

$$\frac{\sigma}{\sigma_y} = 0.5 \cdot \left(\left(1 + \frac{\sigma_E}{\sigma_y} \cdot (\eta + 1) \right) - \sqrt{\left(1 + \frac{\sigma_E}{\sigma_y} \cdot (\eta + 1) \right)^2 - 4 \cdot \frac{\sigma_E}{\sigma_y}} \right)$$

Table 21: Perry-Robertson results, no imperfection, H-400 major axis

Length (mm)	Euler's stress, σ_E (MPa)	Stress ratio, $\frac{\sigma}{\sigma_y}$
1	1.93e^10	1.000
500	77113.53	1.000
1000	19278.38	1.000
1500	8568.17	1.000
2000	4819.60	1.000
2500	3084.54	1.000
3000	2142.04	1.000
3500	1573.75	1.000
4000	1204.90	1.000
4500	952.02	1.000
5000	771.14	1.000
5500	637.30	1.000
6000	535.51	1.000
6500	456.29	1.000
7000	393.44	1.000
7500	342.73	1.000
8000	301.22	1.000
8500	266.83	1.000
9000	238.00	0.952
9500	213.61	0.854
10000	192.78	0.771
10500	174.86	0.699
11000	159.33	0.637
11500	145.77	0.583
12000	133.88	0.536
12500	123.38	0.494
13000	114.07	0.456
13500	105.78	0.423
14000	98.36	0.393
14500	91.69	0.367
15000	85.68	0.343
15500	80.24	0.321
16000	75.31	0.301

Appendix E: Imperfect cross-section calculations

E.1. H-400 Cross-section with varying geometry

To gain a better understanding of the effect that varying the width of the flange and height of the web has on flexural buckling resistance, some calculations must be performed. As mentioned in Chapter 5, this will be a worst-case scenario where both deviations of the width and deviations of the height occurs simultaneously.

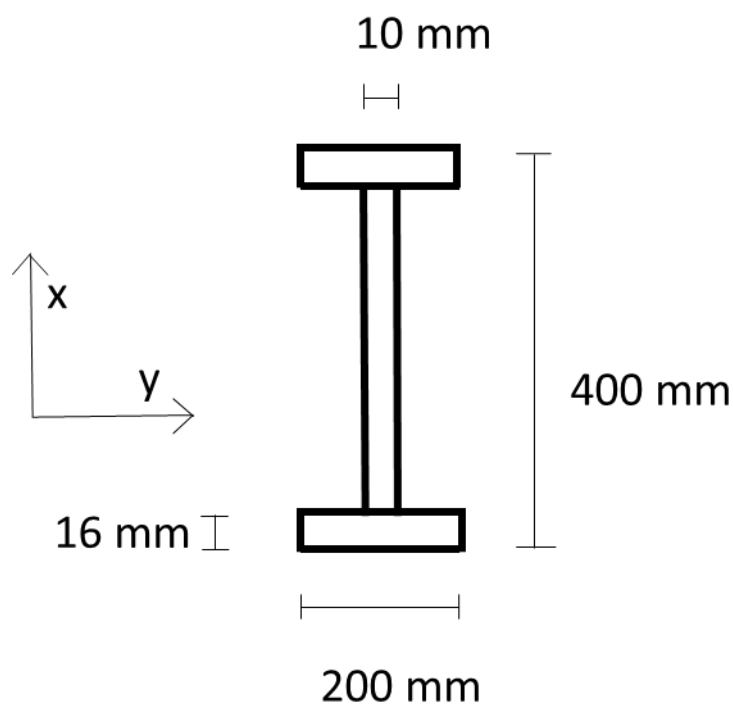


Figure 49: H-400 cross-section

The calculations will be carried out for a H-400 cross-section. With changes being done to the cross-section, it is necessary to perform the classification calculations again. With class 4 components, a thickness reduction factor must be determined and implemented into the relevant thickness. This will create a new effective area that is to be used in the resistance calculations. A new moment of inertia must also be determined. The moment of inertia for both axes is determined with regards to the gross cross-section geometry.

The classification calculations and moment of inertia calculations are done in the same manner as in Appendix A.2.

The resistance calculations are done in the same manner as in Appendix B.2.

The results have been tabulated:

Table 22: Classification and thickness reduction, H-400

Change	Geometry				Classification		Thickness reduction factor	
	Width	Height	Thickness flange	Thickness web	Flange	Web	Flange	Web
- 5 mm	195 mm	395 mm	16 mm	10 mm	Class 3	Class 4	-	0.715
- 3 mm	197 mm	397 mm	16 mm	10 mm	Class 3	Class 4	-	0.712
0 mm	200 mm	400 mm	16 mm	10 mm	Class 3	Class 4	-	0.707
+ 3 mm	203 mm	403 mm	16 mm	10 mm	Class 4	Class 4	0.998	0.703
+ 5 mm	205 mm	405 mm	16 mm	10 mm	Class 4	Class 4	0.995	0.700

Table 23: Moment of inertia, H-400

Change	Effective thickness		Area		Moment of inertia	
	Flange	Web	Gross	Effective	I_x	I_y
- 5 mm	16.00	7.146	9870.0	8833.9	19803250.0	264073202.5
- 3 mm	16.00	7.116	9954.0	8901.3	20418078.0	269430825.5
0 mm	16.00	7.070	10080.0	9002.2	21364000.0	277596160.0
+ 3 mm	15.97	7.027	10206.0	9091.7	22338722.0	285917446.5
+ 5 mm	15.91	7.000	10290.0	9135.5	23004750.0	291552317.5

For the resistance calculations the column is assumed to be 3000 mm long with pinned end supports.

Table 24: Compression and flexural buckling resistance, H-400

Change	Compression resistance	Flexural buckling resistance	
		x-axis	y-axis
- 5 mm	2007.7	1058.7	1910.8
- 3 mm	2023.0	1083.9	1926.3
0 mm	2045.9	1121.8	1949.6
+ 3 mm	2066.3	1159.4	1970.4
+ 5 mm	2076.3	1186.8	1981.1

It can be determined from these results that the resistances increases with the larger cross-sections. Therefore it can be concluded that the positive effects from a larger cross-section is overall beneficial, even with the added negative effect from local buckling.

E.2. H-200 Cross-section with varying geometry

Since the production tolerances listed in NS-EN 1090-3 states an actual measurement for the permitted deviation of flange width and web height and not an expression, as is the case with many other tolerances, the effect should prove more influential in a smaller cross-section.

To test this a new cross-section will be presented, the H-200. This cross-section will be half the size of the H-400 cross-section

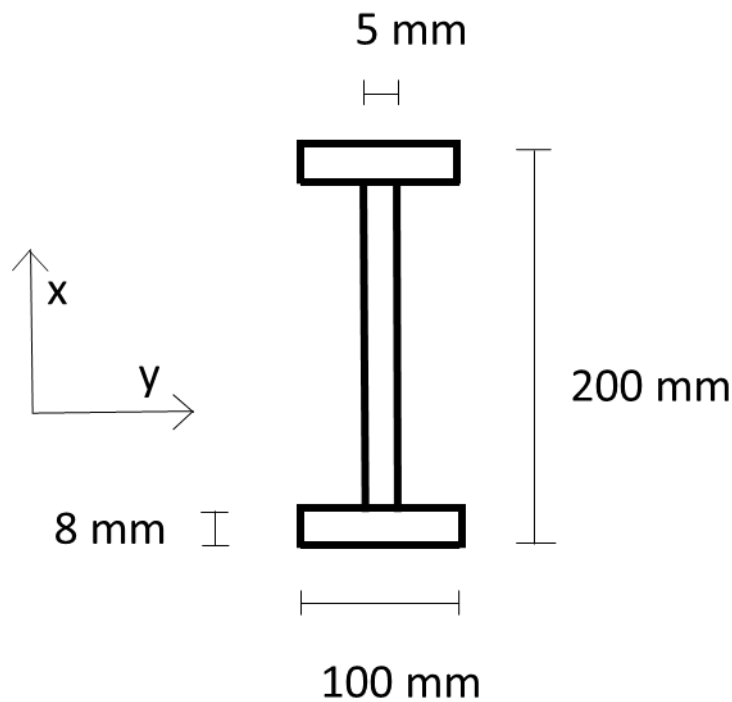


Figure 50: H-200 cross-section

The calculations are done in the same manner as for the H-400 cross-section. This cross-section is exactly half the size of the H-400 cross-section and so the slenderness ratio for the different cross-section components remains unaltered. This will lead to the same required thickness reductions for the various changes in the geometry.

The results have been tabulated:

Table 25: Classification and thickness reduction, H-200

Change	Geometry				Classification		Thickness reduction factor	
	Width	Height	Thickness flange	Thickness web	Flange	Web	Flange	Web
- 5 mm	95 mm	195 mm	8 mm	5 mm	Class 3	Class 4	-	0.722
- 3 mm	97 mm	197 mm	8 mm	5 mm	Class 3	Class 4	-	0.716
0 mm	100 mm	200 mm	8 mm	5 mm	Class 3	Class 4	-	7.070
+ 3 mm	103 mm	203 mm	8 mm	5 mm	Class 4	Class 4	0.993	0.698
+ 5 mm	105 mm	205 mm	8 mm	5 mm	Class 4	Class 4	0.986	0.693

Table 26: Moment of inertia, H-200

Change	Effective thickness		Area		Moment of inertia	
	Flange	Web	Gross	Effective	I_x	I_y
- 5 mm	8.00	3.61	2415.0	2166.4	1145031.25	15686051.25
- 3 mm	8.00	3.58	2457.0	2200.1	1218782.75	16338750.75
0 mm	8.00	3.54	2520.0	2250.5	1335250.00	17349760.00
+ 3 mm	7.94	3.49	2583.0	2289.3	1458917.25	18399787.25
+ 5 mm	7.89	3.46	2625.0	2310.3	1545468.75	19121768.75

For the resistance calculations the column is assumed to be **1000 mm** long with pinned end supports.

Table 27: Compression and flexural buckling resistance, H-200

Change	Compression resistance	Flexural buckling resistance	
		x-axis	y-axis
- 5 mm	492.4	378.7	480.1
- 3 mm	500.0	389.9	487.8
0 mm	511.5	406.4	499.4
+ 3 mm	520.3	420.7	508.5
+ 5 mm	525.1	429.2	513.5

